Bulletin 153

New Mexico Bureau of Mines & Mineral Resources

A DIVISION OF
NEW MEXICO INSTITUTE OF MINING & TECHNOLOGY

Facies, diagenesis, and mineralogy of the Jurassic Todilto Limestone Member, Grants uranium district, New Mexico

Augustus K. Armstrong
U.S. Geological Survey, c/o New Mexico Bureau of Mines & Mineral Resources, Socorro, New Mexico 87801

SOCORRO 1995

Original Printing

Published by Authority of State of New Mexico, NMSA 1953 Sec. 63-1-4
Printed by University of New Mexico Printing Services, December 1995

Available from New Mexico Bureau of Mines & Mineral Resources, Socorro, NM 87801

Contents

Figures

Table

Abstract—The Todilto Limestone Member, the basal member of the Wanakah Formation of the Grants uranium district, is 1-30 ft (0.3-9.1 m) thick and records the change in depositional environment from a restricted marine embayment with an ephemeral connection to the Curtis-Summerville Sea to a completely enclosed salina/playa and shrinking body of gypsiferous water. The salina measured 300 mi (483 km) from east to west and 250 mi (402 km) from north to south, and was fringed by an extensive belt of limestone-gypsum sediments. The arenaceous lime-mudstone sediments record salina/playa deposition in alternating brackish to hypersaline waters and extended periods of exposure to desiccation. Dolomite is absent in the study area. The calcite-lime mudstones were derived primarily from an aragonite-mud precursor and were subjected to extensive neomorphism. The aragonite-to-calcite diagenetic history is evident in the poorly preserved ooids.

The salina waters supported a small invertebrate fauna and flora, and there is no evidence of an infauna in the lime mudstone. Rare bioclasts of calcareous algae, dasyclads of the tribe Salpingoporellae, are found in the Todilto sediments. Ostracodes were abundant in the salina's ephemeral gypsiferous waters. The salinity of the waters was influenced by seasonal influx from streams, rainfall, periods of drought, and intermittent connections to the Curtis-Summerville Sea. The overlying 0-110 ft (0-33.5 m) thick gypsum unit found to the east of the study area was deposited in the center of the basin during the final salina phase. Playa-type alkaline evaporites, such as trona and shortite, are not known from the Todilto Limestone Member.

Syndepositional intraformational folds in a vertical stack up to 10 ft (3 m) high and 45 ft (14 m) wide occur in the playa (inland sabkha) lime mudstone and are associated with calcite pseudo-morphs of anhydrite-gypsum and anhydrite ptygmatic-enterolithic layers. The intraformational folds are overlapped and buried by thick-bedded microbial mat, ostracode-lime mudstone. Prior to Beclabito Member deposition, the Todilto Limestone Member was subjected to sub-aerial weathering and vadose solution which formed sink holes, rundkarrens, and solution pipes that are filled with limestone breccias and ferruginous sands. The smaller vadose-solution cavities are partially filled with multiple cycles of spar calcite and iron-stained quartz sands. Commercial bodies of uranium ore are found in the Todilto intraformational folds and associated solution cavities. Isotope dates (150-155 m.y.) indicate that the uraninite is nearly syngenetic with the carbonates.

Introduction

This is a study of the sedimentology, facies, and diagenesis of the Todilto Member of the Wanakah Formation (Jurassic) in the Grants uranium district (Fig. 1).

Wanakah Formation is U.S. Geological Survey nomenclature for the upper San Rafael Group in northwestern New Mexico. The Todilto forms the basal member of the Wanakah. Lest the appearance of the name Wanakah in this publication be interpreted as acceptance by the New Mexico Bureau of Mines & Mineral Resources, the following statement is included herein. The New Mexico Bureau of Mines & Mineral Resources recognizes the Todilto as a formation-rank unit within the San Rafael Group and further recognizes that the name Wanakah is preoccupied (in the state of New York) and therefore unavailable as a stratigraphic name.

The primary objective of this research was to determine the depositional environments of limestones in the Todilto Member. The separation of marine, salina, and lacustrine depositional environments in Proterozoic, Paleozoic, and Mesozoic rocks is difficult. Criteria that may be used to separate the two include (1) packaging of respective facies, (2) suites of evaporite minerals or pseudomorphs contained in sedimentary assemblages, (3) organic remains, and (4) petrographic and geochemical evidence (Southgate et al., 1989).

Studies of lacustrine carbonate facies (Platt & Wright, 1991), modern saline lacustrine depositional environments (Hardie et al., 1978), and the marine tidal deposits of Andros Island (Shinn et al., 1969; Hardie, 1977) and Holocene and Jurassic evaporites of the Arabian Gulf provide us with much of the basic knowledge for deciphering the Todilto sedimentary structures. In recent years the literature on modern and ancient salinas has greatly increased our ability to interpret these ancient deposits. The work of Warren (1982,1990), Kendall (1984), Handford et al. (1984), Warren & Kendall (1985), and Logan (1987) on the modern marine-influenced salina deposits of Australia has helped in understanding the Todilto Limestone Member.

Hardie et al. (1978) defined an ephemeral salina lake as a body of water, normally a concentrated brine, that at least once every few years dries up, leaving in the low central area an exposed layer of salts that precipitated out as the brine evaporated. This subenvironment has been described as a salina, alkali lake, or playa lake when wet and as a playa, dry lake, alkali flat, salt pan, or inland sabkha when dry.

Dunham's (1962) classification of carbonate rocks is used throughout this report.

Acknowledgments

Frank E. Kottlowski, Director Emeritus of the New Mexico Bureau of Mines & Mineral Resources, suggested the study of the Todilto Limestone. Fred Craft, Resident Manager of Homestake Mining Company, gave permission to study the mineralized Todilto Limestone on the company properties in the Grants district. Scanning electron microscope (SEM) studies and energy-dispersive x-ray analyses (EDX) were made by R. L. Oscarson of the U.S. Geological Survey, Menlo Park, California. Calcareous algae were identified by B.L. Mamet of the University of Montreal. Chris McKee of the New Mexico Bureau of Mines & Mineral Resources performed x-ray analyses of the carbonate rocks. Christopher R. Scotese of the University of Texas at Arlington generously provided his prepublication copy of paleomagnetic and paleogeographic map of the Callovian in the Western United States. Robert N. Ginsburg spent several days (April 1994) in the field with me and gave invaluable advice on the interpretation of the sedimentary structures and the organization of the manuscript. I appreciate the critical reviews by Eu-

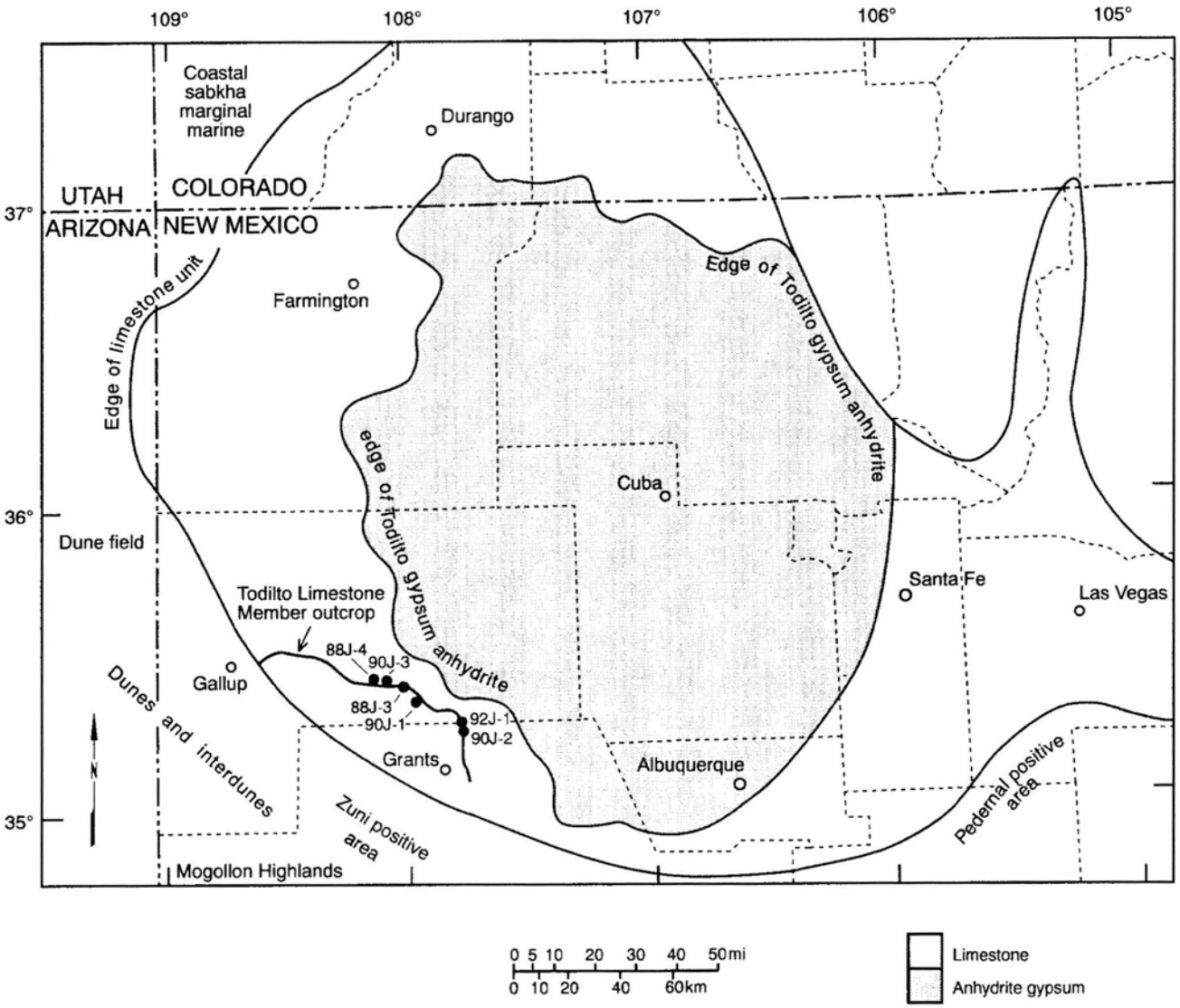

FIGURE 1—Map showing distribution of the Todilto Limestone Member of the Wanakah Formation in northwestern New Mexico and equivalent rocks in southwest Colorado and east-central New Mexico. Distribution of the gypsum unit is shown by dark stippled pattern and the limestone unit by light stippled pattern. The Todilto Limestone Member deposition shows a bull's eye pattern consisting of a carbonate rim surrounding a central zone of massive-bedded gypsum–anhydrite. Locations of the measured sections in the Grants uranium district are marked by black dots and the line of stratigraphic section. Distribution of Gypsum Member is in part from Vincelette & Chittum (1981).

gene A. Shinn and Robert B. Halley of the U.S. Geological Survey, James Lee Wilson of New Braunfels, Texas, and William R. Berglof of the University of Maryland.

Previous studies

The reader is referred to Lucas et al. (1985) for a chronological account of the literature and history of the stratigraphic nomenclature for the Jurassic System and the Todilto in east-central New Mexico, where they designated it the Todilto Formation. Condon & Peterson (1986) and Condon (1989) carefully documented the Jurassic stratigraphy of the southeast San Juan Basin. They discussed the evolution of the stratigraphic nomenclature for the Todilto Limestone Member since Dutton's (1885) original description of the rocks. Gregory (1916, 1917) defined and first used the name Todilto Limestone. In the Grants mining district (Fig. 2) the Wanakah Formation consists of three members, in ascending order the Todilto Limestone, the Beclabito, and the Horse Mesa (Condon & Huffman, 1988; Condon, 1989). In east-central New Mexico, the Todilto has been designated the Todilto Limestone or the Todilto Formation. Rocks equivalent to the Todilto across the state line in Colorado (Fig. 2) have been assigned to the Pony Express Limestone Member, the basal member of the Wanakah Formation.

Environments of deposition

Lacustrine deposition

The Todilto has been interpreted as lacustrine, deposited in low-energy, fetid, toxic, and anoxic water (Silver, 1948; Rapaport et al., 1952; Gabelman, 1956; Ash, 1958; Anderson & Kirkland, 1960; Bell, 1963; Mankin, 1972; Tanner, 1974; Campbell, 1976; Green & Pierson, 1977).

Lucas et al. (1985) analyzed the Todilto fauna and facies, and envisioned the Todilto environment as a salina formed by the flow of marine waters from the Curtis Sea through the Entrada Sandstone along the northwestern margin of the basin. The water body had a fresh-water

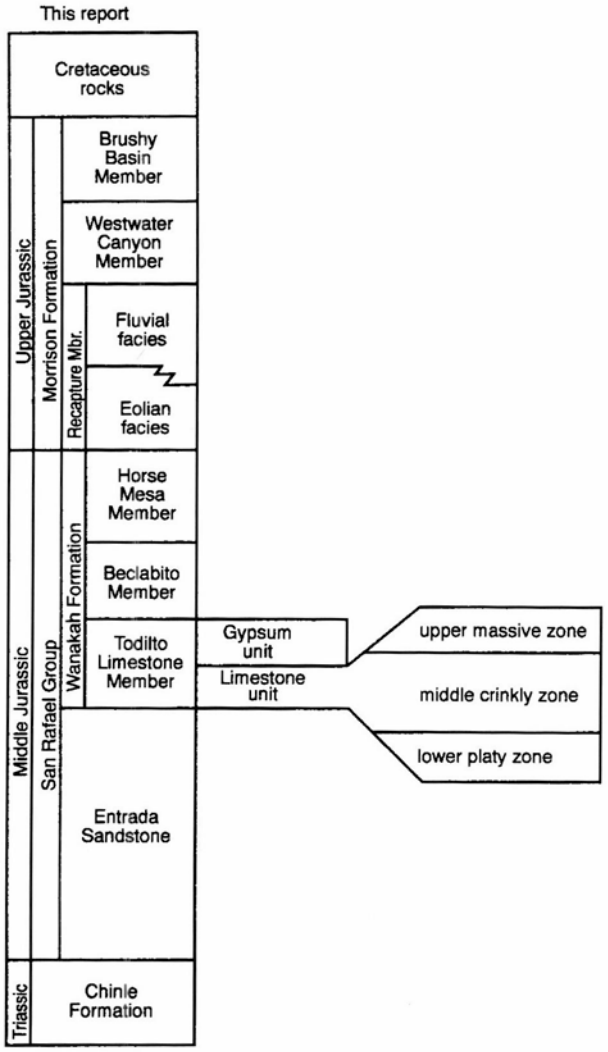

FIGURE 2—Jurassic nomenclature for the southern San Juan Basin and the Gallup and Acoma sags (after Condon, 1989).

component in the form of streams and ground water which entered the basin from the east, south, and west.

The Todilto carbonates cannot be traced into marine sediments, which is in part why various authors concluded that the Todilto Limestone Member was deposited in a lacustrine environment. The Todilto Limestone does not interfinger with or extend into any known marine strata, and stratigraphically it lies between continental or marginal-marine sandstones.

Marine deposition

Baker et al. (1947), Smith (1951), Harshbarger et al. (1957), and Ridgley (1989) favored a marine environment of deposition for the Todilto Limestone Member. Harshbarger et al. (1957) cited the abundance of sulfate and the absence of chloride salts as evidence indicating that the Todilto was deposited from abnormal (anoxic, toxic, reducing, and fetid) marine waters in a gulf connected to the Curtis Sea. Thick deposits of gypsum/anhydrite are possible in a lacustrine basin only under very special conditions. The Todilto deposits do not contain alkaline salts such as trona, ankerite, or siderite, which are common in some ancient lacustrine deposits. Rawson (1980, p. 304), who studied deposits of the Todilto Limestone Member, concluded that "the carbonates were deposited in a sabkha environment in or near a large lake that became restricted at times and evaporated to dryness." Anderson (1982, p. 149) stated that the Todilto Basin was connected to the ocean. The evaporite sequence never progressed to the point of halite precipitation, and the occurrence of insects and brackish-water fishes suggests a substantial nonmarine influence.

Ridgley & Goldhaber (1983) presented isotopic evidence that the Todilto evaporites were marine in origin, and Ridgley (1989) again stated that the environment of deposition for the Todilto Limestone Member was restricted marine. Evans & Kirkland (1988) found that "The sulfur isotopes of the Gypsum Member indicate that the sulfate anions had a marine source." Ridgley's (1986) petrographic study of the Todilto Limestone in the Chama Basin of north-central New Mexico indicated that the carbonate sediments had a varied and complex diagenetic history, including dolomitization followed by dedolomitization, an evaporate replacement of carbonate and subsequent carbonate replacement of the evaporite, and an early formation of styolites. Ridgley's (1989, figs. 9,10) paleogeographic maps show her ideas on the access of the Todilto embayment to the Curtis—Pine Butte (the Pine Butte is a member of the Sundance Formation) Sea during the middle Callovian time in areas of Utah, Colorado, New Mexico, and Arizona.

Evans & Kirkland (1988) stated that "strontium isotope data establish clearly that cations forming the Todilto Limestone Member were derived mainly from a marine source."

Lucas et al. (1985) envisioned a large, landlocked salina. McCrary's (1985) regional study of the Todilto Limestone Member indicated to her that the limestone and gypsum recorded the changes in depositional environment from a restricted-marine embayment with an ephemeral connection to the sea to a completely enclosed basin (lake). The limestone member was deposited under restricted-marine conditions, and the gypsum member formed during the lake stage. The Todilto embayment was fed by (1) periodic excursion of the Curtis—Summerville Sea across the Entrada dune barrier during storms and unusually high tides, (2) marine ground water, (3) continental surface water and ground water, and (4) rainfall.

Age

Lucas et al. (1985) provided an extensive list of fishes and invertebrates found in the Todilto Formation of east-central New Mexico. They also described in detail the various environments in which these animals lived, and discussed the biostratigraphic and regional- stratigraphic relationships of the Todilto. They concluded from the fossil evidence that "the Todilto is most likely of middle Callovian age," or late Middle Jurassic. It is interesting to note that this is also the presumed age of the great evaporite filling of the Gulf of Mexico, the Louann Formation (James Lee Wilson, written comm. 1992).

Regional paleolatitude and paleoclimates

Kocurek & Dott's (1983, fig. 3) analysis of the Jurassic paleogeography and paleoclimates of the central and southern Rocky Mountains used the paleopole positions as determined by Steiner & Helsley (1975), Steiner (1978), and Lienert & Helsley (1980) from data gathered on the Triassic to Jurassic red beds on the Colorado Plateau. C. R. Scotese's (written comm. 1993) paleomagnetic studies indicate that the Todilto Limestone Member of the

Wanakah Formation in the Grants district was deposited at a latitude of about 13° north (Fig. 3), while Kocurek & Dott (1983) suggested about 15-16° north. Frakes (1979) suggested that global temperature means may have been as much as 18°F (10°C) warmer than they are today. Widespread eolian deposits in the study area have been interpreted by Poole (1962) as representing trade-wind desert deposits. During the Middle Jurassic, the region occupied the paleolatitude range typically associated with trade winds. Most modern hot deserts of the world occur within the trade-wind belt (Hardie, 1991). Kocurek & Dott's (1983) and Vakhrameer's (1991) syntheses of the data have shown that with respect to paleoclimate, paleolatitude, and location on the western edge of North America during the Mesozoic, the conditions of the western United States were similar to the modern Sahara (Fig. 3).

Stratigraphy

Studies by Santos & Turner-Peterson (1986) show that during the Middle and Late Jurassic the structural configuration of the area occupied by the San Juan Basin was different from the present-day configuration, which developed in response to Laramide deformation. The Todilto and equivalent rocks were deposited in an elliptical basin which extended about 300 mi (483 km) east—west and about 250 mi (402 km) north—south (Fig. 1). The Todilto is composed of two units, (1) a lower, thin, regionally extensive limestone unit and (2) an upper, more restricted, thick gypsum unit. In the eastern part of the San Juan Basin, the limestone unit is generally from 5 to 10 ft (1.5-3.1 m) thick, and the overlying gypsum unit reaches a thickness of up to 95 ft (29 m). In the west part of the basin only the limestone unit is present. This unit

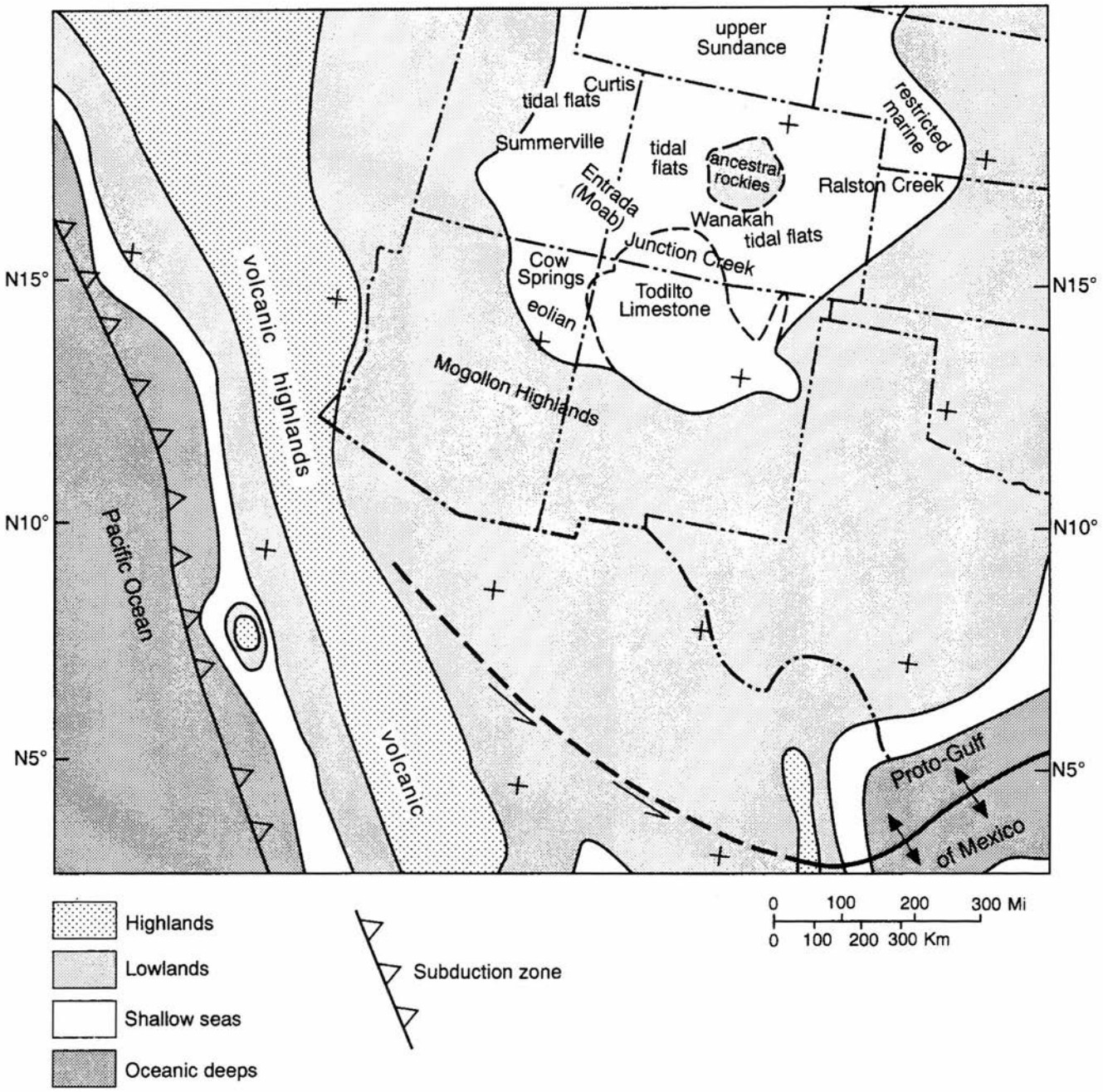

FIGURE 3—Callovian paleomagnetic latitude and paleogeography. From Scotese (written comm. 1993), with some modifications from Kocurek & Dott (1983).

ranges in thickness from about 25 ft (8 m) in the Grants district to 1 ft (0.3 m) or less near the southwest strandline of the basin a few miles east of Gallup (McLaughlin, 1963).

On the southwest side of the San Juan Basin, in the area of this study, the Todilto Limestone Member crops out along the northeast-dipping Thoreau homocline in a belt trending generally northwest—southeast across southern McKinley and northern Cibola Counties.

In the Grants district the Todilto is composed of medium- to dark-gray carbonaceous, thinly laminated to thin-bedded limestone and gypsum. The limestone is from 2 to 25 ft (0.6-8 m) thick (Fig. 4). Many workers (Hilpert &

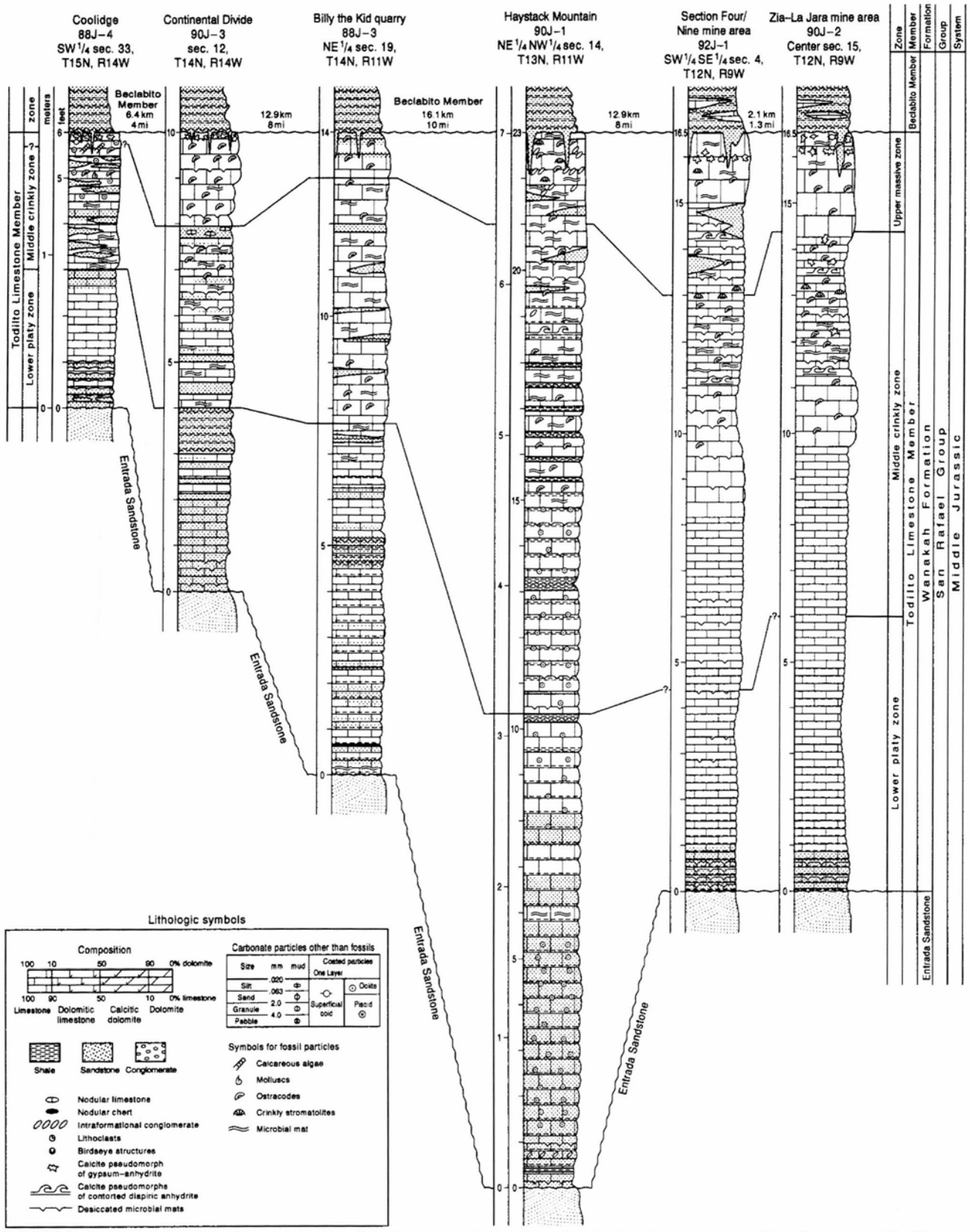

FIGURE 4—Regional stratigraphy, correlation, lithology, and facies chart for the Todilto Limestone Member in the Zia/La Jara mine area, Grants uranium district, New Mexico.

Moench, 1960; McLaughlin, 1963; Thaden et al., 1967; Rawson, 1980) have recognized three informal stratigraphic units within the Todilto carbonates. They are known as the lower platy zone, the middle crinkly zone, and the upper massive zone (which may be locally absent) of the limestone member.

The Todilto gradationally overlies the eolian, cross-bedded, cliff-forming, reddish-orange Entrada Sandstone. Immediately beneath the Todilto contact the Entrada Sandstone is a leached, varicolored, fine-grained, well-sorted sandstone unit 5-30 ft (1.5-9.1 m) thick. Colors range from light gray to lavender, contrasting markedly with the predominantly orangish-brown typical Entrada (McLaughlin, 1963).

Above its contact with the Entrada Sandstone, the Todilto Limestone Member consists of thin beds of calcareous sandstone or siltstone that are commonly interbedded with limestone (Condon, 1989). To the east of the study area at Mesita, about 110 ft (33.6 m) of white, crudely bedded gypsum of "chickenwire" texture overlies the limestone. However, it is absent in the study area.

The Beclabito Member is composed of reddish-brown to white silty sandstone, sandy siltstone, and claystone. Condon (1989) interpreted the Beclabito Member as mainly marginal-marine or marginal-lacustrine and sabkha deposits that grade southward into fluvial deposits. Most of the Beclabito Member was deposited in a low-lying area that was transitional between highlands to the south and the Todilto Sea to the north. The area was marginal to a body of water. Ridgley (1989) described trace fossils and nonmarine, lacustrine mollusks from the upper member of the Wanakah Formation in the Chama Basin, New Mexico.

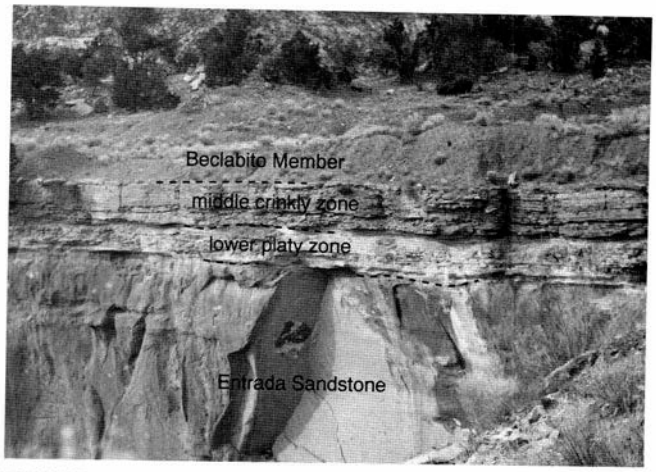

FIGURE 5—Measured section 88J-4 north of Coolidge. The section is some 6 ft (2 m) thick and consists of the lower platy zone overlain by the crinkly zone. No intraformational folds were observed in the outcrops or in the limestone quarry.

Measured sections

Coolidge section 88J-4—The stratigraphic samples from the Coolidge section 88J-4 were collected in an abandoned limestone quarry 3 mi (4.8 km) north of the Interstate 40 interchange at Coolidge, New Mexico. From the overpass a dirt road leads north to the cliffs of Jurassic rocks and the outcrops of the Todilto Limestone Member. The samples were collected on an abandoned quarry road that was cut on the south side of a canyon wall and leads to the quarry floor. The map location is SW¼ NE¼ sec. 33, T15N, R14W. Green's (1976) geologic map of the Continental Divide quadrangle shows the quarry in the Todilto Limestone Member and the various access roads from Interstate 40.

The section was measured and studied on the highwall of an abandoned quarry. The Todilto Limestone Member is 6-7 ft (1.8-2.1 m) thick and consists of a thin-bedded arenaceous limestone which rests with a gradational contact on the Entrada Sandstone. As can be seen in Figure 5, the limestone consists of a lower platy zone some 2-3 ft (0.6-0.9 m) thick and a middle crinkly zone also about 3 ft (0.9 m) thick. The top of the middle crinkly zone is formed by a 1-2 ft (0.3-0.6 m) thick interval of ooid and dense, micritic limestone (Fig. 6). At the top of the section, thin beds some 6 inches (15 cm) thick, with abundant calcite pseudomorphs of gypsum, may represent the upper massive zone. The contact of the Todilto Limestone Member with the Beclabito Member is sharp and well defined (Fig. 6), but can be seen in only a few places because in much of the quarry the Beclabito clastic beds have been removed or covered by waste rock.

Petrographic studies show the lower 1 ft (0.3 m) of the limestone to have stringers and pods of detrital silt to fine sand composed of angular grains of quartz with minor amounts of feldspar. The limestone is composed of 2-6 pm calcite crystals that form a vaguely clotted lime mudstone (micrite). In the lower part of the section, a feature which is not readily recognized in plane light under the petrographic microscope but becomes apparent under cathodo-

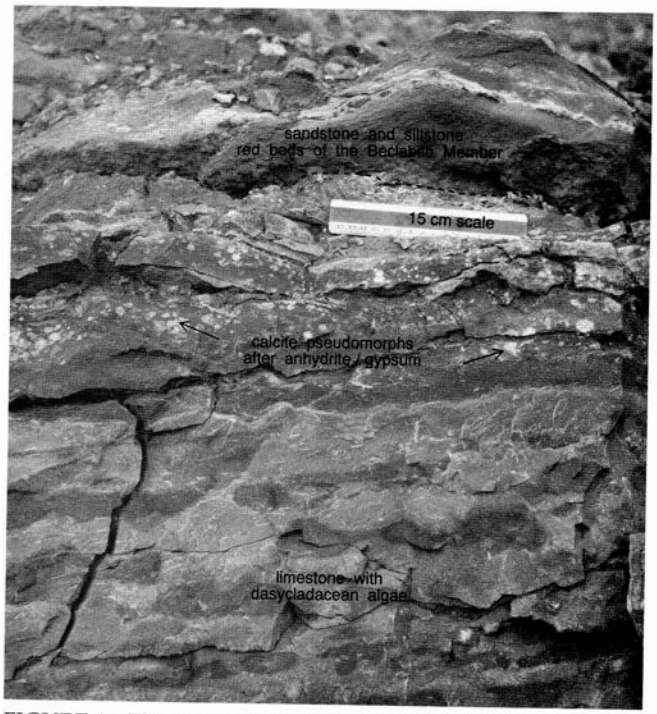

FIGURE 6—The highest beds of the Todilto Limestone Member at the Coolidge section. The gray limestone in the lower part of the photo contains dasyclad algae of the tribe Salpingoporellae. The highest beds of the Todilto Limestone Member at the Coolidge section are similar to those of the Continental Divide section 90J-3 in that they are also characterized by abundant white calcite pseudomorphs after gypsum–anhydrite in a gray microbial mat–ostracode–lime mudstone. Pale red–maroon eolian siltstones and sandstones with nodular-limestone interbeds of the Beclabito Member (Wanakah Formation) overlie the Todilto. This final phase of the Todilto represents a playa (inland sabkha) that was covered by wind-blown sands (see Butler et al., 1982, figs. 18–22 of Abu Dhabi coastal flats). Scale is 6 inches (15 cm) long.

luminescence is the calcite coating of many of the angular quartz grains. They are concentrically coated by 10-25 pm calcite-spar crystals. This coating tends to produce rounded carbonate grains superimposed on angular detrital-quartz nuclei. The ooid-like grains are supported in a micrite matrix composed of 2-6 pm calcite rhombs or a neomorphic microspar calcite matrix (5-20 pm crystals). This microspar appears to be the result of lime-mud (micrite) neomorphism or grain growth. Above the basal silty beds are 2 ft (0.6 m) of 4-6 inch (10-15 cm) thick beds of silty lime mudstones with varying amounts of soft, poorly defined peloids, calcite-coated detrital-quartz grains which form the nuclei of rounded ooids and thin, lenticular beds of ooids. The bed above is 2 ft (0.6 m) of lime mudstone (micrite) with abundant angular-quartz silt and thin, lenticular beds of calcareous siltstone. The uppermost 1-2 ft (0.3-0.6 m) of the section has imbricated lime-mud chips composed of ooid packstone. The top of the section is characterized by large white sparry-calcite pseudomorphs after gypsum/anhydrite (Fig. 6).

Continental Divide section 90J-3—The Continental Divide section 90J-3 was sampled and studied immediately beside an abandoned limestone quarry on a natural west-facing outcrop near the center of sec. 12, T14N, R14W, some 3.1 mi (5 km) northeast of the Continental Divide interchange on Interstate 40. A dirt road leads from the overpass north to the cliffs of Jurassic rocks and the outcrops of the Todilto Limestone Member. Green's (1976) geologic map of the Continental Divide quadrangle shows the quarry in the Todilto Limestone Member and the various access roads from the Interstate.

The Continental Divide section was measured on top of an Entrada Sandstone cliff (Figs. 7-9). The Todilto Limestone Member is some 10 ft (3 m) thick. Thin-bedded an

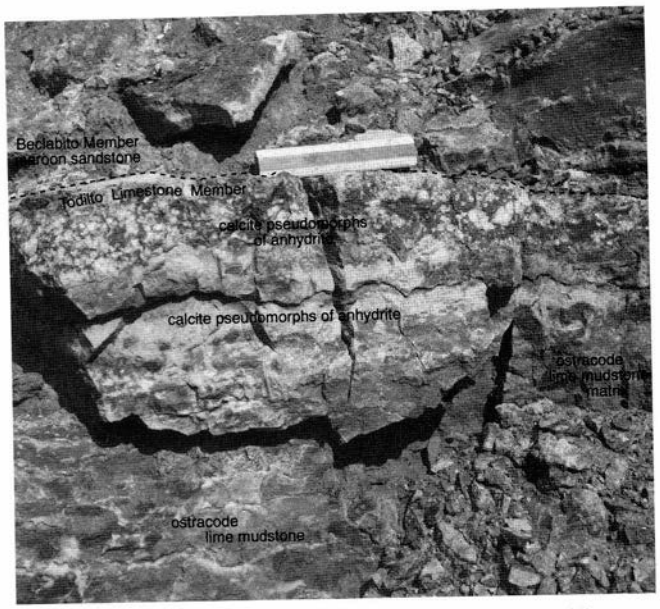

FIGURE 8—The uppermost limestones of the Todilto are characterized by abundant white calcite pseudomorphs after gypsum–anhydrite in a gray, microbial mat–ostracode–lime mudstone. Pale red–maroon eolian siltstones and sandstones with nodular-limestone interbeds of the Beclabito Member (Wanakah Formation) overlie the Todilto Limestone Member Continental Divide section, 90J-3. This final phase of sedimentation of the Todilto represents a playa (inland sabkha) that was covered by wind-blown sands (see Butler et al., 1982, figs. 18–22, Abu Dhabi coastal flats).

gular-quartz siltstones and sandstones compose a significant part of the section interbedded with the lime mud-stones. Ostracodes are found only in the upper third of the section. Well preserved microbial filament tubes are present in the ostracode-lime mudstone, and abundant calcite pseudomorphs after gypsum are found in the limestones at the top of the section.

Billy the Kid mine section 88J-3—Billy the Kid mine section 88J-3 was collected in NE¼ sec. 19, T14N, R11W. The geology, roads, and location of the mine are shown on Green & Pierson's (1971) geologic map of the Thoreau NE quadrangle.

This section was studied along the extensive highwalls of an active quarry (Fig. 10). The exposures of carbonate rocks are excellent except for extensive fracturing caused by quarry blasting. The Todilto Limestone Member is 14-15

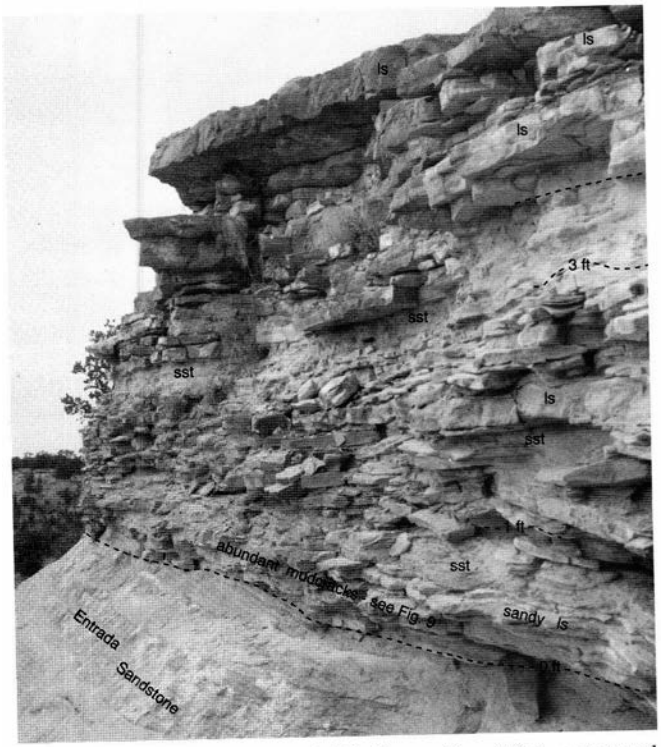

FIGURE 7—The Continental Divide section 90J-3, a natural outcrop adjacent to the northwest side of a small limestone quarry. The section is characterized by interbedded quartz sandstones (sst) with limestones (ls) deposited on a playa surface (inland sabkha).

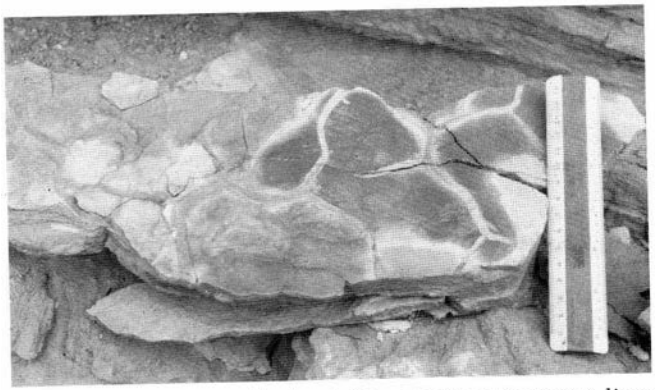

FIGURE 9—Desiccated microbial mats in arenaceous lime mudstone at the base of the Todilto Limestone Member above the Entrada Sandstone, Continental Divide section, 90J-3 (see Shinn, 1983, figs. 7–9A; Butler et al., 1982, Holocene examples from the coastal flats of Abu Dhabi).

FIGURE 10—Billy the Kid mine section 88J-3, studied on the extensive highwalls of an active quarry. The Todilto Limestone Member section is 14–15 ft (4.3–4.6 m) thick. The quarry floor is on the top of the Entrada Sandstone, and the limestone is overlain by maroon sandstones of the Beclabito Member, Wanakah Formation. The lower platy zone is 7 ft (2.1 m) thick and is composed of angular grains of detrital quartz floating in a matrix of neomorphic microspar calcite. This zone is capped by a 1–2 inch (2.5–5 cm) bed of white gypsum followed by the middle crinkly zone, 8.7–9.7 ft (2.7–3.0 m) of arenaceous ostracode–lime mudstone. The massive unit is 1 ft (0.3 m) of arenaceous ostracode–lime mudstone. The contact with the overlying Beclabito Member sandstones is gradational over a thickness of 1–2 ft (0.3–0.6 m). Small intraformational folds are developed at the base of the middle crinkly zone and extend to the top of the section.

ft (4.3-4.6 m) thick. The quarry floor is on the top of the Entrada Sandstone, and the limestone is overlain by maroon sandstones of the Beclabito Member of the Wanakah Formation. The basal 7.7 ft (2.3 m) of the section are the lower platy zone which is composed of angular grains of detrital quartz floating in a matrix of neomorphic microspar calcite. This zone is capped by a 1-2 inch (2.5-5 cm) bed of white gypsum. This is followed by the middle crinkly zone, which is 8.7-9.7 ft (2.7-3.0 m) of arenaceous ostracode-lime mudstone that has undergone a variable amount of neomorphism. The massive unit may be represented by 1 ft (0.3 m) of arenaceous ostracode-lime mudstone. The contact with the overlying Beclabito Member sandstones is gradational over a distance of 1-2 ft (0.3-0.6 m).

Haystack Mountain section 90J-1—The Haystack Mountain section 90J-1 was collected in the NE¼ NW¼ sec. 14, T13N, R11W. The samples were collected in a deep arroyo that has an excellent exposure. Thaden & Ostling's (1967) geologic map of the Bluewater quadrangle shows the road and access to the Todilto outcrops.

This section was measured in an arroyo re-entrance at the top of a cliff (Fig. 11). The section is 23-25 ft (7-7.6 m) thick. The three informal lithologic units of the Todilto are not readily recognized at this outcrop. The lower platy zone is 10 ft (3.0 m) thick and consists of 6-10 inch (15-25 cm) thick beds of arenaceous lime mudstone separated by 1-3 inches (2.5-6.3 cm) of dark, calcareous, argillaceous-siltstone partings. The lime mudstones have been subjected to extensive calcite neomorphism. Many of the angular detrital-quartz grains have calcite coatings. The middle crinkly zone is 11 ft (3.4 m) thick, with beds up to 12 inches (31 cm) thick and abundant ostracodes and microbial laminations in the upper part of the section. Adjacent to and over the intraformational fold developed in the middle crinkly zone is a 2-4 ft (0.6-1.2 m) thick bed of the upper massive zone which is draped on and over the fold (Fig. 11). The original microfabric was arenaceous, laminated ostracode-lime mudstone with nodular gypsum/anhydrite which is now replaced by void-filling spar calcite and neomorphic microspar with calcite in 10-75 pm size range. The overlying maroon Beclabito Member siltstones and sandstones have a sharp contact with the underlying Todilto Limestone Member.

Section Four and Nine mines 92J-1—The outcrop was measured on a south-facing cliff in the SW¼ SE¼ sec. 4, T12N, R9W. The Todilto Limestone Member is 16.5 ft (5 m) thick, and was studied in outcrops and numerous open pits in sections 4 and 9. The lower platy zone is 4.5 ft (1.4

FIGURE 11—A well-developed intraformational fold exposed in an arroyo on the southwest side of Haystack Mountain. The Todilto Limestone Member section is some 25 ft (7.6 m) thick, rests on the Entrada Sandstone, and is overlain by the Beclabito Member of the Wanakah Formation. The intraformational fold developed in the lower platy zone and is expressed by swelling or mound-like beds. The north side of the upper part of the fold has vertical beds. Ostracode–lime mudstones of the massive zone onlap and cover the fold.

m) thick and contains interbeds of gray sandstone which grade laterally into lime mudstone. The middle crinkly zone is 8.5 ft (2.6 m) thick and is thin-bedded and platy ostracode-lime mudstone. The upper massive zone is 3.5 ft (1.1 m) thick, composed of limestone breccia and lime mudstone, and contains abundant calcite pseudomorphs of anhydrite/gypsum. The upper massive-zone limestone shows extensive evidence of subaerial vadose weathering, karsting, and brecciation preceding the deposition of the overlying terrigenous clastics of the Beclabito Member, Wanakah Formation.

Zia/La Jara mine section 90J-2—The Zia/La Jara mine section 90J-2 was studied in sections 15, 16, and 22 and measured and sampled near the center of sec. 15, T12N, R9W, on a northwest-facing highwall of a bulldozed cut some 50-100 ft (15-30 m) south of a dirt road. The cut is marked on the Thaden et al. (1967) geologic map.

The Todilto Limestone Member is exposed in the Zia/La Jara mine area in continuous outcrop above the Entrada Sandstone and in numerous bulldozed cuts and open pits. The outcrops can be easily walked out and the sedimentary structures observed and studied. The section is 16.5 ft (5 m) thick, composed of arenaceous lime mudstone, and relatively free of calcite neomorphism. The lower platy zone is 6 ft (1.8 m) thick, yellowish brown to gray, and devoid of ostracodes. The middle crinkly zone is 8.4 ft (2.6 m) thick and formed by lime mudstone with microbial laminae, abundant ostracode and calcite pseudomorphs of gypsum, and anhydrite diapir structures. The middle crinkly zone has numerous intraformational folds. The upper massive zone is 2.1 ft (0.64 m) thick, and is ostracode-lime mudstone with microbial laminations and spar-calcite pseudomorphs after gypsum/anhydrite. The top of the Todilto Limestone shows the effects of pre-Beclabito solution activity and vadose weathering. The overlying maroon Beclabito Member silt-stones and sandstones were deposited over an irregular and weathered Todilto surface.

Carbonate particles

The Todilto Limestone Member is typically an arenaceous calcite-lime mudstone with some clay minerals and vague, irregularly shaped clots, pellets, or peloid texture that can grade into neomorphic microspar (Figs. 12, 13). Petrographic and SEM studies of the Todilto carbonate rocks indicate that the primary and original carbonate

depositional constituent was aragonite—lime mud (Figs. 14, 15B, D, F, 16C—F). When the aragonite was exposed to meteoric waters, it was altered by diagenetic process to calcite, micrite, and neomorphic microspar (Figs. 15E, 16A, 17A—C). Extensive petrographic, x-ray, and SEM—EDX studies have failed to reveal any dolomite in the Todilto Limestone in the Grants uranium district.

Origins of Todilto lime mud

Studies by Warren & Kendall (1985) and Warren (1990) on the modern salinas of South Australia have shown the differences in carbonate mineralogy between sabkhas and salinas. Aragonite is the predominate carbonate precipitate in the gypsiferous salinas where the ions for the evaporating salina water are supplied by resurging, chemically unaltered sea water. Dolomite does form, but only as rare, very isolated, localized zones around the extreme periphery of the salina carbonate fringe where waters with a strong meteoric influence seep into the lake. Dolomite is rare in gypsiferous salinas, in contrast to open-marine coastal sabkha deposits where dolomite is a common diagenetic mineral.

Studies on the Miocene evaporative limestones of Sicily have application to understanding the origin of the Todilto lime muds and microfacies. Decima et al. (1988) have developed two basic models which may account for the large amount of evaporative carbonates found in most basins. The simplest depositional model is an evaporative basin which receives continued marine inflow and has reflux circulation during the various phases of evaporative concentration. Biologically induced carbonate precipitation from concentrated sea water is common in euryhaline environments. The precipitation is induced by specialized plants and bacteria which live in extraordinary numbers within restricted hypersaline environments.

A second model by which large amounts of carbonate may accumulate in an evaporative setting is through meteoric-water input from ground water, rivers, streams, and springs into a restricted basin, as in the Dead Sea. This inflow may add considerable quantities of bicarbonate to the waterbody, resulting in greater amounts of carbonate deposition than would occur from sea water alone.

In the Todilto a possible addition to the production of aragonite—lime mud may have occurred by diagenetic alteration of calcium-sulfate precipitates (both gypsum and anhydrite) to form calcium carbonate through the action of sulfate-reducing bacteria (Shearman & Fuller, 1969).

Inorganic precipitation of aragonite may have been the major contributor of lime mud to the Todilto Limestone Member (Shinn et al., 1989). Milliman et al. (1993) found that inorganic precipitation produces much of the aragonite mud on the Bahama Bank and is the only possible source of fine-grained aragonite in the Persian Gulf.

Calcareous microbialites

Aitken (1967), Logan et al. (1974), and Monty (1976) proposed the term cryptalgae for sedimentary rocks believed to have originated through the sediment-binding and/or carbonate-precipitating activities of nonskeletal algae. Although it has been widely used in the literature, the term is here abandoned in favor of the term microbialite.

Microbialites are organosedimentary deposits that have accreted as a result of a benthic-community trapping and binding detrital sediment and/or forming the locus of mineral precipitation. Calcareous microbialites have been traditionally classified as algal limestones because they are produced by benthic microbial communities which commonly contain cyanobacteria, organisms that until recently were termed blue-green algae (Burn & Moore, 1987; Golubic, 1991).

The trapping and binding of detrital sediments produces unlithified but cohesive mound-shaped structures and flat microbial mats (Burn & Moore, 1987). Carbonate deposition is often an integral part of stromatolite formation. The role of microbial activity in this process is not easily determined and remains controversial (Golubic, 1991). These structures have been referred to as stratiform stromatolites, algal mats, and algal laminated sediments.

Microbialite lithoherms include domal laminated types termed stromatolites and nonlaminated types termed thrombolites. Weakly developed stromatolites are found in the upper parts of the Todilto Limestone Member. Planar to crinkly microbialite laminates are abundant in much of the limestone section, in particular in the middle crinkly unit in the area from Haystack Mountain east to the Zia/La Jara area. In their simplest form, these laminations are preserved through an alteration of microstructure formed by vague, clotted peloids composed of 2-6 pm calcite rhombs and small desiccation cracks and fenestrae lined and filled by spar calcite (Figs. 18, 19). Microbial filament tubes were found in association with the calcite-spar pseudomorphs of gypsum in the highest limestones of the Continental Divide section.

Neomorphic processes

Folk (1965) proposed the word "neomorphism" as a "comprehensive term of ignorance" to embrace "all transformations between one mineral and itself *or* a polymorph...whether the new crystals are larger or smaller or simply differ in shape from the previous ones. It does not include simple pore-space filling; older crystals must have gradually been consumed and their place simultaneously occupied by new crystals of the same mineral or its polymorph."

"Aggrading neomorphism is the process whereby a mosaic of finely crystalline carbonate is replaced by a coarser sparry mosaic. It is a complex process combining some of the in-situ processes, namely polymorphic transformation and recrystallization" (Folk, 1965).

The Todilto Limestone Member has changed from originally unconsolidated carbonate sediments (assumed to have been a mixture of aragonite and a range of magnesian calcite) immersed in hypersaline water to a fabric of low-Mg calcite with low porosity. Decima et al. (1988) stated that aragonite is the most common carbonate mineral found in hypersaline environments and is unstable in the presence of fresh water (meteoric). The process of calcitization and recrystallization of the original Todilto aragonite—lime muds probably was a wet (fresh water) polymorphic transformation of aragonite to calcite. This recrystallization was a growth of certain crystals at the direct expense of smaller ones of the same mineral species, and development of neomorphic spar. Bathurst (1971) stated that "the neomorphic process of micrite yields a sparry calcite that is difficult to distinguish from the sparry calcite of cement."

The Todilto Limestone Member was primarily carbonate mud that was subjected to aggrading neomorphism. The micrites originally contained abundant cavities formed by the dissolution of enclosed gypsum/ anhydrite nodules and enterolithic structures, desiccation cracks, rip-up breccias, microbial-mat fenestrae, and cavities within ostracode shells. These cavities are now filled by various types of calcite-spar cements.

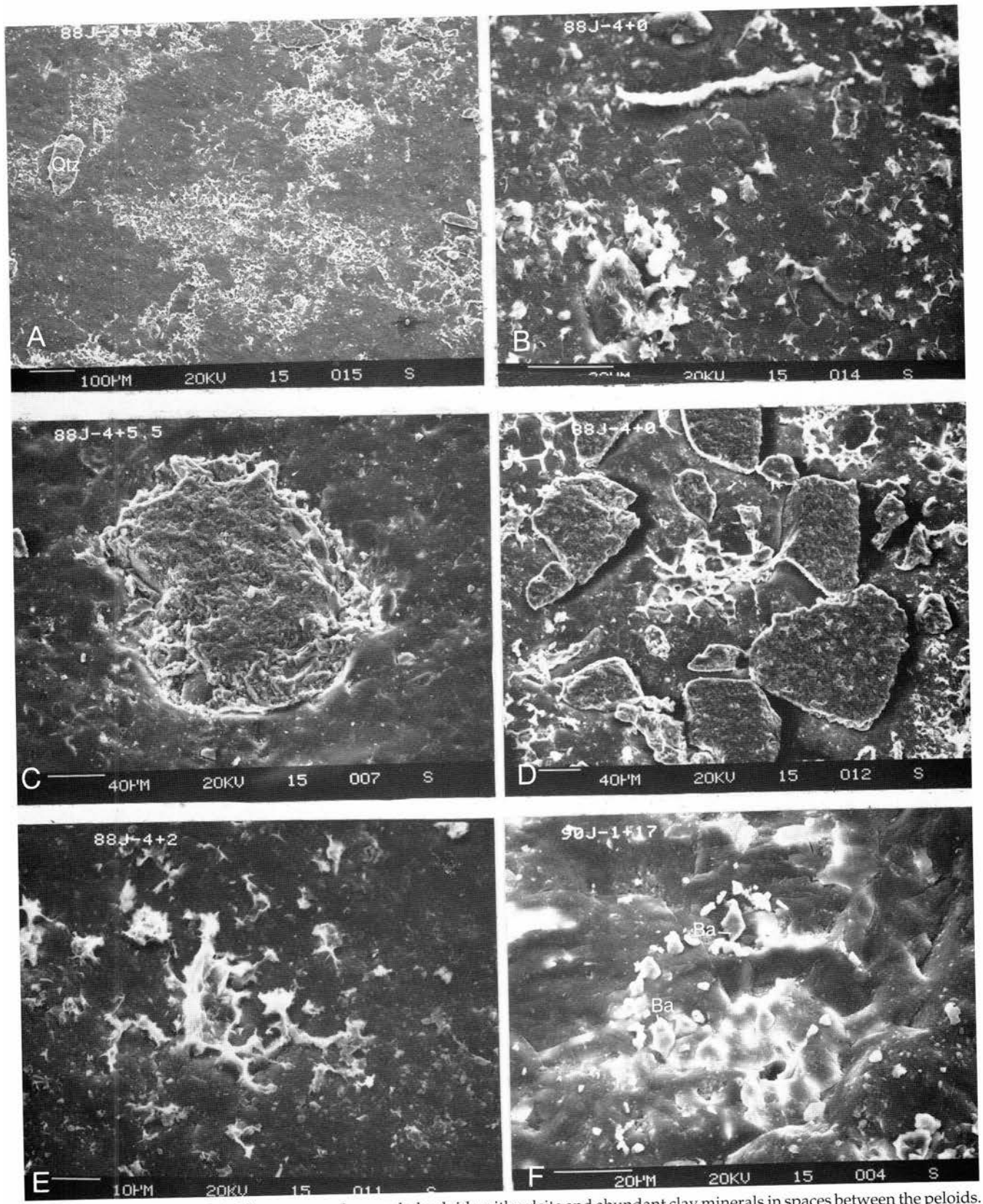

FIGURE 12—All SEM. **A**, Mud lump or poorly rounded peloids with calcite and abundant clay minerals in spaces between the peloids. Angular detrital-quartz grains (100–150 µm, Qtz) are also present. 88J-3+13. **B**, Clay minerals filling spaces between neomorphic calcite crystals. The photo also illustrates the low intercrystalline porosity typical of the Todilto Limestone Member. 88J-4+0. **C**, Detrital feldspar grain embedded in neomorphic microspar. The feldspar grain has a rim of clay minerals thought to be derived from weathering of the feldspar before deposition. 88J-4+5.5. **D**, Arenaceous lime mudstone at the base of Todilto Limestone Member. The photomicrograph shows the angular shape of the detrital-quartz grains and the abundance of clay minerals in the basal limestones above the Entrada Sandstone contact. 88J-4+0. **E**, Clay minerals concentrated between crystal boundaries of neomorphic calcite microspar. Note the lack of porosity in these limestones. 88J-4+2. **F**, Neomorphic calcite microspar with crystals in the 25–50 µm size range (Ba). Barite crystals in the 2–5 µm range are found as inclusions in the calcite crystals. Dejonghe (1990) thought that barium can be trapped in aragonite during early precipitation of marine carbonates and expelled when the aragonite is converted to calcite. 90J-1+17.

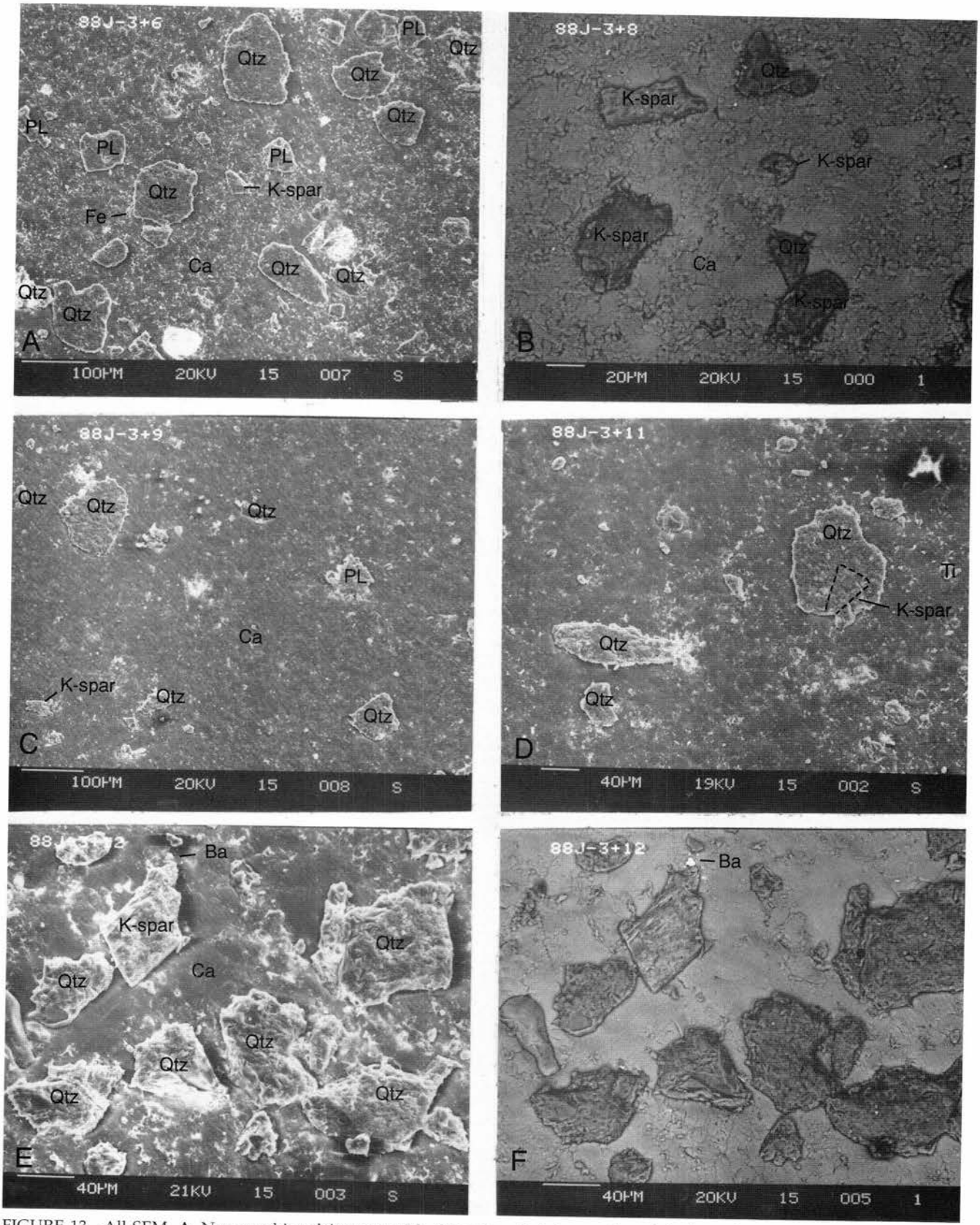

FIGURE 13—All SEM. **A**, Neomorphic calcite spar with clay minerals between the calcite boundaries. Angular detrital-quartz (Qtz) and plagioclase (PL) and potassium-feldspar (K-spar) grains floating in a calcite (Ca) matrix. 88J-3+6. **B**, Background scatter setting. Crystal size of the calcite (Ca) is graphically shown in the photomicrograph. Angular detrital-quartz (Qtz) and potassium-feldspar (K-spar) grains floating in a calcite matrix. 88J-3+8. **C**, Neomorphic calcite spar derived from arenaceous lime mud. Detrital grains are angular fragments of quartz (Qtz), plagioclase (PL), and potassium-feldspar (K-spar) set in a matrix of calcite. 88J-3+9. **D**, Neomorphic calcite spar with some clay minerals and detrital grains of potassium-feldspar (K-spar) and quartz (Qtz). Small grains of detrital rutile (Ti) were also found. 88J-3+11. **E**, Standard SEM photomicrograph of a sample from top of the limestone section below the Beclabito Member sandstones. Increased amount of quartz sand in the calcite matrix is apparent. The angular detrital quartz (Qtz) and potassium feldspar (K-spar) may be of eolian origin. Small grains of barite (Ba) were observed. **F**, SEM background scatter, same as in **E** but with a better view of the crystal surface and boundaries. 88J-3+12.

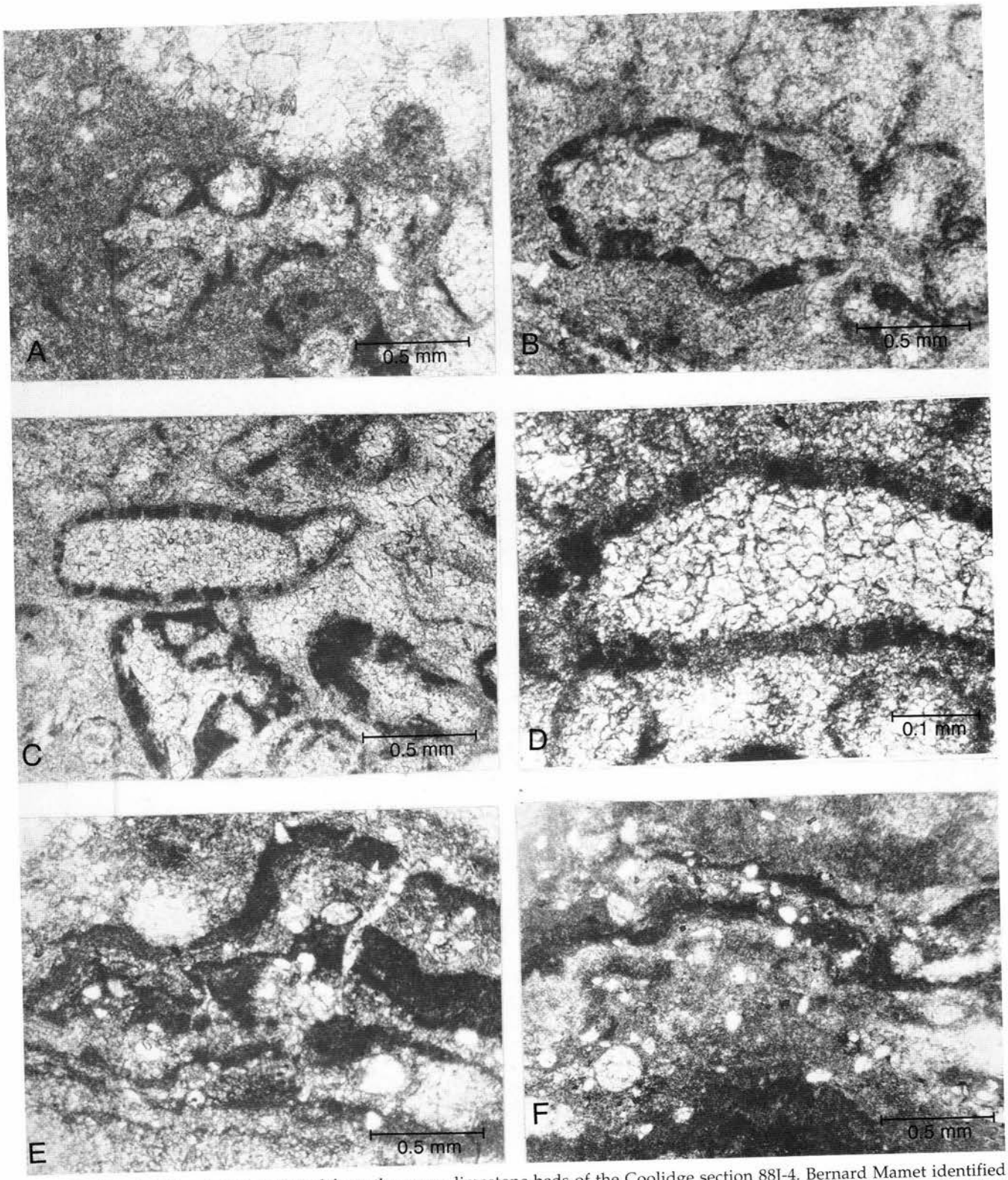

FIGURE 14—**A–D**,Specimens collected from the upper limestone beds of the Coolidge section 88J-4. Bernard Mamet identified abundant ostracodes, scarce dissolved mollusks, and crushed dasyclad algae of the tribe Salpingoporellae. The thallus is cylindrical and appears to have been unramified. Pores are simple and ploiophore. The tribe is abundant from the Jurassic through the Cretaceous. 88J-4+6; plane polarized light. **E, F**, Microbial-mat–ostracode–arenaceous-lime mudstone. Microbial laminations are dark, wavy bands of micritic calcite encased in arenaceous neomorphic microspar. This Todilto microfacies is typical of the higher beds and consists of microbial-stromatolite mats, calcite pseudomorphs after gypsum, and abundant ostracodes, suggesting sedimentation in intermittent gypsiferous ponds or lakes developed on the salina/playa (inland sabkha). During the wet phase ostracodes flourished in great numbers. 88J-3+13; plane polarized light.

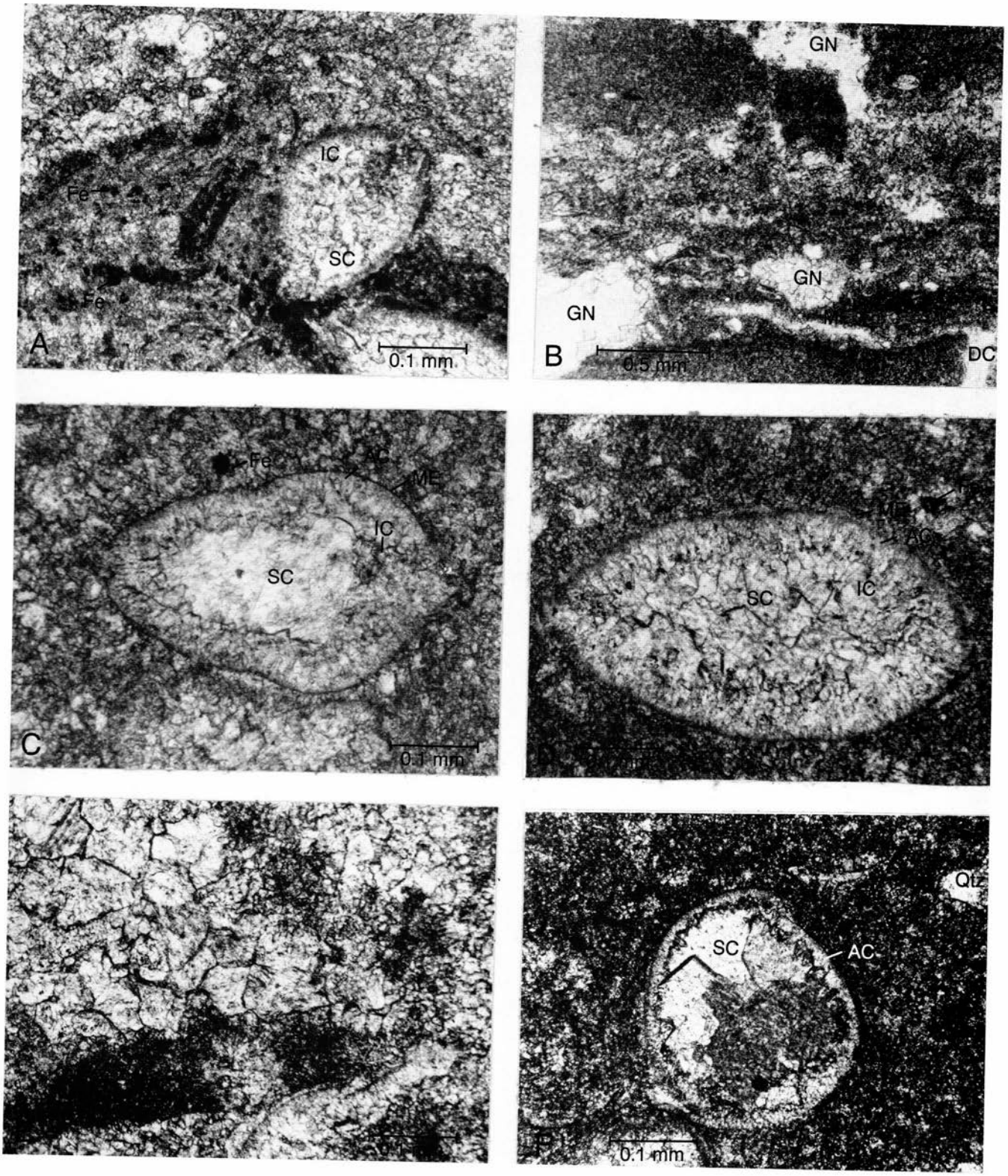

Skeletal grains

Ostracodes are the only abundant fossil bioclasts in the Todilto carbonate rocks (Figs. 15A—D, F, 16C—F). Minor amounts of dasycladacean fragments and vague ghostlike outlines of calcite-filled molluscan molds (Figs. 16A—B) are found in some thin sections from the Coolidge section. Normal-marine invertebrates such as foraminifers, brachiopods, echinoderms, or bryozoans are absent in the Todilto, which clearly indicates abnormal salinities.

Dasycladacean algae

In the upper limestone beds of the Coolidge section, Bernard L. Mamet identified abundant ostracodes, scarce dissolved molluscs, and crushed Dasycladaceae. These are real dasyclads of the tribe Salpingoporellae (Bassoulet et al., 1979), but they cannot be identified down to genus because the complete morphology is not discernible. The thallus is cylindrical and appears to be unramified, and pores are simple and ploiophore. The tribe is abundant in the Jurassic and Cretaceous. Interpretation of the envi-

FIGURE 15—A, Group of ostracode tests enclosed by microbial laminations, with black hematite crystals (Fe) and organic-rich(?) dark material surrounded by neomorphic calcite microspar. The interiors of ostracode tests are lined by acicular-calcite cement followed by isopachous-calcite cement (IC), and the remaining voids are filled by equant-spar cement (SC). This is the microfacies which caps and extends over the intraformational fold structure at Haystack Mountain seen in Figure 11.90J-1+25; plane polarized light. **B,** Upper part of the Todilto Limestone Member at Haystack Mountain. The carbonates were deposited in a gypsiferous salina /playa (inland sabkha) environment. The white areas (GN) are calcite pseudomorphs after gypsum. Sedimentary structures include microbial-stromatolite mats, fenestrae (MF) and desiccation cracks (DC), and lime muds with abundant entombed ostracode tests. The porosity and cavities were filled by isopachous calcite and equant-spar cements. 90J-1+20; plane polarized light. **C-F,** Ostracode valves are abundant in the upper parts of the five sections studied. The tests are generally surrounded by lime mud (micrite) and have a thin micritic envelope. The interior walls are lined by acicular-calcite cement, and the central cavities are filled by blocky calcite spar. Some tests have geopetal crystal silt or are partially filled by micritic muds, while others have been crushed or broken before entombment. Ostracode tests were composed of calcite and their microstructure is well preserved. This is in marked contrast to the poor preservation of the primarily aragonitic ooids and micritic material that form the bulk of the limestones. **C,** Ostracode test showing a thin but well-developed micritic envelope (ME), acicular-calcite cement (AC), isopachous-calcite cement (IC) and the central space filled by equant-spar cement (SC) and hematite (Fe). The matrix was lime mud that has been subjected to calcite neomorphism. 90J-1+16; plane polarized light. **D,** Ostracode test with thin micritic envelope (ME) and acicularcalcite cement (AC) lining the interior, followed by 40-60 pm crystals of isopachous-calcite cement (IC). The center of the test is filled by equant-spar cement (SC). The matrix was lime mud that has been subjected to neomorphic crystal growth. The neomorphic microspar is composed of 10-15 pm calcite crystals with small, scattered areas of hematite (Fe). 90J-1+15; plane polarized light. **E,** An example of incomplete neomorphism in which a mosaic of finely crystalline carbonate is replaced by a coarser sparry mosaic (Folk, 1965). It is a complex process involving in-situ polymorphic transformation and recrystallization. The dark material is relic lime-mud lumps formed by 6-10 pm calcite crystals that have not been subjected to grain growth as extensive as the surrounding matrix. 88J-3+7; plane polarized light. **F,** Ostracode test with a thin acicular-calcite cement (AC) coating its interior; this was followed by void-filling equant-spar calcite (SC). Matrix is formed by calcite-lime mudstone in the 5-10 pm crystal-size range. Some floating grains of detrital quartz (Qtz). 88J-3+8; cross polarized light.

ronment is restricted lagoonal grading to semievaporitic (Figs. 14A—D).

According to Wray (1977), Barattolo (1991), and Flügel (1991), extant dasycladaceans most often occur in tropical and subtropical marine waters. As a group they seem to prefer normal-marine salinities, but the Acetabularieae, for example, tolerate wide temperature variations and salinities ranging from hypersaline to brackish.

Ostracodes

The relatively abundant ostracodes [assumed to be *Metacypris todiltensis* (Swain)] are supposedly a brackish-water species unique to the Todilto Limestone Member. Swain's (1946) type material was collected by R. H. Wilpolt and **J.** B. Reeside, Jr., 6 mi north of Thoreau on NM Highway 57, probably near to, and on strike with, the section at the Billy the Kid mine. Kietzke (1992) reassigned this Todilto ostracode to the genus *Cytheridella.*

Ostracode valves are abundant in the upper parts of the outcrop sections studied (Figs. 15A—D, F, 16C—F). The tests are generally surrounded by lime mud (micrite) and have a thin micritic envelope on their exterior and interior surfaces. The interior walls of the valves are lined with acicular-calcite cement, and the central cavity is filled by blocky calcite spar. Some tests have geopetal crystal silt or are partially filled by micritic muds. Some valves have been crushed upon entombment. Ostracode tests were formed as calcite, and their microstructure is well preserved. This is in marked contrast to the poor preservation of the original aragonite ooids and aragonite—lime mud that have suffered dissolution and neomorphic grain growth, and are now calcite.

Logan (1987, p. 21) found in the MacLeod evaporite basin, Western Australia, that "gypsum-pond assemblages are reduced to cyanobacteria and ostracodes with seasonal colonization by seagrasses, green algae and fish."

The ostracodes are envisioned to have lived in profusion during times of expansion of the cyclic ephemeral Todilto saline lake.

Compound grains

Grains with compound architecture or an uncertain, multigenetic origin are grouped in this category. They can be divided into pellets, peloids, and ooids, with a range of gradations between these end members; many are semirounded. Interclasts, although grouped as detrital grains, are commonly compound in internal architecture (Reijers & Hsu, 1986).

Pellets, peloids, and ooids

The term peloid was originally introduced by McKee & Gutschick (1969) to describe ovoid particles of aphanitic limestone, believed to have been largely derived from rocks currently forming nearby. The term is now taken to mean aggregates of micrite limestone of unknown origin (MacIntyre, 1985). The term pellet is generally applied to pellets of fecal origin, as indicated by a characteristic shape.

In the study area, the Todilto contains lime mudstones to packstones that are composed of mud lumps (Figs. 12A, 15A, B, E), pellets, peloids, ooids (Figs. 16A, 17A—C) and quartz sand grains which are coated by fibrous calcite (Figs. 17E—F). Many of the lime mudstones still retain the vague outline patterns of former peloid packstones (Fig. 17E).

The ooid grains have had a complex diagenetic history as a result of having been formed primarily of aragonite with varying amounts of calcite and then subjected to meteoric waters, partial dissolution, and neomorphic re-crystallization to calcite (Fig. 20). Texture and fabric similar to those found in the Todilto ooids have been described by other workers studying Phanerozoic ooids (Sandberg, 1975; Wilkinson et al., 1984) and Precambrian ooids (Tucker, 1984; Singh, 1987). The Todilto ooids are 0.6-0.8 mm in diameter, and their center usually contains an angular detrital-quartz grain on which the carbonate nucleated. A typical Todilto ooid has neomorphic fabrics that range from incipient microspar in the outer layers to a coarse mosaic of spar calcite in the center. In the least neomorphosed ooids the crystals are somewhat equigranular and toward the periphery have relic concentric bands or rings. The rims of the ooids are typically 100-200 pm thick and contain relic concentric banding preserved by 10-30 pm crystals of neomorphic calcite that forms the outer layers of the ooids. Most ooids have centers that were dissolved and later filled by blocky spar calcite. This

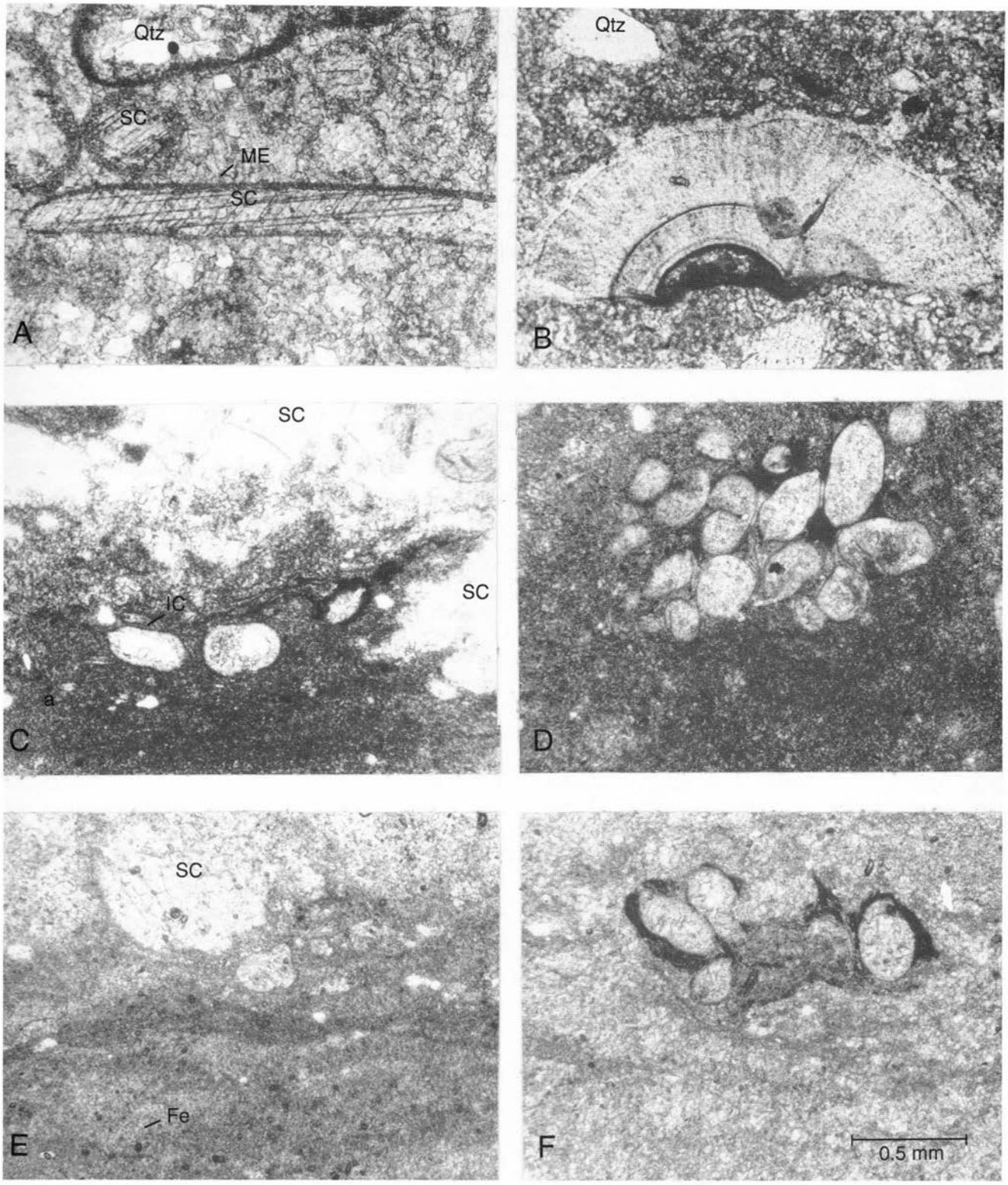

suggests a micrite center composed of aragonite which was dissolved and the voids filled by spar calcite. Dissolution of the center and cementation by spar calcite are also suggested by the geopetal orientation of the detrital-quartz grain, which has fallen to the lower part of the spar-filled center (Figs. 16A, 17A). The ooids are set in a matrix of cloudy, inclusion-rich calcite rhombs 50-100 pm across (neomorphic spar).

Tucker (1984) found it difficult to explain the origin of mixed calcite and aragonite ooids in the Proterozoic Belt Supergroup, and similar questions apply to the Todilto ooids. Modern marine ooids normally are all aragonite. Land et al. (1979) described from Baffin Bay, Texas, a lagoon which is generally hypersaline but can be fresh to brackish water after a hurricane. The Baffin Bay ooid nuclei are primarily quartz with minor amounts of skeletal allochems. Ooids with cortical layers of aragonite and high-Mg calcite are being precipitated, but the factors controlling ooid mineralogy are not known. The rate of nucleation and precipitation, degree of agitation, and presence of certain types of organic compounds appear to be the most likely factors.

FIGURE 16—A, Ooid-molluscan arenaceous packstone. The carbonate sediment, which was primarily aragonite, has undergone extensive fresh-water dissolution, calcite-cement void filling, and polymorphic transformation and recrystallization. Neomorphism is evident in the ooids and the matrix which are now composed of calcite crystals (SC) in the 50-150 pm range. The large linear object is a micritic-envelope (ME) mold of an originally aragonitic molluscan shell filled by equant-spar calcite (SC). 88J-4+5; plane polarized light. **B,** Section through a fragment that may possibly be the fragmocone of a belemnoid cephalopod. Matrix is neomorphic microspar with angular fragments of detrital quartz (Qtz). 88J-3+7; plane polarized light. C, Ostracode-lime mudstone with faint microbial-stromatolite mat laminations. Equant-spar (SC) white areas are calcite pseudomorphs after gypsum. The lime mudstone is composed of calcite crystals in the 10 pm range. The lime muds originally contained abundant cavities formed by the dissolution of enclosed gypsum nodules, desiccation cracks, rip-up breccias, microbial-mat fenestrae, and cavities within ostracode tests. These cavities are filled by isopachous-calcite cement (IC) and equant-spar cement (SC). 88J-3+13; plane polarized light. **D,** Arenaceous ostracode-algal-lime mudstone. Cluster of ostracode tests is bound by dark microbial material apparently rich in organics and disseminated hematite. The tests are filled by isopachous-calcite cement and minor amounts of equant-spar cement. 901-1+20; plane polarized light. E, Arenaceous ostracode-lime mudstone. Weakly developed microbial laminations. Calcite pseudomorphs after gypsum and cavities with ostracode tests are filled by equant-spar calcite. Dark spots are concentrations of hematite (Fe). The calcite in the lime mudstone has not been subjected to extensive grain growth. 90J-1+21; plane polarized light. F, Ostracode-microbial-mat-lime mudstone. Ostracode tests are bound together by dark, organic-rich, hematitic, microbial material. The original lime mud has been converted by neomorphism to a matrix composed of 20-40 pm size calcite crystals. Faint images of microbial laminations can be seen. 90J-1+25; plane polarized light.

The texture of the Todilto ooids suggests that they were an original mixture of calcite and aragonite. This mineralogy most likely resulted from reworking of ooids from different sites. These Jurassic salina oolite beds could reflect water traction transport and mixing of sediments from several sources by storms and currents, and also by wind transport across playa flats.

Larger coated grains, such as grapestone, pisoids, and oncoids, have not been found in the Todilto Limestone Member of the Grants uranium district.

Carbonate cements

Bathurst (1971) stated that ooids are the most obvious example of precipitation on a grain surface, and hardened fecal pellets are products of cementation within a loosely bound mixture of carbonate mud and adhesive organic material. Both aragonite and high-Mg calcite cements filled the deserted boreholes of dead endolithic algae in carbonate grains of lime sand, forming the dark micritic envelopes.

Micritic envelopes

Micritic envelopes are found on the carbonate allochems in the study area. A two-step process of micritization has been documented by Bathurst (1971). The micrite envelope is believed to form largely as a result of the precipitation of carbonate in discarded microbial bores.

Micritic envelopes are common on the outer surfaces of ostracode shells (Figs. 15A, C, D) and as dark bands on and in ooids (Figs. 16A, 17A—C). The relict concentric micritic bands are evidence that these poorly preserved circular bodies were ooids prior to calcite neomorphism. Similar reasoning is used to identify peloids, which are now typically only outlines of clots with circular micritic envelopes. Most of the peloids have been obliterated by neomorphism and by the development of microspar during the transformation from aragonite to calcite.

Acicular-calcite cement

This is cement consisting of radially arranged needle-like crystals. It is characteristically 30-90 pm thick and the individual crystals are bladed with scalenohedral terminations. Shinn (1969) found in Recent sediments of the Persian Gulf that acicular cement forms as aragonite and high-Mg calcite. Prezbindowski (1985) thought acicular cement formed as high-Mg calcite and was marine in origin. In the Todilto Limestone Member, isopachous bladed cement is found as the first cement lining the inside and outside walls of ostracode shells (Figs. 15A, C—F), desiccation cracks, fenestral cavities of stromatolite microbial mats, and calcite-filled gypsum/anhydrite pseudomorphs preserved in the lime mudstones.

Drusy dogtooth cement

This is a variety of sparry-calcite cement in sharply pointed crystals of acutely scalenohedral shape resembling dog teeth. Drusy dogtooth cement is found on the interior lining and in the centers of peloids, vugs, microbial-mat fenestrae, ostracode shells, and as coating on detrital, angular quartz and feldspar grains (Figs. 15C, D, F, 17D, F). This cement nucleates on pore wall, earlier bladed isopachous cement, internal sediments, or crystal silt, and is prevalent on the surface of detrital-quartz grains. It is also a pervasive isopachous cement filling the voids, the leached centers of ooids, and spaces between particles in peloid—ooid packstones and grainstones.

Equant-spar calcite cement

Fine to very coarsely crystalline (16 pm to 4 mm) equant-spar calcite cements (drusy mosaic or isopachous cement in Reijers & Hsü, 1986) are volumetrically the most important cement types in the Todilto. This cement fills the voids in ostracode shells (Figs. 15A, C, D, F), molds of molluscan shells (Fig. 16A), calcite pseudomorphs after gypsum/anhydrite (Fig. 16E), desiccation cracks (Fig. 14E), leached voids in the centers of ooids (Figs. 16A, 17A—C), and microbial-mat and stromatolite fenestrae (Figs. 14E, F, 19A, **B).**

According to Prezbindowski (1985), equant-spar calcite develops in two general sequences. The most common is one in which crystal size increases at a more or less uniform rate toward the center of the filled pore along with a corresponding increase in the number of straight crystal boundaries and triple junctions. The second, less common sequence consists of a bimodal population of equant-spar calcite cement crystals. The sequence is typified by an early, fine to medium crystalline equant-spar calcite with irregular crystal boundaries and a sharp transition to well-defined linear crystal boundaries.

Diagenetic minerals

Dolomite

In the Grants district dolomite has not been observed in any of the thin sections, SEM and energy-dispersive x-ray (EDX) analyses, or x-ray studies. However, Ridgley

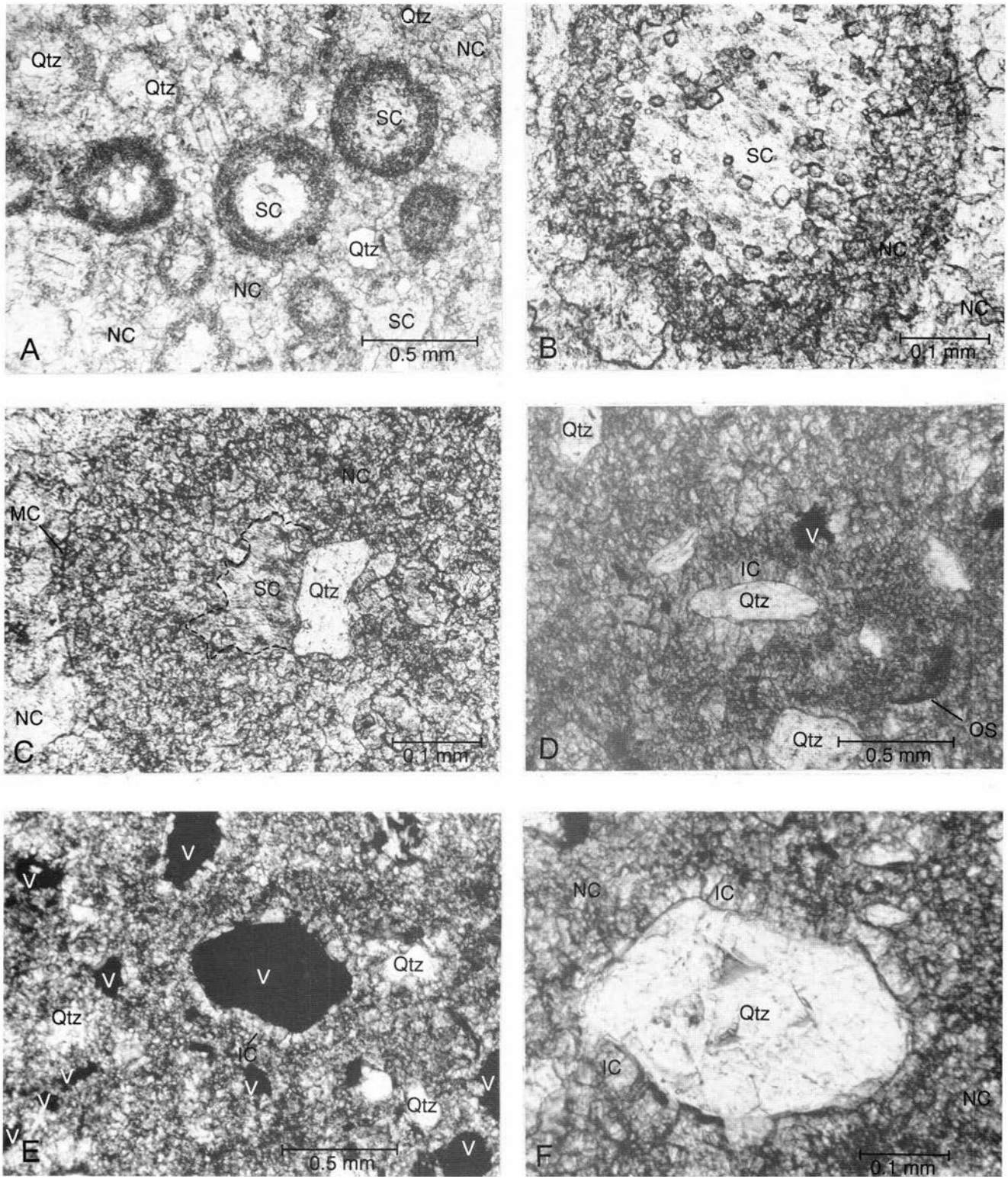

(1986) reported dolomite from the Todilto Limestone Member in the Chama Basin some 100 mi (161 km) northeast of Grants. The dolomite occurs as remnant patches in micrite and microspar matrix. The limestones in the Chama Basin are associated with gypsum beds, and the carbonates have many features suggestive of intertidal-supratidal environments.

Hematite

Hematite pseudomorphs after pyrite are found in the lime mudstones (micrites) (Figs. 13A, 15A, C), in the neomorphic calcite spar, in close association with the ostracode shells, and often concentrated along and in stylolites. It is abundant parallel to the laminations in the middle crinkly zone, often staining the outcrops rusty brown. The presence of cubic hematite after pyrite indicates development in reducing conditions below the water—lime-mud interface. Love et al. (1984) demonstrated the importance of organically derived and organically reduced sulfides in the formation of framboidal pyrite in sediments.

Hematite after pyrite was observed in all the thin sections studied and occurs as 5-50 pm bodies and clusters. Aggregates of hematite only 5-10 pm across are found

FIGURE 17—A, The ooids are 0.6-0.8 mm in diameter and generally have at their center a detrital-quartz grain (Qtz) on which the carbonate nucleated. Many ooids show evidence of aragonite centers which were later dissolved and the spaces filled by spar calcite (SC). The rims of the ooids are typically 100-200 pm thick and contain relic concentric bands preserved by 10-30 pm size crystals of neomorphic calcite (NC) that form the outer layers. The ooids are set in a matrix of cloudy, inclusion-rich, neomorphic calcite spar with crystals in the 50-100 pm range. 88J-4+5; plane polarized light. **B,** Enlargement of a relic ooid that is outlined by poorly defined concentric bands of smaller, darker, neomorphic-calcite crystals (NC). The center of the ooid has been dissolved and is filled by a large, inclusion-rich crystal of spar calcite (SC). The matrix is also neomorphic calcite. 88J-4+5; plane polarized light. **C,** Enlargement of a typical ooid with a detrital-quartz grain (Qtz) forming a center. The center has been partially dissolved and the void is filled by a spar-calcite crystal. The shell of the ooid is now formed by microspar that is composed of darker and smaller crystals than the surrounding microspar (MC) matrix. The poor preservation of this ooid is typical for the Todilto Limestone Member in the Grants district. 88J-4+5; plane polarized light. **D,** Vuggy (V) packstone with extensive neomorphic microspar. It has a clotted grumous-like fabric that suggests the microfacies was a packstone composed of pellets, peloids, and possibly ostracode tests (OS), and also contained detrital-quartz (Qtz) sand-size grains coated by isopachous calcite (IC). The isopachous-calcitecement coatings on many of the angular detrital-quartz and feldspar grains are one of the most diagnostic features of the Todilto Limestone Member in the Grants district. In much of the microspar the former lime-mudstones (micrite) matrix can be discerned by the vague or ghost patterns of former peloids. 90J-1+1; cross polarized light. **E,** Vuggy limestone near the base of the Todilto Limestone Member. Vugs (V) are thought to have been formed by the solution of aragonite peloids; a rim of isopachous-calcite (IC) cement that was on the surface of the peloids now lines the cavities. Neomorphism has converted the lime mudstone to microspar. White spots are detrital-quartz (Qtz) grains. 90J-1+1; cross polarized light. F, Enlargement of a detrital-quartz grain (Qtz) coated by isopachous-calcite cement (IC) and encased in a neomorphic calcite-spar matrix (NC) derived from lime mud. 901-1+17, plane polarized light.

concentrated on the outer surface and within the walls of ostracode valves. This is thought to be related to the higher concentration of organic matter associated with the tests. In the Zia/La Jara mine area the middle crinkly zone may be stained reddish brown by hematite that was leached from the microbial-mat laminations and the fenestrae. The iron oxides are derived from pyrite that was deposited in the organic-rich microbial mats in the wet playa surface. This interpretation is supported by Golubic's (1991, p. 546) studies of modern stromatolitic mats. He found that below the layer of blue-green algae is a layer of purple sulfide bacteria which is followed by layers in darkness dominated by fermenting decomposers and possibly methanogens. Excess H2S is bound in a black FeS precipitate, which diagenetically recrystallizes into pyrite.

Barite

SEM studies of limestone sample 901-1+17 from the Haystack Mountain section (Fig. 12F) and sample 88J-3+12 from Billy the Kid quarry (Figs. 13E, F) have 5 pm crystals of authigenic barite as inclusions in calcite crystals. Dejonghe (1990) studied Frasnian sedimentary barites in carbonate rocks of Belgium and concluded that barium could be trapped in aragonite during early precipitation of marine carbonates and expelled when aragonite was converted either to calcite or dolomite, or barium ions could also be derived from submarine hot springs, possibly in connection with magmatic activity. The Todilto uranium deposits contain abundant barite and fluorite. Emanuel (1982) considered the "hypogene" event to be "early" and implied a Laramide age, but did not cite much evidence.

Detrital grains

Clays

SEM studies have shown that clay minerals occur in the limestones between crystal boundaries of calcite (Figs. 12B, D, E). A typical specimen 88J-3+13 from Billy the Kid quarry is a mud-lump peloid packstone with the space between the mud-lump peloids filled by calcite microspar and clay minerals concentrated between the crystal boundaries (Fig. 12A).

Detrital-quartz and feldspar grains

Angular and subangular detrital-quartz and feldspar (orthoclase and plagioclase) grains are ubiquitous in the limestones of the Todilto. They vary in abundance from bed to bed but are more abundant in the lower horizons and show little evidence of corrosion. These grains are generally associated with clay minerals and are believed to be primarily of eolian origin (Figs. 12C, D, 13A—F).

Chert

Outcrop studies indicate that the Todilto Limestone Member is devoid of bedded or nodular chert in the Grants uranium district. Thin-section studies show that silicification or the replacement of carbonates by chalcedony is very rare.

Replacement of spar-calcite crystals by chalcedony was observed in the centers of calcite pseudomorphs of gypsum at the top of the Zia/La Jara mine section. The chalcedony appears to have developed in the capping caliche in the upper massive zone.

X-ray studies by Christopher McKee

Twenty-one thin-section billets and powdered samples were analyzed qualitatively by x-ray diffraction. A Rigaku powder diffractometer equipped with a long, fine-focus copper tube and a graphite monochromator were used for analysis.

Most of the samples are calcite with traces of quartz, and only a few contain feldspar, either plagioclase or potassium feldspar, or both. The most interesting result of this x-ray study is the total absence of dolomite.

The field samples with stratigraphic location numbers are listed in the results (Table 1). The stratigraphic levels of the specimens in each section above the Entrada Sandstone are graphically shown in Figure 4.

Carbonate depositional structures

Layering: Origins and depositional environments of Todilto laminations

Hardie & Ginsburg *(in* Hardie, 1977, pp. 50-123), in their studies of the carbonate sedimentation of Andros Island, Bahamas, demonstrated that "the type of layering and its associated structures are a very sensitive record of the depositional subenvironment in which they are formed."

The most characteristic feature of the Todilto carbonates is the varied but persistent types of laminations (Figs. 18, 19A—E). Anderson & Kirkland (1960), Anderson (1982), and Anderson & Dean (1988, p. 227) interpreted the laminations in the limestone and gypsum units as varves in

Table 1—X-ray diffraction analysis of mineralogy. B = billet samples, P = powdered samples, X = major phase, M = minor phase, tr = trace phase, ? = questionable identification.

Sample number	Sample type	Calcite	Quartz	Plag.	K-Spar
88J-3+0.5	B	X	M	—	—
88J-3+3	P	X	tr	—	—
88J-3+5	B	X	X	—	tr?
88J-3+6	P	X	tr	—	—
88J-3+8	P	X	tr?	—	—
88J-3+9	P	X	tr	tr	—
88J-3+11	P	X	tr	—	—
88J-3+12	P	X	tr	tr	tr
88J-3+14	P	X	X	—	—
88J-4+0	P	X	M	tr	tr
88J-4+1	P	X	X	tr	tr
88J-4+3	B	X	M	—	—
88J-4+5	B	X	tr?	—	—
88J-4+5.5	P	X	tr?	—	—
88J-4+6	P	X	tr?	—	—
90J-1+1	P	X	tr	—	tr?
90J-1+8	B	X	tr	—	—
90J-1+10	P	X	tr	—	—
90J-1+21	P	X	tr?	—	—
90J-1+22	P	X	—	—	—
90J-1+25	P	X	tr	—	—

cyclic sequences and believed they were related to 10-13 year and longer period sun-spot cycles.

Rawson (1980) attributed the laminations of the lower platy zone to sedimentation in poorly circulated basin waters below wavebase and devoid of life. He thought the middle crinkly zone was formed in algal (microbial mat) flats which were frequently exposed and desiccated. The deposition of the overlying upper massive zone occurred in the supratidal zone where algal (microbial) lime muds and gypsum were interbedded and later, through meteoric ground water and solution of the gypsum, formed breccias.

In modern salinas /playas most of the fine carbonate crystals are formed by evaporation (Dean & Anderson, 1982; Warren & Kendall, 1985). In permanent to perennial saline lakes layering results from seasonal or climatically controlled variations in water inflow, temperature or evaporation rates, and non-periodic events such as the influx of storm-generated waters (Kendall, 1984; Bell, 1989).

Reese's (1981) studies in northeast and southeast San Juan Basin show eolian-transverse-dune buildup in the upper Entrada perpendicular to the dominant wind directions shown by crossbed foresets. Some bevelling of the sand occurred prior to the deposition of limestone and gypsum. In the Grants region, Todilto carbonate sedimentation began with flooding, some wave cutting and filling of the irregular Entrada sand-dune surface, and the development of a large marine-influenced Salina/ playa with an exceedingly impoverished biota and no infauna. The preservation of the laminations in the lower platy and middle crinkly zones and the lack of evidence of bioturbation by a burrowing infauna indicates a very inhospitable environment. The lower platy zone has large, well developed mudcracks, which are similar to those illustrated by Shinn (1983, figs. 8A, B) from thick algal mats at Inagua Island in the Bahamas and from algal mats on tidal flats of the Trucial Coast in the Persian Gulf, and disrupted flat laminations and flat-pebble gravel described by Hardie & Ginsburg *(in* Hardie, 1977) from the algal marsh of Andros Island, Bahamas (Figs. 9, 27C). Butler et al. (1982, fig. 16) illustrated Recent salt polygons in the supratidal deposits of Abu Dhabi, Trucial Coast, that are similar to those of the basal Todilto Limestone Member. The laminations in the lower platy zone are the result of lime-mud deposition by traction. The laminations are of irregular thickness and in length, are terminated by small-scale erosional structures, and contain abundant evidence of desiccation (Fig. 26A). In the area of this study the lower platy zone represents carbonate sedimentation in a shallow, ephemeral salina /playa (inland sabkha).

Weathered outcrops of the middle crinkly zone (Fig. 18) also display thin but wavy laminations. Study of polished rock surfaces and thin sections (Figs. 19A—D) shows millimeter-thick disrupted flat laminations with intraclast chips, crinkly and wavy fenestral laminations with desiccation cracks and chips, and spar-calcite pseudomorphs after nodular gypsum/ anhydrite and cumulous enterolithic structures (Figs. 19C, D). The fenestrae and the desiccation pull-aparts between the lime-mudstone layers are filled with white spar calcite (Figs. 19A, B). These sedimentary features are similar to those illustrated by Davies (1970, fig. 10) as "intra-laminar shrinkage polygons" from the Recent supratidal sediments of Shark Bay, Western Australia, and Hardie & Ginsburg's *(in* Hardie, 1977, figs. 43, 67) "crinkled fenestral lamination" from the Recent supratidal zone of Andros Island. In contrast to the the relatively flat laminations of the lower platy zone, the laminations of the middle crinkly zone are probably the result of a much higher original organic content of the dark bands (R. N. Ginsburg, written comm. 1994). The size range of structures extends from millimeter-size folded microbial-mat laminations through centimeter-size ptygmatic—enterolithic structures to tens of meters large intraformational folds.

Shinn et al. (1969) and Hardie (1977) conducted studies at Andros Island and demonstrated that in the high intertidal and supratidal deposits each millimeter-thick lamina is a storm layer, whereas in an ephemeral-salina (inland sabkha) subenvironment the layers probably represent a recharge of the salina by runoff and/or reconnection to the Curtis Sea.

Diagnostic evaporative sedimentary features in the middle crinkly zone are calcite pseudomorphs of gypsum/ anhydrite chicken-wire texture and enterolithic structures (Figs. 19C, D, 27B). Laminated contorted anhydrite diapirs (ptygmatic—enterolithic structures) are found in the Section Four and Nine open pits, the Zia /La Jara mine outcrop, and the extensive outcrops east of Haystack Mountain (Figs. 21, 22, 25). The gypsum/anhydrite chicken-wire textures and diapiric structures grew displacively in the sediments in a capillary zone between the top surface of playa-derived saline water table and the surface of the playa flats. The anhydrite nodules and diapiric/enterolithic structures were precipitated from

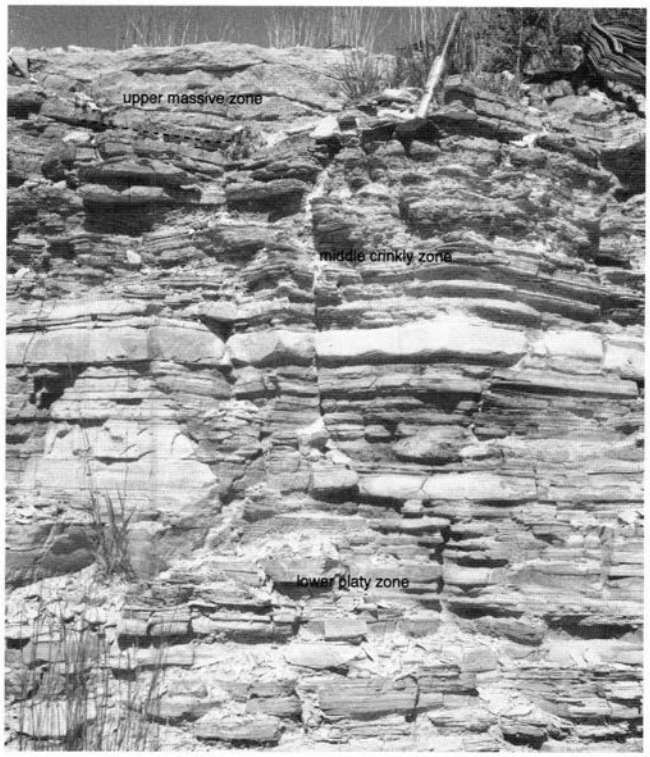

FIGURE 18—A weathered exposure of the lower platy and middle crinkly zones, Todilto Limestone Member. Natural etching of the bedding surfaces accentuates the fissile nature of the limestone partings, which results from the micromillimeter bedding induced by the concentration of clay- and silt-size particles in the lime mudstone. In the open-pit mines, fresh surfaces of the middle crinkly zone have a solid and massive appearance. See Figures 35, 38, 39. Sledge hammer for scale. Section Nine mines.

sauna /playa-derived ground-water brines. Above the saline water table and within the interstitial lime muds in the playa sediments these gypsum/anhydrite fluids became more concentrated, and gypsum/anhydrite crystals grew as a result of capillary movement and evaporation. Upper surfaces of some of the Todilto diapir structures are truncated (Figs. 22A, 25A), indicating that contemporaneous playa deflation surfaces formed before deposition of the overlying beds (see Shinn, 1983, figs. 38-41, from the Trucial Coast). Surface trenches in the Recent supratidal sediments of Abu Dhabi (Shearman, 1981, pls. 16-17; Butler et al., 1982, fig. 16) show diapiric layers of anhydrite which have a structure similar to those of the Todilto middle crinkly zone (Figs. 21, 22, 25). The Todilto spar-calcite pseudomorphs after diapiric structures can be laterally continuous into intraformational conglomerates composed of broken limestone clasts that were formed by the dissolution of anhydrite in the diapirs (Figs. 22A, B, 25B). The middle crinkly zone also contains well developed calcite pseudomorphs after anhydrite-gypsum mush (Figs. 19C, D). Similar sedimentary structures are known from the modern sabkha of Abu Dhabi (Butler et al., 1982, figs. 7-15).

The limestones of the upper massive zone are microbial mats and ostracode-lime mudstones. The sedimentary structures are desiccation cracks, chips, abundant spar calcite pseudomorphs after nodular gypsum-anhydrite, and solution breccias. The top of the zone is characterized by spar-calcite pseudomorphs of anhydrite (chicken-wire texture) and gypsum-anhydrite mush (Figs. 6, 8, 19E). Sedimentary structures and facies relationships indicate that the upper massive zone was deposited in the final phase of drying and evaporation of the Todilto salina. Field studies show that the upper massive zone can laterally grade into the middle crinkly zone (Figs. 35, 38, 39).

Layering and laminations are not as well developed or as conspicuous in the upper massive zone. Sedimentary laminations were interrupted by the growth of gypsum/anhydrite nodules (Figs. 6, 8, 19E) in the capillary zone above the saline water table. The nodules were disolved by vadose fresh water before deposition of the overlying Beclabito Member. The dissolution of the gypsum/anhydrite nodules and their replacement by spar calcite, the development of a karsted surface, and extensive areas of calcite recrystallization and brecciation combined to obscure the original sedimentary structures in the upper massive zone. The carbonate rocks of this zone are overlain by red beds of the clay-quartz sand clastic sequence of the Beclabito Member, which is a marginal-lacustrine and playa deposit that grades southward into fluvial deposits.

Alsharhan & Kendall (1994, fig. 7) illustrated a core from the Holocene carbonate and evaporite facies belt of the Abu Dhabi sabkha, which is very similar lithologically to the Todilto sequence. The sedimentary structures of their lower tidal-flat lime mudstone with gypsum are similar to the lower platy zone of the Todilto, their "crinkly" algal peat is similar to the Todilto middle crinkly zone, and their anhydrite-after-gypsum mush is similar to the Todilto upper massive zone.

Intraformational folds in the Todilto Limestone Member

Intraformational folds are present north and west of Grants in the Ambrosia Lake mining district (Green, 1982), from the west flank of Mount Taylor westward across the Zia /La Jara mine area and the Sections Four and Nine mines (Figs. 10, 11, 23, 24, 30-31, 33-39), and in the outcrops west of Haystack Mountain (Fig. 11). The folds are associated with salina /playa sedimentary structures. These are desiccated crinkly microbial mats with chips and gypsum pseudomorphs of gypsum, calcite pseudomorphs of supratidal gypsum mush, and anhydrite diapirs/ enterolithic structures. Intraformational folds vary considerably in size and shape. The Todilto folds are typically asymmetrical and range from simple structures 12 inches (0.3 m) high and a few feet wide to complex mounds up to 10 ft (3 m) high and 45 ft (14 m) wide. Some are simple mounds or dome-like structures that are roughly concentric and equidimensional, while others have clearly defined axial trends and are hundreds of feet long. They are generally represented by thickened or mound-like beds in the lower **platy** zone (Figs. 11, 29). W. R. Berglof (written comm. 1994) observed that many of the intraformational folds he saw in the underground mines during the 1960s (now inaccessible) were also developed, at least in part, in the platy zone.

The folds can project into, and/or are onlapped by, the upper massive zone. Within the folds the beds are often bent over or brecciated in a curve with one side much steeper than the other (Figs. 11, 28, 29A, 30), and fracturing is common (Figs. 23-24, 28, 29, 30-32). Fracturing and distention of beds in the folds are greatest where dips are nearly vertical (Figs. 23, 24, 28-38). The flanks of some folds exhibit penecontemporaneous soft-sediment slumping within the lime mudstones of the middle crinkly unit

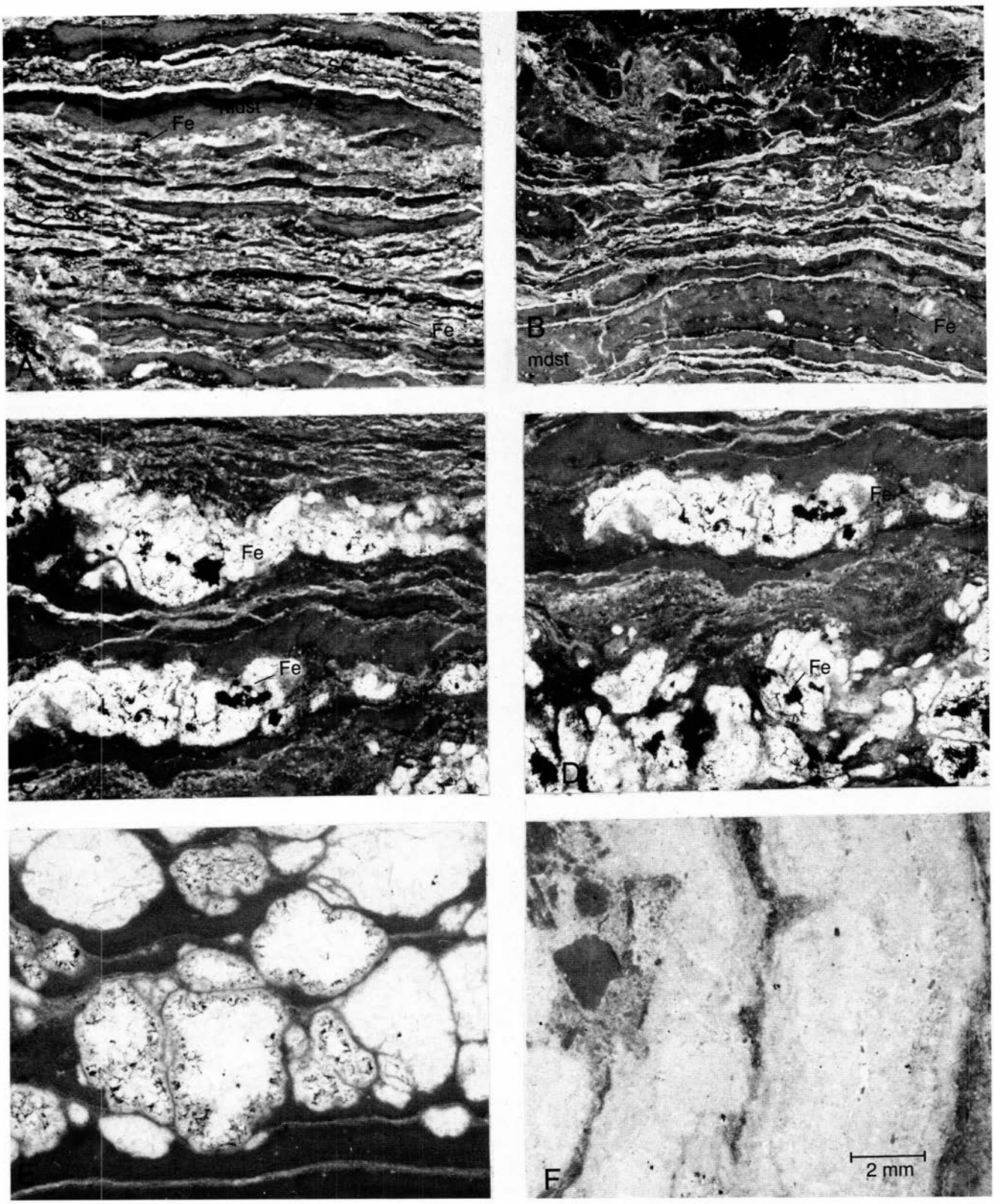

(Figs. 23, 24, 32), and the tops of the folds may be eroded or truncated (Figs. 28, 29A), but are also onlapped and buried by ostracode—lime mudstone of the upper massive zone (Figs. 11, 23). A nearly symetrical fold with a curved, wedge-shaped cross section and inward dipping 45° fracture zone is exposed on Haystack Mountain (Fig. 29B).

Almost all of the folds have a fracture zone or fault surface which may be horizontal to nearly vertical. The faulted or fractured limestone indicates that the lime mudstones were partly cemented and lithified before folding.

The intraformational folds in the Todilto Limestone Member show considerable range in their development and morphology. A natural outcrop in the Zia /La Jara mine complex (Fig. 33) displays a fold that is composed of penecontemporaneous soft-sediment breccia fragments that contain fragments of calcite pseudomorphs of anhydrite diapirs/enterolithic structures. These brec-

FIGURE 19—Photomicrographs (plane light, same scale) of sedimentary structures in the crinkly and massive zones. A, B, Vertical thin sections from the middle crinkly zone showing desiccated microbial-mat formed by lime mudstone (mdst). The microbial-mat laminations were separated by drying and the space was then filled by white spar calcite (SC). Black spots are hematite pseudomorphs after pyrite (Fe). Desiccated microbial mats, mud cracks, spar-calcite-filled fenestrae, and mud chips are visible. Davies (1970, fig. 10) illustrated "intra-laminar shrinkage polygons" from the Recent supratidal deposits of Shark Bay, Western Australia, whose physical attributes are similar to the Todilto specimen. Cores from the supratidal deposits of Andros Island (Hardie, 1977, fig. 43) have "crinkled fenestral lamination" which also displays the same sedimentary fabric. The specimen was collected from an open pit, Section Four mine area, Bunny mine. See Figure 35 for location of specimen. C, D, Laminations disrupted due to desiccation and growth in the capillary zone of small-scale anhydrite cumulus enterolithic structures which are preserved as spar-calcite pseudomorphs of anhydrite. Relict cumulus texture of the anhydrite is preserved by the calcite. Abundant hematite pseudomorphs of pyrite (Fe). Lime mudstone contains abundant ostracode valves. Similar cumulus enterolitic structures are shown by Shearman (1981, pl. 12) from the lower Purbeck of England and Shearman & Fuller (1969, fig. 4) from the Devonian of Canada. Middle crinkly zone, Bunny mine. See Figure 35 for location of specimen. E, Spar-calcite pseudomorphs of nodular "chicken-wire" anhydrite displaced the microbial laminations in the upper massive zone limestone. Bunny mine. F, Vertical cross section of an enterolithic structure shown at outcrop in Figure 25A. The translucent band is composed of 100-150 pm calcite crystals with abundant fluid inclusions. The calcite has replaced calcium sulfate (Shearman & Fuller, 1969). The enclosing lime mudstone contains contorted laminations, clasts, and numerous ostracode valves. Middle crinkly zone, sec. 20, T13N, R9W.

cia fragments are cemented by lime mudstone and spar calcite.

At some localities on the west side of Haystack Mountain the Todilto Limestone Member is less than 10 ft (3 m) thick. Drape-fold structures have developed over Entrada Sandstone paleohighs. At this locality the Todilto Limestone Member contains interbeds of quartz sandstone and limestone. The Entrada Sandstone is continuous and shows no evidence of faulting or folding (Fig. 34) below the Todilto–Entrada contact.

At the Zia/La Jara and Sections Four and Nine mines, natural outcrops and bulldozed scraped-top bedding surfaces of the Todilto Limestone Member show in planar view that the apexes of the folds are linear to sinuous, can be traced for hundreds of feet, and can converge with the apexes of other folds.

Faulting associated with intraformational folds—Evidence of a shear surface and some movement or a plane of slippage are often found along the axes of the intraformational folds.

Many of the intraformational folds are associated with low-angle faults or shear zones. The fault surfaces have slickenside marks that were developed on lithified lime stone. A south-facing fold in the Bunny mine in the Section Four area (Fig. 35) has a fault with a dip of 35° and a N30°E strike. The displacement on the fault appears to be about 3 ft (1 m). The age or timing of this fault is uncertain, but the movement did occur after the lithification of the carbonate sediments. The fault could have been superimposed over an earlier sedimentary fold. It is difficult to determine how much the fault contributed to the size and shape of the intraformational fold. In the same open-pit workings the exposed south face of the same fold, 131 ft (40 m) away, shows no evidence of a fault (Fig. 36).

At Billy the Kid quarry a low-angle fault is associated with, and underlies a set of, small intraformational folds (Fig. 10) that developed in the middle crinkly and upper massive zones.

The intraformational folds show a variety of stratigraphic relationships within the Todilto Limestone Member which could suggest timing of the folding and associated shear zones. A fold developed within the middle crinkly zone is overlain by unfolded and parallel beds of the upper massive zone. This suggests that the folding occurred before the deposition of the upper massive zone

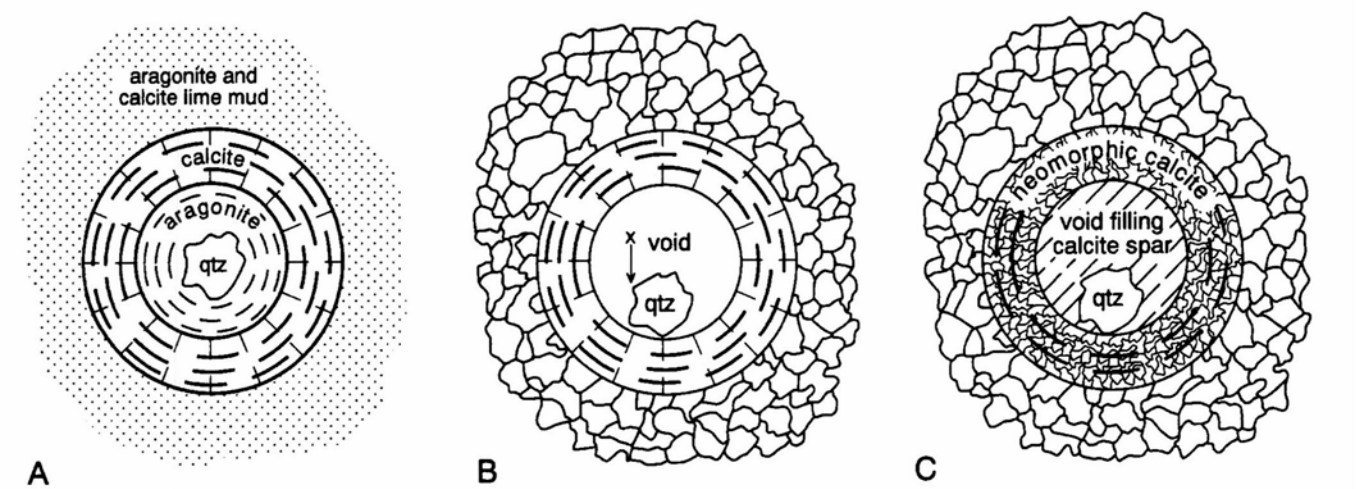

FIGURE 20—Diagrammatic illustration of the diagenetic history of typical Todilto ooids. **A**, The ooids are encased in lime mud and their diameter ranges from 0.6 to 0.8 mm. They were originally composed of alternating concentric layers or bands of aragonite and calcite. The crystals of aragonite were 2–6 µm, and lesser amounts of calcite nucleated on a detrital-quartz grain. **B**, The aragonite center of the ooid was dissolved by fresh water, allowing the quartz grain to fall to the bottom of the cavity. The cavity was subsequently filled by spar calcite. **C**, The outer concentric rim of the ooid is typically 100–200 µm thick, composed primarily of calcite, and contains relic concentric banding that represents micritic envelopes. These micritic envelopes are preserved by 10–30 µm crystals of dark, neomorphic calcite. The ooids are preserved in a neomorphic-spar matrix of cloudy, inclusion-rich spar calcite occurring in 50–100 µm rhombs.

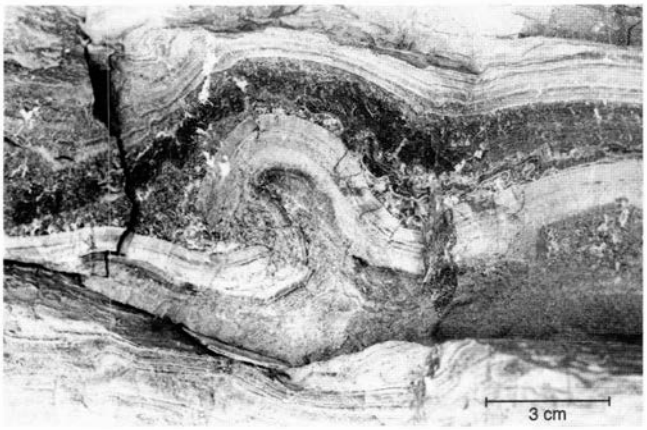

FIGURE 21—Calcite pseudomorphs of anhydrite diapirs/enterolithic structures in the middle crinkly zone on the east flank of an intraformational fold exposed in the Bunny open-pit mine Section Four, some 30 ft (9 m) north of the right portal shown in Figure 35. Photo shows calcite pseudomorph of contorted diapiric-anhydrite enterolithic structure that is truncated by a deflation surface (compare with Shinn, 1983, fig. 4). Some of the diapiric folds are truncated on their upper surfaces, suggesting the development of a penecontemporaneous sabkha deflation surface before the deposition of the overlying beds (see Shinn, 1983, figs. 38–41, from the Trucial Coast). Butler et al. (1982, fig. 16) made trenches in the Recent supratidal sediments of Abu Dhabi that show white diapiric layers of anhydrite with configurations that are very similar to the Todilto Limestone Member examples.

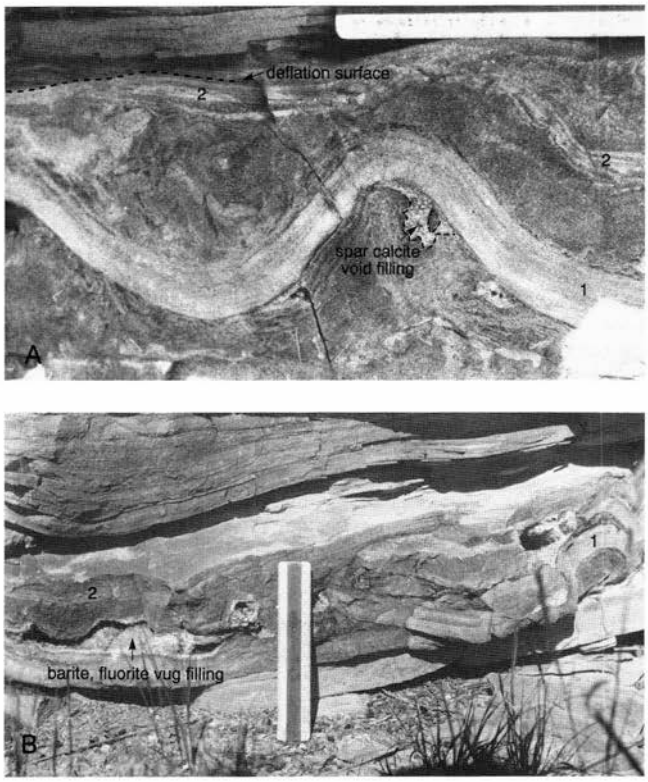

FIGURE 22—**A**, Calcite pseudomorph of anhydrite diapirs/enterolithic structures and penecontemporaneous soft-sediment deformation. Two diapirs/enterolithic structures are visible in the center of photo, and a less well defined diapir is present near the top of the bed. Both of the contorted diapiric beds were truncated by a deflation surface. La Jara mines. In arid climates winds deflate sediment down to the permanent capillary zone (Shinn, 1983, fig. 40; Shearman, 1981). **B**, The same bed becomes an intraformational breccia only a few feet from (A). This penecontemporaneous breccia is composed of broken clasts derived from the solution of the anhydrite within the diapirs/enterolithic structures. The breccia and vugs were subsequently partially filled with barite, fluorite, and minor amounts of uranium minerals. The stratigraphic location of the diapirs beneath the intraformational fold is shown in Figure 31. Zia/La Jara mine area. Scale is 6 inches (15 cm) long.

(Fig. 28A). In contrast, adjacent intraformational folds involve both the middle crinkly and upper massive zones (Figs. 28B, 29).

Todilto paleokarst—The top of the Todilto Limestone Member shows evidence of pre-Beclabito Member solution activity. The outcrops at Coolidge, Continental Divide, and Billy the Kid quarry all contain in the upper few feet or meters of the section abundant spar-calcite pseudomorphs of nodular and chicken-wire anhydrite in ostracode–lime mudstone (Figs. 6, 8, 19). The anhydrite was dissolved before the deposition of the overlying quartz sands of the Beclabito Member. The highest few feet or meters of the Todilto Limestone Member may also contain well-developed incipient platy caliche horizons.

In the open-pit workings of the Zia /La Jara and Sections Four and Nine mines are intraformational-fold structures with impressive solution and paleokarst features that developed in the upper massive and middle crinkly zones (Figs. 35-40). Also observed were karst features such as vadose-weathering sinkholes, recemented solution-collapse breccias, breccia pipes, solution-enlarged joints, and in places a thin purple–maroon terra-rossa soil developed on top of the Todilto surface.

The limestones of the upper massive zone contain sedimentary breccias formed in part by the dissolution of anhydrite/gypsum and the recementation of broken and desiccated lime mudstone, and microbial-mat clasts. These lithoclasts were cemented by spar-calcite and lime-mud matrix. The karst features developed in the upper massive and middle crinkly zones are sinkholes, rundkarrens, and solution pipes that have been filled in part with limestone breccias and ferruginous sands from the overlying Beclabito Member. The smaller vadose-solution cavities are partially filled with multiple cycles of spar calcite, and quite often with iron-stained quartz sands from the overlying Beclabito Member (Figs. 35, 37). The thickness of the upper massive zone varies due to lateral facies relationships with the middle crinkly zone (Figs. 35, 39), irregular pre-Beclabito erosion, extensive karst features and solution breccias, and sinkhole development. The internal apexes of the intraformational folds contained penecontemporaneous soft-sediment breccias that had higher porosities and were sites of pre-Beclabito solution activity. These are now sinkholes that have been subsequently filled with sands from the overlying Beclabito Member. Examples of these sinkholes can be seen in the open-pit workings of the Sections Four and Nine areas (Figs. 35-40). The most interesting example is a long and sinuous open-pit uranium mine that followed the axis of an intraformational fold. The north end of the pit shows that the axis of the fold involves both the middle crinkly and upper massive zones, and demonstrates that prior to the deposition of the Beclabito Member (Fig. 37) the Todilto Limestone Member was subjected to extensive subaerial weathering and sinkhole development adjacent to the fold.

The residual void spaces and solution porosity were subsequently filled with epigenetic minerals including fluorite, barite, hematite, and uranium minerals.

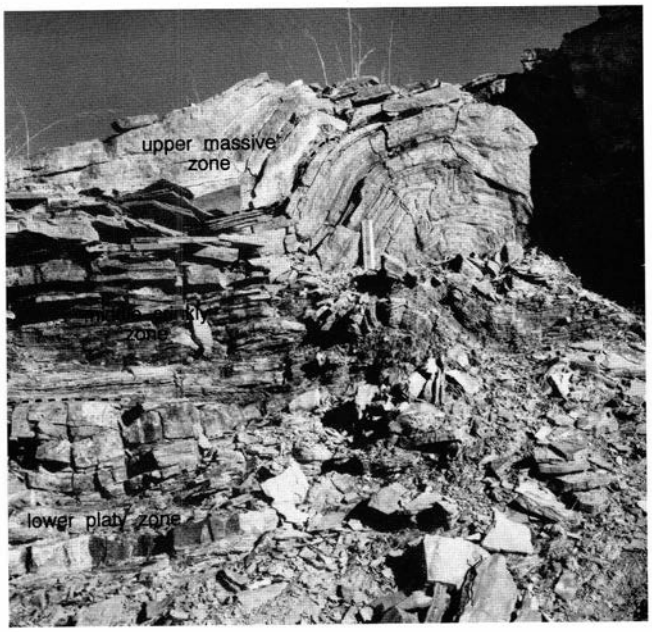

FIGURE 23—A bulldozer cut at Number 1 mine, La Jara mines, showing the stratigraphic relationships of an intraformational fold that formed in both the middle crinkly and upper massive zones. The fold is not developed in the beds of the lower platy zone. Scale is 6 inches (15 cm) long.

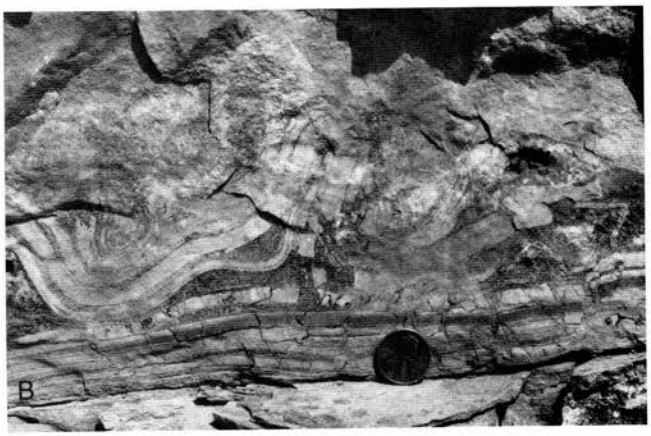

FIGURE 25—**A**, Diapiric/enterolithic structure preserved by calcite pseudomorphs of anhydrite. Note the contorted beds or laminations associated with the white enterolithic structure. The beds above and below the structure are parallel. A thin section cut across the white calcite of the enterolithic structure is shown in Figure 19F. Sec. 20, T13N, R9W. Coin is 16 mm in diameter. **B**, Diapiric enterolithic structure resting on flat-lying, desiccated, and cracked lime-mudstone microbial mat. The enterolithic structure has penecontemporanous brecciation with spar-calcite vug filling and vugs lined with calcite. Contorted lime-mudstone matrix has abundant ostracode valves. Sec. 20, T13N, R9W. Coin is 18 mm in diameter.

Intraformational folds: Previous concepts—The origins of the Todilto intraformational folds have intrigued many geologists over the decades, which has resulted in numerous theories.

Hilpert & Moench (1960, p. 462) thought the folds or "deformation may have been caused by the flowage of unconsolidated lime muds on the flanks of Jurassic flexures, for the intraformational folds are localized along these flexures and many are elongate parallel to them." They also stated that in the F-33 deposit (an underground mine) "in contrast with much of the folding in the Todilto limestone

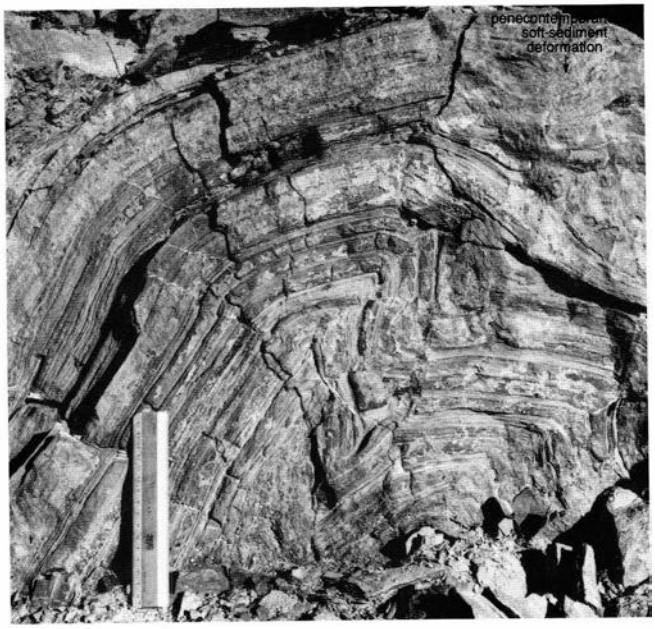

FIGURE 24—Details of the apex and internal sedimentary structures of the intraformational fold shown in Figure 23. The center of the fold shows overturned beds, penecontemporaneous soft-sediment deformation, and brecciation. Scale is 6 inches (15 cm) long.

the largest fold exposed in this mine involves the upper part of the Entrada Sandstone." Hilpert (1969) stated that "These folds are related to broader open folds in the Jurassic rocks, which are dated as post-Todilto and pre-Dakota."

Moench & Schlee (1967, p. 39) thought that "large-scale warping that took place during the Jurassic sedimentation appears to have induced slumping and sliding of semiconsolidated limestone into the synclines. Under a probably thin cover, then, plastic limestone apparently slid down the limbs of synclines and piled up near the trough."

Gabelman & Boyer (1988) attributed these structures to nearly orthogonal sets of tectonic folds developed during a mild orogeny in the Lower and Middle Cretaceous.

Perry (1963) and Rawson (1980) believed the folds were algal structures forming reefs, whereas Bell (1963, p. A14) proposed that "These folds probably were caused by hydration of calcium sulfate and subsequent leaching of this material."

Green (1982) viewed the intraformational folds in the Todilto Limestone Member as the result of encroachment of the Summerville eolian dunes over soft, unlithified Todilto lime muds. Sedimentary loading by migrating sand dunes on layers of Todilto lime mud resulted in dif-

FIGURE 26—**A**, Arenaceous lime mudstone near the base of the lower platy zone. Bed shows possible stromatolitic structure with abundant desiccation cracks, mud chips, and breccias. Contorted and diapiric penecontemporaneous sedimentary structures indicating subaerial exposure are also common in the lower platy zone. Sec. 20, T13N, R9W. Scale is 6 inches (15 cm) long. **B**, Small intraformational fold developed in the middle crinkly zone. The fold developed in a single bed which is bounded above and below by laminations and bed surfaces that are parallel. This indicates that the intraformational fold formed penecontemporaneously with sedimentation. Intraformational folds in the Todilto Limestone Member grade from small (millimeter size) to very large, embracing the entire Todilto section. Sec. 20, T13N, R9W. Scale is 6 inches (15 cm) long.

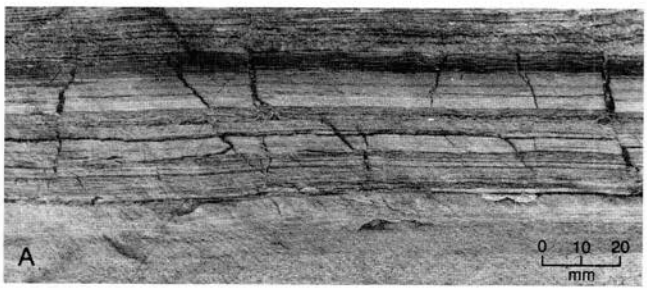

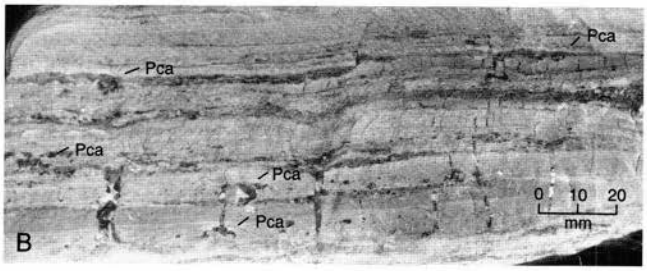

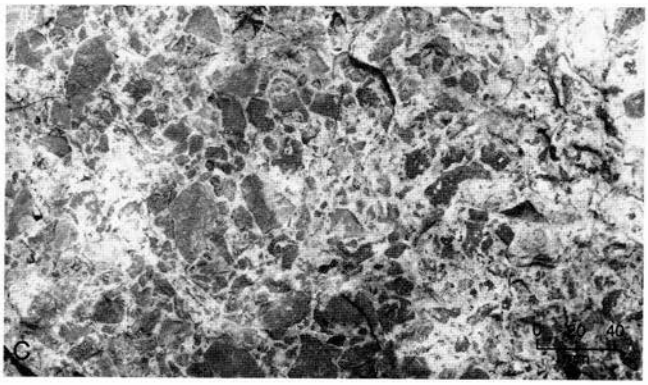

FIGURE 27—**A**, Vertical section of a weathered bed in the middle crinkly zone that shows desiccation cracks in the millimeter-thick laminated microbial mat. Sec. 20, T13N, R9W. **B**, Large, vertical desiccation cracks filled by spar-calcite and numerous spar-calcite pseudomorphs of gypsum/anhydrite (Pca); lower platy zone, Haystack Mountain. **C**, Flat lime-mudstone pebbles displayed on a weathered bedding surface near the base of the lower platy zone, Haystack Mountain. These were microbial-bound clasts (interclasts) similar to those illustrated by Hardie & Ginsburg (*in* Hardie, 1977, fig. 57) from the inland algal marsh on Andros Island.

ferential compaction, contortion, and dewatering, producing both small and large-scale plastic-deformation structures such as convolute laminations, mounds, rolls, folds, and small anticlines and synclines.

Tepee structures—The term "tepee" was introduced by Adams & Frenzel (1950) to describe structures which look like cross sections of American Indian tents and are common in the back-barrier facies of the Permian Carlsbad Group [designated Artesia Group by some] in the Guadalupe Mountains (Smith, 1974; Assereto & Kendall, 1977; Pray & Esteban, 1977). These structures are a common geologic phenomenon in many carbonate platforms of different ages and their analogues are now forming in modern peritidal zones of the Persian Gulf and in the salinas of Australia (Warren, 1982, 1991; Handford et al., 1984).

Tepees in the lagoon (shallow subtidal) grow by aragonite crystallization within the crust, a probable result of suprasaturated bottom waters immediately above the crust and hard grounds; submarine tepees also record a very low rate of sedimentation. In contrast, the intertidal/supratidal sabkha tepees form under repeated cycles of thermal cracking, mud infilling, and cementation (Warren, 1991). According to Assereto & Kendall (1977, p. 201), the presence of tepee structures is evidence of reduced deposition or hiatus. The presence of peritidal tepees implies a period of exposure during which marine vadose diagenesis took place.

Warren's (1983, 1991) studies on the coastal salinas of South Australia found that tepees form where *marine-derived ground water* resurges from a surrounding dune aquifer into the margins of the salina. Tepees form in the "boundstone" (hardground) as a response to ground-water-induced seasonal change in pore pressure of the underlying sediments. Warren (1983) and Handford et al. (1984) found that the tepee structures form openings in the pavement aquitard, and that tepee zones are sites of preferential ground-water (saline) overflow. Ground water trickles from tepees throughout the year, but outflow is greatest during spring and early summer. Warren's (1983) research on the development of tepees in the sali-

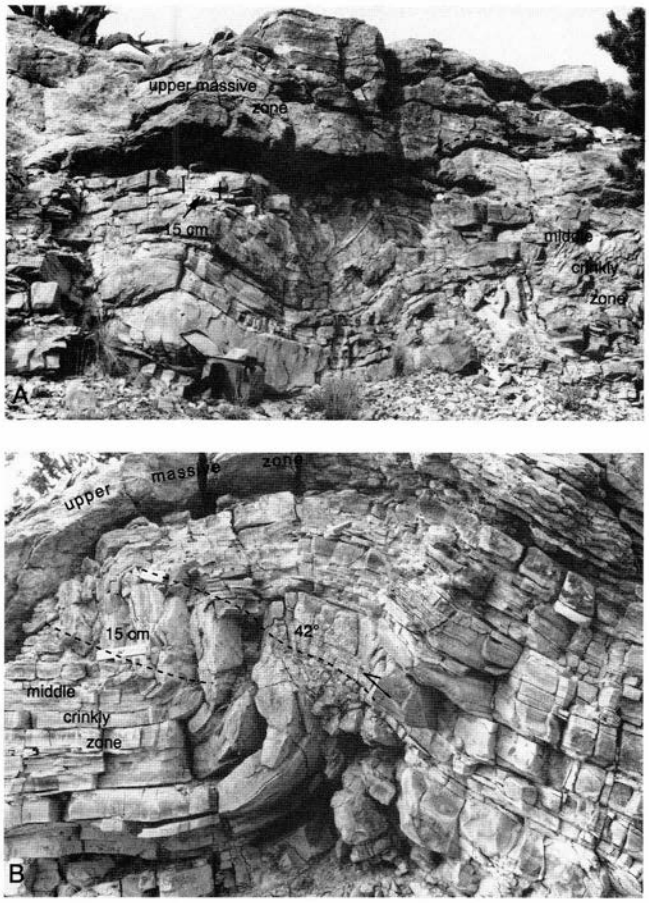

FIGURE 28—Intraformational folds at Haystack Mountain. Scale is 6 inches (15 cm) long. **A**, Fold developed within the middle crinkly zone and overlain by unfolded and parallel beds of the upper massive zone. **B**, Fold within the middle crinkly zone, with a fold-axis trend of about 42°W. The fold also involves the overlying beds of the upper massive unit, west side of Haystack Mountain.

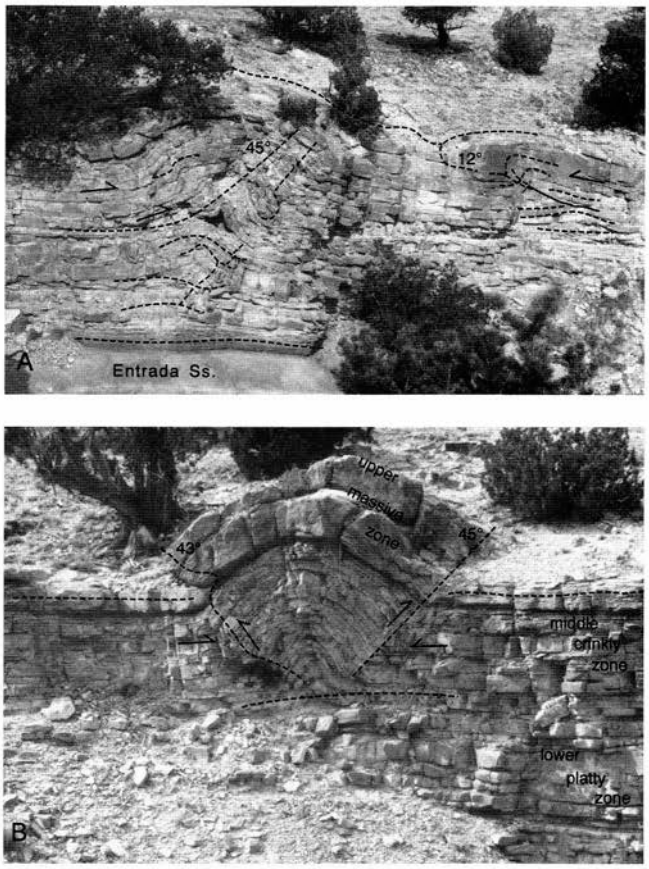

FIGURE 29—Intraformational folds at adjacent outcrops, Haystack Mountain. **A**, The fold rests on a flat surface of the Entrada Sandstone, and the lower platy zone shows swelling or mounding at the base of the section and development of the fracture zone. Two parallel 45° fracture zones are well developed in the middle crinkly zone and extend into the upper massive unit. Facing this fold is a smaller fold developed in the middle crinkly and upper massive zones, with a fracture surface of 12°. **B**, Nearly symmetrical, wedge-shaped intraformational fold that has developed in the middle crinkly zone and extends into the massive zone. The fold is bounded by fractures which are 43°and 45° from the horizontal. West side of Haystack Mountain.

nas of Australia has revealed their intimate relationship with the aquitard-veneer boundstone and its response to fluid movement in the underlying boxwork limestones. His boxwork limestones are fenestral, and are composed of curved to straight plates and filaments of aragonite. Saline-inflow ground waters move within the porousboxwork limestones.

Warren (1983) reported that Holocene tepees in the coastal salinas of South Australia have a relief up to 3.2 ft (1 m). Assereto & Kendall (1977, p. 157, fig. 3C) reported tepees in the Triassic dolomites of Italy that are 13 ft (4 m) tall, with a 33 ft (10 m) base.

Assereto & Kendall (1977) found that peritidal tepees are generally associated with abundant marine-vadose pisolites and exotic fibrous- or cellular-aragonite or calcite-pseudomorph cements.

Origin of Todilto intraformational folds—The Todilto Limestone intraformational folds have many of the attributes of tepee structures.

(1) The folds can develop within the lower platy zone. Initially the limestone beds swell or thicken on top of each other and are vertically stacked. A shear zone or plane of movement may develop in the lower part of the middle crinkly zone and may extend into the upper massive zone (Figs. 23, 24, 30, 31, 35, 38). Little or no expression of the intraformational fold can be seen in the overlying clastics of the Beclabito Member or in the stratification of the un derlying Entrada Sandstone.

(2) Associated with the intraformational folds are salina/playa (inland sabkha) sedimentary structures which are calcite pseudomorphs of anhydrite/gypsum, gypsum mush, chicken-wire structures, and anhydrite diapirs/enterolithic structures.

(3) The flanks of many of the folds exhibit penecontemporaneous soft- or semilithified-sediment slumping within the lime mudstones of the middle crinkly unit (Figs. 24, 30, 32). The sediment slumping and brecciation indicate compressional folding in a salina/playa (inland sabkha) environment.

(4) At the Zia/La Jara and Sections Four and Nine mines, outcrops and bulldozer-exposed top surfaces of the Todilto Limestone Member show, in planar view, that the fold apexes are linear to sinuous, and that they can be traced for hundreds of feet and can converge with the apexes of other folds. The surface expression of the fold apex is commonly fractured and filled by quartz sands.

(5) Berglof (written comm. 1994) measured the direction of hundreds of folds exposed in outcrop and in underground mines, and statistically found no preferred axis orientation for the intraformational folds on a district-

FIGURE 30—Close-up of a small intraformational fold developed in the upper part of the middle crinkly zone, some 30 ft (10 m) to the north of the fold shown in Figures 23 and 24. Penecontemporaneous soft-sediment deformation and breccias at the base of the fold, and abundant small soft-sediment folds on the flank of the larger intraformational fold. Zia/La Jara mines. Scale is 6 inches (15 cm) long.

wide basis, although they exhibit a strongly preferred orientation within some individual mines or closely spaced groups of deposits.

Sedimentary features of tepees absent in Todilto folds—(1) The Todilto intraformational folds are not associated with pisolites; in fact pisolites have not been found in the Todilto. Pisolites are intimately associated with tepees described by Assereto & Kendall (1977) from the Triassic of Italy and by Esteban & Pray (1983) from the Permian of New Mexico. Warren (1982) and Handford et al. (1984) described the close genetic relationship between the pisolites and tepees now forming in the salinas of South Australia.

(2) Sedimentary structures similar to the boxwork limestones described by Warren (1983) have not been found in the Todilto Limestone Member. Warren described the boxwork boundstone and associated tepees and pisoids as formed by saline ground-water inflow. The Todilto Limestone Member does show extensive evidence of PreBeclabito vadose weathering that resulted in the development of vuggy porosity and poorly cemented breccias (Figs. 35, 36-40).

Evidence from this study—A definitive statement cannot be made about the origin of the Todilto intraformational folds. The folds appear to be the result of compressional forces that developed during, or very shortly after, limestone deposition. The folds are not expressed in the underlying Entrada Sandstone and developed before the vadose karsting and deposition of the overlying Beclabito Member. The compressional force could be the result of the interstitial growth of aragonite cement and/or gypsum/anhydrite crystals within the lime-mud sediments, with the growth of these crystals resulting in lateral compressional forces. Much of the interstitial crystal growth occurred from concentrated saline brines in the capillary zone above the saline ground-water zone (Figs. 19C-F, 40). Assereto & Kendall (1977) contended that the expansion indicative of tepee formation is caused by a continual repetition of the following processes: (A) desiccation and thermal contraction causing small fractures; **(B)** a phase of wetting causing the enlargement of fractures; (C) a phase of crystallization of calcium carbonates and other minerals causing the enlargement, filling, and cementation of the fractures (precipitation is from

FIGURE 31—A natural exposure of an intraformational fold developed in the middle crinkly zone in the Zia/La Jara area. The north half of the fold is preserved on a cliff. The fold is underlain by supratidal sediments that have calcite pseudomorphs of gypsum/anhydrite mush and anhydrite diapirs/enterolithic structures. A 6 inch (15 cm) scale is shown in upper center of photo. See Figure 22 for photos of these sedimentary structures.

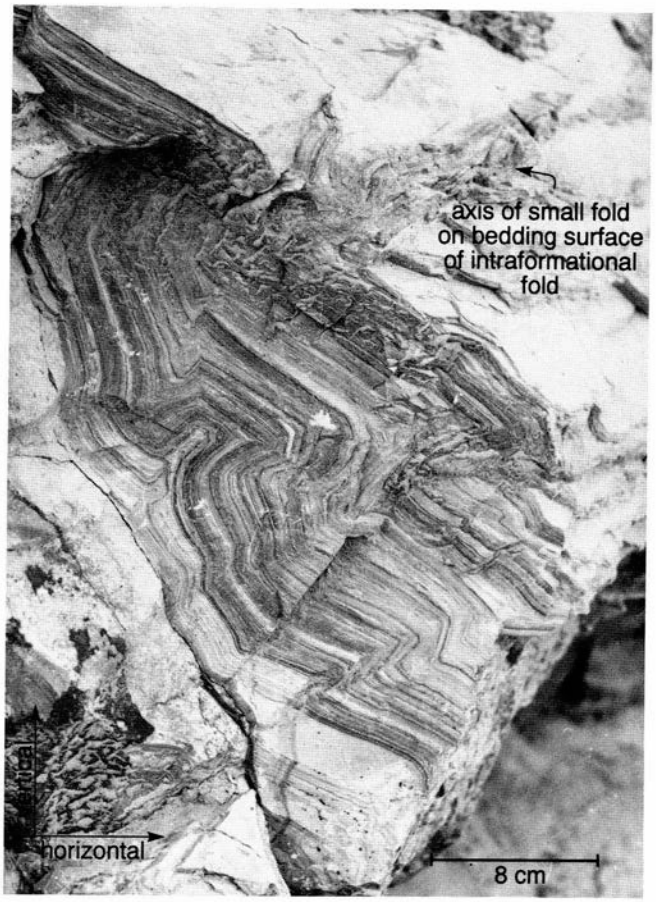

FIGURE 32—Penecontemporaneous soft-sediment slump folds developed on the east flank of a large intraformational fold that was mineralized with uranium. Photograph was taken some 3 ft (1 m) south of Figure 21. The unlithified microbial-mat lime mudstone slumped downslope as the intraformational fold was forming. Section Four, Bunny mine.

brines and meteoric waters); and (D) hydration of minerals, thermal expansion, breaking waves, and faulting all may add to the disruption.

Hilpert & Moench (1960), Hilpert (1969), Moench & Schlee (1967) and Gabelman & Boyer (1988) attributed the Todilto intraformational folds to tectonic compressional forces or gravity sliding on a paleoslope during or after Todilto Limestone deposition.

It is interesting to note that Bell (1989) described a salina-lake carbonate sequence in an Upper Jurassic—Lower Cretaceous continental red-bed sequence in the Atacama region of northern Chile that is very similar to the Todilto sequence. The Chilean carbonates contain what Bell (1989) described as box folds and thrust faults in a thin carbonate section, and he considered them to be the result of deformation by early Tertiary compression caused by tectonism. The Chilean box folds of Bell (1989) are very similar in appearance to the Todilto intraformational folds in the Grants district.

Uranium deposits in the Todilto Limestone Member

A detailed historical review of the uranium production from the Todilto Limestone Member can be found in Chenoweth (1985). The following discussion is taken in part from McLemore & Chenoweth (1989). The Grants uranium district is one of the few localities in the world where economic peneconcordant uranium deposits occur in limestone beds. The orebodies range in size from a few to hundreds of feet long and wide, and up to 20 ft (6.5 m) thick. Most deposits contain less than 20,000 tons of ore averaging 0.2-0.5% U_3O_8, although a few deposits are larger.

Three types of deposits occur in the Todilto Limestone Member: (1) unoxidized primary deposits, (2) oxidized (weathered) primary deposits, and (3) vagrant secondary deposits (Jones, 1978). Unoxidized primary deposits

FIGURE 33—Natural outcrop of an intraformational fold that developed within the middle crinkly and massive zones, Zia/La Jara area. The fold has a massive appearance, but grades laterally into the middle crinkly zone. The center of the fold is composed of penecontemporaneous soft-sediment breccia fragments that have supratidal sedimentary structures, including calcite pseudomorphs of anhydrite diapirs/enterolithic structures, gypsum mush, and crinkly microbial mats. La Jara claim number 9.

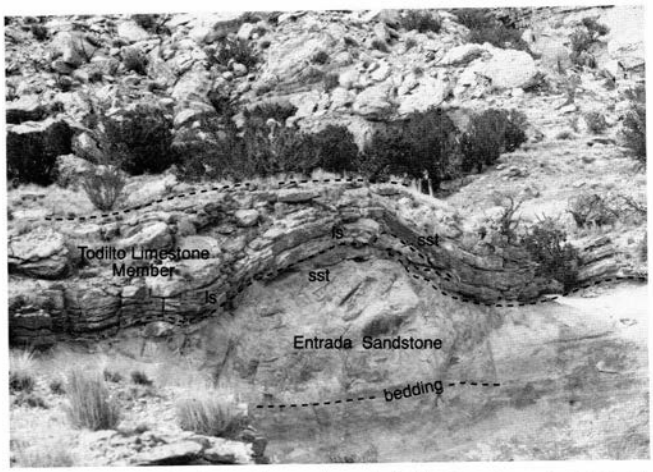

FIGURE 34—An intraformational fold developed over an Entrada Sandstone paleohigh on the west side of Haystack Mountain. The Todilto Limestone Member appears to be draped over the relict Entrada Sandstone high with interbeds of quartz sandstone (sst) between limestones (ls). Beneath the Entrada/Todilto contact the bedding in the Entrada Sandstone is continuous and shows no evidence of faulting or folding. The Todilto Limestone Member at this location is less than 8 ft (2.4 m) thick, shows rapid facies changes, and contains numerous lenses and interbeds of quartz sandstone.

contain uraninite and coffinite as fine blades and fibers along grain boundaries, as veinlets, and as replacements of calcite along bedding planes and fractures. McLemore & Chenoweth (1989) stated that unoxidized and oxidized primary uranium deposits occur in the Todilto Limestone Member *within intraformational folds* where an overlying gypsum bed is absent. The largest orebodies occur in the anticlinal portions of the folds (Green, 1982).

Rawson's (1980, p. 308) paper indicated that "most of the economic deposits are found in the middle crinkly and upper massive zones. The primary (reduced) ore appears to be uraninite that is restricted to layers parallel to bedding and/or small irregular-shaped blobs rich in carbonaceous residue." He further stated (p. 309) that "observations suggest that the primary ore was emplaced prior to lithification, owing to the disseminated nature of the uraninite within the limestone." Berglof (1992) added supporting evidence for the penesyngenetic origin from isotopic dates of the uraninite in the Todilto. He dated the uraninite at 150-155 Ma and concluded that it was emplaced shortly after deposition. Some of the isotopic ages are discordant, but they can be interpreted as supporting this conclusion (Berglof, 1992). Harland et al. (1990) placed the Callovian Stage from 157.1 to 161.3 Ma, and Mulholland & Kuryvial (1992) placed the stage from 150.5 to 155.5 Ma.

The age of the Callovian—Oxfordian boundary is of interest since the Todilto Limestone Member may be slightly older. Mulholland & Kuryvial (1992) simply repeated age dates from Haq et al. (1988). The Callovian-Oxfordian age is of concern because, as Berglof (1992) stated, estimates of up to 163 Ma are given for this boundary. If Berglof's (1992) uraninite age dates are correct, then there could be a gap of 10 m.y. between the deposition of the Todilto Limestone Member and the introduction of the uraninite.

Field studies of the Homestake Mining Company's properties shown as Anaconda Section 9 mine on Thaden's (1969) geologic map, in secs. 4 and 9, T12N,

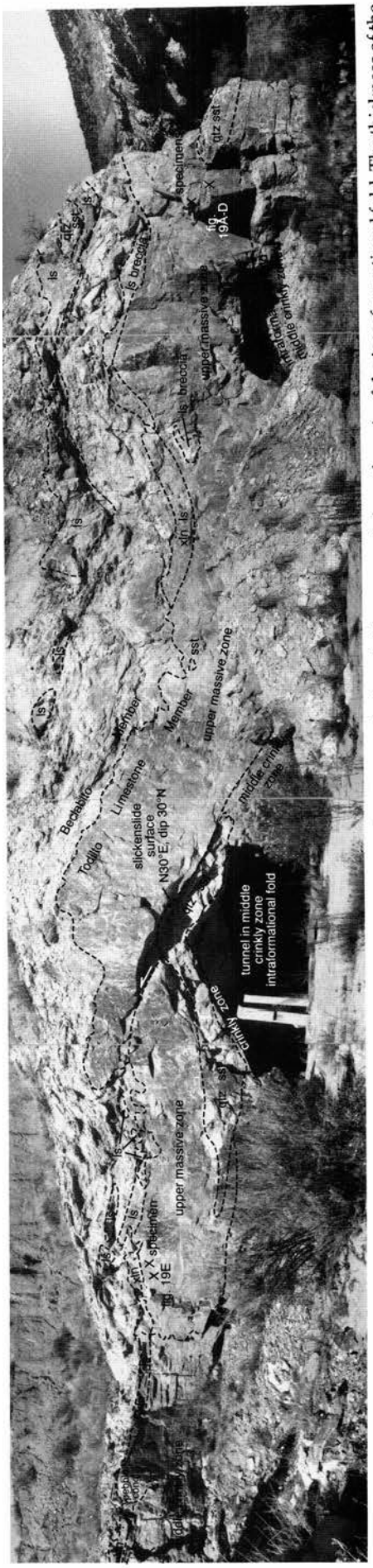

FIGURE 35—A south-facing fold exposed in Section Four, Bunny mine. Uranium mineralization was in the crinkly zone and along the axis of the intraformational fold. The thickness of the massive zone is highly irregular due to slumping and brecciation within the fold as well as pre-Beclabito karsting and erosion. Karst features observed in the massive zone include rundkarrens and solution pipes, and cavities filled with limestone breccias and ferruginous sands from the overlying Beclabito Member. The smaller vadose-solution cavities are partially filled with multiple cycles of vadose spar calcite and frequently also with iron-stained quartz sands from the overlying Beclabito Member. The intraformational fold in the center of the photograph is associated with a small, low-angle fault. The fault surface has slickenside marks developed on lithified limestone. This fault has a 35° dip and a N30°E strike. The displacement on the fault appears to be about 3 ft (1 m). The age or timing of this fault is uncertain, but the movement did occur after the lithification of the carbonate sediments. The fault could have been superimposed over an earlier sedimentary fold. It is difficult to determine how much the fault contributed to the size and shape of the intraformational fold. Within the open-pit workings the exposed north face of the fold shows no evidence of faulting. See Figure 36.

FIGURE 36—View to the south of open-pit and tunnel workings at Section Four, Bunny mine (SE¼ sec. 4, T12N, R9W). The open-pit workings follow the axis and flanks of the intraformational fold, which is developed in the middle crinkly zone. This is overlain by a quartz-sandstone bed within the Todilto Limestone Member that grades laterally into lime mudstones of the middle crinkly zone. The upper massive zone is variable in thickness and contains many solution joints and cavities. The tunnel is some 131 ft (40 m) south of the large portal shown in Figure 35.

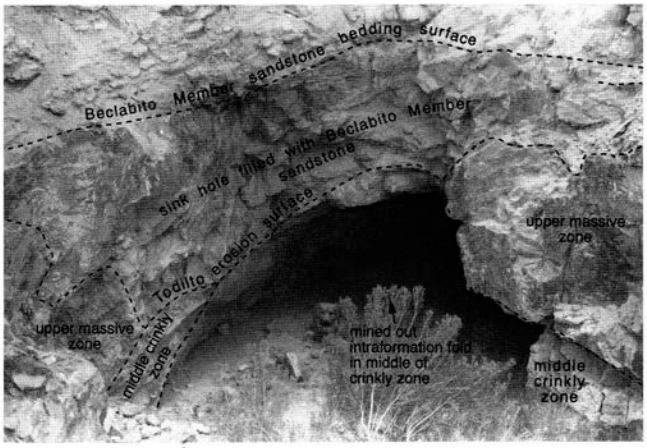

FIGURE 37—A north-facing mine tunnel which follows the axis of an intraformational fold in the Bunny mine, in the same open-pit complex as shown in Figures 35 and 36. The fold can be seen in the wall of the tunnel. The upper massive zone has been removed by solution on the east side of the fold, and the overlying sandstones of the Beclabito Member have filled in the large sinkhole depression.

R9W, reveal that the orebodies in the Todilto Limestone follow the axes of the intraformational folds (Figs. 35-39). The folds are best developed in the middle crinkly zone, 6 ft (2 m) thick, and are associated with calcite pseudomorphs of anhydrite and well-developed enterolithic structures (Fig. 21). The massive-zone limestone is 3-5 ft (1-1.5 m) thick, is draped over the middle crinkly zone, and shows extensive evidence of subaerial vadose weathering, karsting, and brecciation previous to the deposition of the overlying terrigenous clastics of the Wanakah Formation (Figs. 35-40). The top of the massive zone has desiccation cracks that have been enlarged by solution and breccia zones. The solution voids and pore space in the breccia associated with the intraformational folds are the sites of deposition for the epigenetic minerals: spar calcite, barite, pyrite, uranium minerals, and purple fluorite. Truesdell & Weeks (1960) described the paragenesis of the uranium ores in the Todilto Limestone Member near Grants. Granger (1963) listed 27 authigenic minerals found in the mineralization. He also noted that mineralization is largely confined to the axial zones of minor anticlines (intraformational folds) within the Todilto Limestone Member.

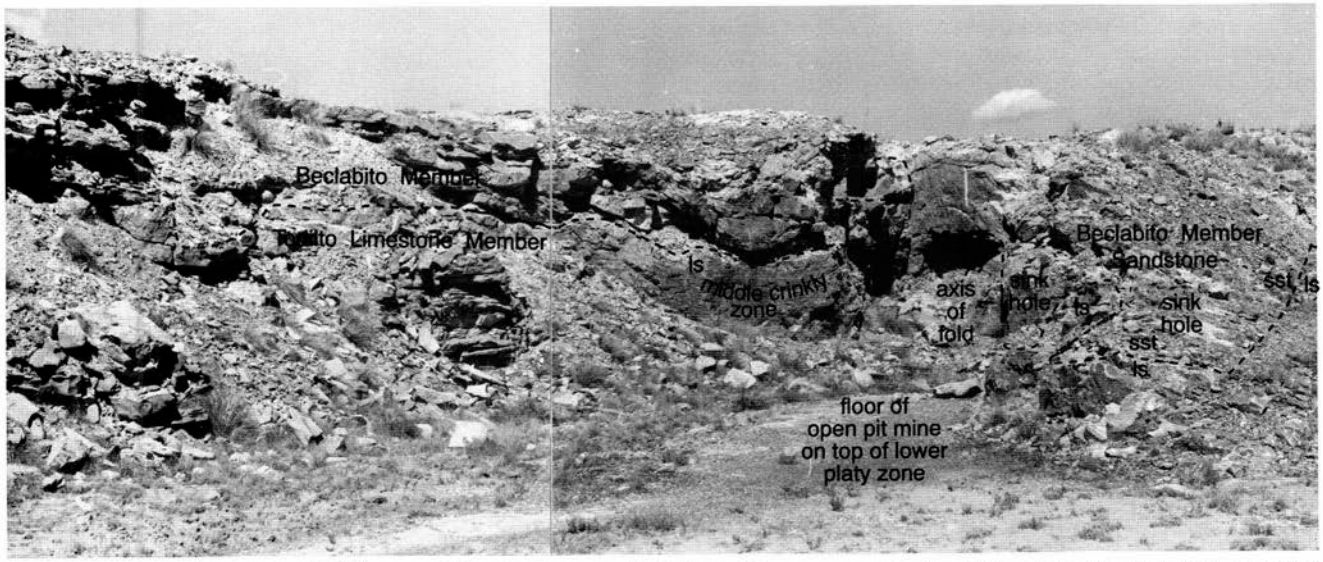

FIGURE 38—Intraformational fold exposed in a long open pit, Section Nine, unnamed mine. This photo illustrates the complex erosional relationship between the Todilto Limestone and Beclabito Members. The axis of the fold is mineralized with uranium minerals both in fracture porosity and in the fenestrae of the microbial mats. The contact between the Todilto Limestone and Beclabito Members is an irregular erosion surface marked by numerous solution sinkholes. Two sinkholes are on the steep east flank of the fold and are filled by detrital-quartz sands from the overlying Beclabito Member. This is similar to the sinkhole above and to the side of the fold seen in Figure 37. Limestone = ls, sandstone = sst.

McLaughlin (1963) thought the Todilto uranium deposits were influenced by hydrothermal solutions, based on "the chemistry of the mineral fluorite, which is considered insoluble under conditions associated with ordinary ground water."

Truesdell & Weeks (1959) stated that "Because the uranium deposits in the Todilto limestone near Grants, New Mexico, are different lithologically, they have also been considered different genetically from the uranium deposits in sandstone of the Colorado Plateau."

Characteristics of the deposits in sandstones are: (1) The chemistry and mineralogy are simple. Uranium is usually associated with vanadium, and few other elements are abundant. The primary ore contains uraninite, vanadium oxides, and coffinite and oxidizes chiefly to uranyl vanadates. (2) Deposition was epigenetic from circulating waters, controlled by primary sedimentary structures and organic matter, and usually limited to a single formation over a wide area. (3) The consistent association of the deposits with tuffaceous (or arkosic) sedimentary rocks suggests a mechanism of formation involving leaching of uranium from the tuff (or arkose) by carbonate ground water with formation of uranyl-tricarbonate complexes, which then move to a different chemical environment where the uranium precipitates.

Deposits in the Todilto, like the sandstone ores, have uraninite, coffinite, and the vanadium oxides haggite and paramontroseite, which oxidize to uranyl vanadates and silicates. Mineralization occurs within intraformational folds and is associated with organic matter which is incorporated into the limestone. The acid-insoluble fraction of the Todilto Limestone Member is 4-45% of the unmineralized limestone and is arkosic and possibly tuffaceous silt-size material. Thus uranium deposits in the Todilto Limestone are considered basically similar to the Colorado Plateau sandstone uranium deposits in mineralogy, occurrence, and origin.

Brookins (1980) and Ludwig et al. (1984) presented evidence from Rb—Sr and U—Pb dating that uranium orebodies in the overlying Jurassic Morrison Formation began to form soon after deposition of the host rock.

Falkowski (1980) summarized earlier dating evidence that the Morrison orebodies formed during or immediately after deposition. He further stated that "the most plausible source of the uranium in the overlying sandstone-type uranium deposits in the Grants region is the volcanic ash; ore elements were released to the host sediments contemporaneously with deposition of the sediments. The uranium is thus envisioned as forming either essentially on the surface as the sediments were being deposited or at very shallow depth." Hansley's (1989) detailed study also shows that fluids responsible for mineralization "were at least in part derived from the alteration of tuffaceous material." A similar source for the uranium and mineralization is plausible for the underlying Todilto Limestone Member.

Emanuel (1982), in his geochemical and fluid-inclusion investigation of the Zuni Mountain fluorspar district and trace-element studies of uraniferous fluorite from the Todilto Limestone Member, Grants district, suggested that these two occurrences may be genetically related hydrothermal systems.

W. R. Berglof (written comm. 1994) expressed the view that any attempt to make the Todilto fluorite deposits a regional hydrothermal event and relate them to the Zuni Mountain fluorite orebodies is difficult if the uranium/

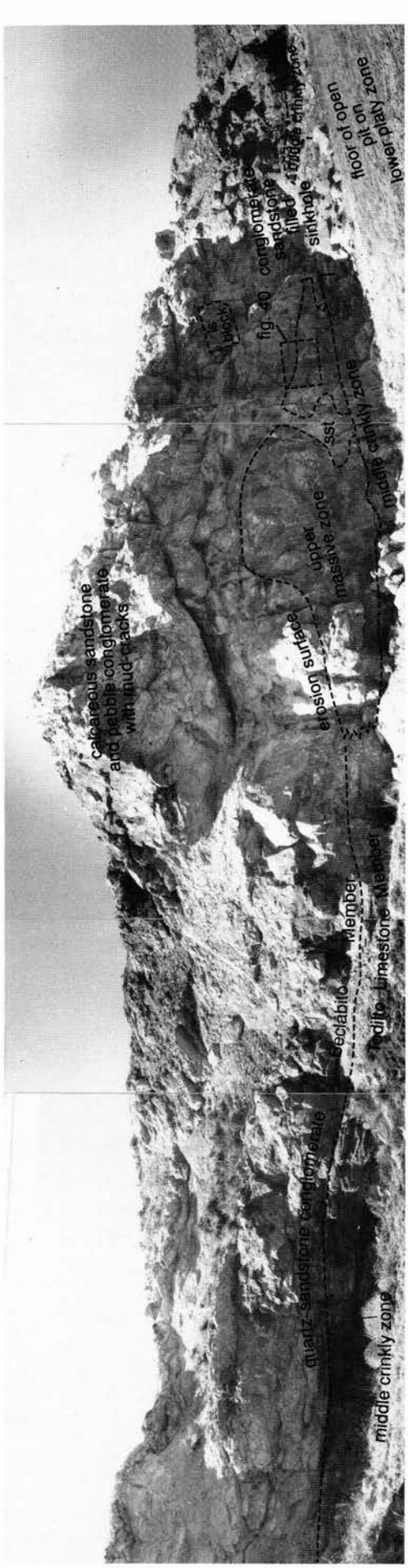

FIGURE 39—South side of Section Nine, unnamed mine, developed along the axis of an intraformational fold. The contact between the Todilto Limestone and Beclabito Members is an irregular erosion surface marked by numerous solution sinkholes and cavities filled by spar calcite, with minor amounts of barite and fluorite. Other cavities are filled by quartz sands derived from the overlying Beclabito Member. See Figure 40 for the various cavity shapes and fillings. The massive zone is composed of lime-mud-cemented sedimentary breccias formed by clasts of broken microbial mats.

FIGURE 40—Pre-Beclabito solution fissures and cavities in the lower part of the massive zone. The fissure has been filled by vadose spar-calcite cement. The contact between the Todilto Limestone and Beclabito Members is an irregular erosion surface marked by limestone- and sandstone-pebble conglomerate at the base of the Beclabito Member. The massive zone is composed of lime mudstone with abundant calcite pseudomorphs of anhydrite and limestone clasts cemented by lime mudstone. Same location as Figure 39, Section Nine, unnamed mine.

lead ages are accepted for the uranium deposits in the Todilto Limestone Member. Although it is erratically distributed, known fluorite mineralization is roughly coextensive with uranium mineralization on a district-wide basis. The uranium/lead isotope ages indicate that the uranium was deposited soon after the sabkha/salina carbonate sediments.

Rawson (1980) thought the intraformational folds in the Todilto Limestone Member were formed by stromatolites. He recognized (p. 309) that the Entrada Sandstone was an excellent aquifer and that a hydrodynamic gradient was established from the Mogollon highlands to the lake. Before the Middle Jurassic, the Mogollon highlands to the south and southwest were the site of silicic volcanism and possibly the source area for the uranium. The ground water moving from the south and southwest carried trace amounts of uranium leached from the silicic volcanics of the Mogollon highlands. Maxwell's (1990, and written comm. 1991) field studies indicate that there were no Mesozoic volcanic rocks in the eastern Mogollon highlands. This is based on his studies of the stratigraphic onshore—terrestrial equivalents of the Todilto Limestone Member to the south and southeast of Grants, on the Acoma Indian Reservation. Here the Wanakah Formation rests on the Entrada Sandstone and contains conglomerates that are composed of Paleozoic cherts and Precam-

brian metamorphic rocks and quartzites. No volcanic clasts were found. The conglomerate clasts suggest that the Mogollon highlands were composed of Paleozoic sedimentary and unroofed Proterozoic rocks. This mixed terrane of Paleozoic and Proterozoic rocks could have served as a source for the uranium.

Conclusions

(1) Paleomagnetic studies indicate that the Todiltc Limestone Member was deposited at a latitude of about 13-16° north. The Jurassic climate of the western edge of North America was similar to the modern Sahara.

(2) Todilto Limestone deposition began with flooding by the Curtis-Summerville Sea, which caused partial wave-cutting and filling of the irregular Entrada sand-dune surface and the development of a large, marine-influenced salina/playa with an impoverished biota. Occasional rive] discharges created flood sheets and large ephemeral ponds with mixtures of evaporitic precipitates and marine waters. The preservation of laminations in the lower platy and middle crinkly zones and the lack of bioturbation by a burrowing infauna indicate an inhospitable environment. The middle crinkly zone has laminations with desiccation crack and chips, and spar-calcite pseudomorphs after nodular gypsum/ anhydrite and cumulus enterolithic / diapiric structures. The upper massive zone limestones are microbial mats and ostracode-lime mudstones. The sedimentary structures are desiccation cracks, chips, abundant spar-calcite pseudomorphs after nodular gypsum-anhydrite, and solution breccias. The top of the zone is characterized by spar-calcite pseudomorphs of anhydrite (chicken-wire texture) and gypsum-anhydrite mush. Sedimentary structures and facies relationships indicate that the upper massive zone was deposited in the final evaporation phase of the Todilto sauna.

(3) The Todilto Limestone Member shows evidence of pre-Beclabito solution activity. The karst features are sinkholes, recemented solution-collapse breccias, breccia pipes, solution-enlarged joints, rundkarrens, and in places a thin purple-maroon terra-rossa soil developed on top of the Todilto surface.

(4) The origin of the Todilto intraformational folds remains unclear. The folds appear to be the result of compressional forces that developed during or very shortly after limestone deposition. The folds are not expressed in the underlying Entrada Sandstone and developed before the vadose karsting and deposition of the overlying Beclabito Member. The compressional force could be the result of interstitial growth of aragonite cement and/or gypsum /anhydrite crystals in the lime-mud sediments, much of it from concentrated saline brines in the capillary zone above the saline ground-water zone. Hilpert & Moench (1960), Hilpert (1969), Moench & Schlee (1967), and Gabelman & Boyer (1988) attributed the Todilto intraformational folds to tectonic compressional forces or gravity sliding on a paleoslope during or after the Todilto Limestone deposition.

(5) Uranium/lead isotopic dating places the uraninite mineralization in the Todilto folds at 150-155 Ma and indicates that the uraninite was emplaced shortly after deposition.

References

Adams, J. E., and Frenzel, H. N., 1950, Capitan barrier reef, Texas and New Mexico: Journal of Geology, v. 58, pp. 289-312.

Aitken, J. D., 1967, Classification and environmental significance of cryptalgal limestones and dolomites with illustration from Cambrian and Ordovician of southwestern Alberta: Journal of Sedimentary Petrology, v. 37, pp. 1163-1178.

Alsharhan, A. S., and Kendall, G. St. C., 1994, Depositional setting of the Upper Jurassic Hith anhydrite of the Arabian Gulf: An analog to the Holocene evaporites of the United Arab Emirates and Lake Macleod of Western Australia: American Association of Petroleum Geologists, Bulletin, v. 78, no. 7, pp. 1075-1096.

Anderson, R. Y., 1982, Orbital forcing of evaporite sedimentation; *in* Berger, A., Imbrie, J., Hays, J., Kukla, G., and Saltzman, B. (eds.), Milankovich and climate, understanding the response to astronomical forcing: D. Reidel Publishing Co., pp. 147-162.

Anderson, R. Y., and Dean, W. E., 1988, Lacustrine varve formation through time: Palaeogeography, Palaeoclimatology, Palaeoecology, v. 62, pp. 215-235.

Anderson, R. Y., and Kirkland, D. W., 1960, Origin, varves, and cycles of the Jurassic Todilto Formation, New Mexico: American Association of Petroleum Geologists, Bulletin, v. 44, pp. 37-52.

Ash, H. 0., 1958, The Jurassic Todilto Formation, New Mexico: Unpublished MS Thesis, University of New Mexico, Albuquerque, 63 pp.

Assereto, R. L. A. M., and Kendall, C. G. St. C., 1977, Nature, origin and classification of peritidal tepee structures and related breccias: Sedimentology, v. 24, pp. 153-210.

Baker, A. A., Dane, C. H., and Reeside, J. B., 1947, Revised correlations of Jurassic formations of parts of Utah, Arizona, New Mexico and Colorado: American Association of Petroleum Geologists, Bulletin, v. 31, pp. 1664-1668.

Barattolo, F., 1991, Mesozoic and Cenozoic marine benthic calcareous algae with particular regard to Mesozoic dasycladaleans: *in* Riding, R. (ed)., Calcareous algae and stromatolites: Springer-Verlag, New York, pp. 504-537.

Bathurst, R. G. C., 1971, Carbonate sediments and their diagenesis: Elsevier, New York, 620 pp.

Bell, C. M., 1989, Saline lake carbonates within an Upper Jurassic-Lower Cretaceous continental red bed sequence in the Atacama region of northern Chile: Sedimentology, v.36, pp. 651-663.

Bell, K. G., 1963, Uranium in carbonate rocks: U.S. Geological Survey, Professional Paper 474-A, 29 pp.

Berglof, W. R., 1992, Isotopic ages of uranium deposits in the Todilto Limestone, Grants district, and their relationship to the ages of other Colorado Plateau deposits: New Mexico Geological Society, Guidebook 43, pp. 351-358.

Brookins, D. G., 1980, Geochronological studies in the Grants mineral belt; *in* Rautman, C. A. (compiler), Geology and mineral technology of the Grants uranium region 1979: New Mexico Bureau of Mines & Mineral Resources, Memoir 38, pp. 52-58.

Burne, R. V., and Moore, L. S., 1987, Microbialites: Organosedimentary deposits of benthic microbial communities: Palaios, v. 2, pp. 241-254.

Butler, G. P., Harris, P. M., and Kendall, C. G. St. C., 1982, Recent evaporites from the Abu Dhabi coastal flats; *in* Handford, C. R., Loucks, R. G., and Davies, G. R. (eds.), Depositional and diagenetic spectra of evaporites: Core Workshop No. 3, Society of Economic Paleontologists and Mineralogists, Calgary, pp. 33-64.

Campbell, C. V., 1976, Reservoir geometry of a fluvial sheet sandstone: American Association of Petroleum Geologists, Bulletin, v. 60, pp. 1009-1020.

Chenoweth, W. L. 1985, Historical review of uranium production from the Todilto Limestone, Cibola and McKinley Counties, New Mexico: New Mexico Geology, v. 7, no. 4, pp. 80-83.

Condon, S. M., 1989, Revision of Middle Jurassic nomenclature in the southeastern San Juan Basin: U.S. Geological Survey, Bulletin 1808-F, 21 pp.

Condon, S. M., and Hoffman, A. C., 1988, Revision in the nomenclature of the Middle Jurassic Wanakah Formation, northwestern New Mexico and northeastern Arizona: U.S. Geological Survey, Bulletin 1633-A, 12 pp.

Condon, S. M., and Peterson, F., 1986, Stratigraphy of Middle and Upper Jurassic rocks of the San Juan Basin: Historical perspective, current ideas, and remaining problems; *in* Turner-Peterson, C. E., Santos, E. S., and Fishman, N. S. (eds.), A basin analysis case study: The Morrison Formation, Grants uranium region, New Mexico: American Association of Petroleum Geologists, Studies in Geology no. 22, pp. 7-26.

Davies, G. R., 1970, Algal-laminated sediments, Gladstone Embayment, Shark Bay, Western Australia: *in* Logan, B. W., Davies, G. R., Read, J. F., and Cebulski, D. E. (eds.), Carbonate sediments and environments, Shark Bay, Western Australia: American Association of Petroleum Geologists, Memoir 13, pp. 169-205.

Dean, W. E., and Anderson, R. Y., 1982, Continuous subaqueous deposition of the Permian Castile evaporites, Delaware Basin, Texas and New Mexico; *in* Handford, C. R., Loucks, R. G., and Davies, G. R. (eds.), Depositional and diagenetic spectra of evaporites: Core Workshop No. 3, Society of Economic Paleontologists and Mineralogists, Calgary, pp. 324-353.

Decima, A., McKenzie, J. A., and Schreiber, B. C., 1988, The origin of "evaporative" limestones: An example from the Messinian of Sicily (Italy): Journal of Sedimentary Petrology, v. 58, no. 2, pp. 256-272.

Dejonghe, L., 1990, The sedimentary structure of barite: Examples from the Chaudfontaine ore deposit, Belgium: Sedimentology, v. 37, pp. 303-323.

Dunham, R. J., 1962, Classification of carbonates according to depositional texture; *in* Ham, W. E. (ed.), Classification of carbonate rocks: American Association of Petroleum Geologists, Memoir 1, pp. 108-121.

Dutton, C. E., 1885, Mount Taylor and the Zuni Plateau; *in* Powell, J. W., Director, Sixth Annual Report of the United States Geological Survey, 1884-85: U.S. Geological Survey, pp. 105-198.

Emanuel, K. M., 1982, A geochemical, petrographic and fluid inclusion investigation of the Zuni Mountains fluorspar district, Cibola County, New Mexico: Unpublished MS thesis, University of New Mexico, Albuquerque, 161 pp.

Esteban, M., and Pray, L. C., 1983, Pisoids and pisolite facies (Permian), Guadalupe Mountains, New Mexico and west Texas; *in* Peryt, T. (ed.), Coated grains: Springer-Verlag, Heidelberg, pp. 503-536.

Evans, R., and Kirkland, D. W., 1988, Evaporitic environments as a source of petroleum; *in* Schreiber, B. C. (ed.), Evaporites and hydrocarbons: Columbia University Press, New York, pp. 256-299.

Falkowski, S. K., 1980, Geology and ore deposits of Johnny M mine, Ambrosia Lake district; *in* Rautman, C. A. (compiler), Geology and mineral technology of the Grants uranium region 1979: New Mexico Bureau of Mines & Mineral Resources, Memoir 38, pp. 230-239.

Flügel, E., 1991, Triassic and Jurassic marine calcareous algae: A critical review; *in* Riding, R. (ed.), Calcareous algae and stromatolites: Springer-Verlag, New York, pp. 481-503.

Folk, R. L., 1965, Some aspects of recrystallization in ancient limestones; *in* Pray, L. C., and Murray, R. C. (eds.), Dolomitization and limestone diagenesis: A symposium: Society of Economic Paleontologists and Mineralogists, Special Publication 13, pp. 14-48.

Frakes, L. A.,1979, Climate through geologic time: Elsevier Publishing Co., New York, 310 pp.

Gabelman, J. W., 1956, Uranium deposits in limestone: U.S. Geological Survey, Professional Paper 300, pp. 387-404.

Gabelman, J. W., and Boyer, W. H., 1988, Uranium deposits in Todilto Limestone, New Mexico: The Barbara "J" No. 1 mine: Ore Geology Reviews, Elsevier Science Publishers, Amsterdam, v. 3, pp. 241-276.

Golubic, S., 1991, Modern stromatolites: A review; *in* Riding, R. (ed.), Calcareous algae and stromatolites: Springer-Verlag, New York, pp. 541-561.

Granger, H. C., 1963, Mineralogy; *in* Kelley, V. C. (compiler), Geology and technology of the Grants uranium region: New Mexico Bureau of Mines & Mineral Resources, Memoir 15, pp. 21-37.

Green, M. W., 1976, Geologic map of the Continental Divide quadrangle, McKinley County, New Mexico: U.S. Geological Survey, Map GQ-1338, 1:24,000.

Green, M. W., 1982, Origin of intraformational folds in the Jurassic Todilto Limestone, Ambrosia Lake uranium mining district, McKinley and Valencia Counties, New Mexico: U.S. Geological Survey, Open File Report 82-69,26 pp.

Green, M. W., and Pierson, C. T., 1971, Geologic map of the Thoreau NE quadrangle, McKinley County, New Mexico: U.S. Geological Survey, Map GQ-954,1:24,000.

Green, M. W., and Pierson, C. T., 1977, A summary of the stratigraphic and depositional environments of Jurassic and related rocks in the San Juan Basin, Arizona, Colorado, and New Mexico: New Mexico Geological Society, Guidebook 28, pp. 147-152.

Gregory, H. E., 1916, The Navajo country. A reconnaissance of parts of Arizona, New Mexico and Utah: U.S. Geological Survey, Water Supply Paper 380,219 pp.

Gregory, H. E., 1917, Geology of the Navajo country, a geographic and hydrographic reconnaissance of parts of Arizona, New Mexico and Utah: U.S. Geological Survey, Professional Paper 93,161 pp.

Handford, C. R., Kendall, A. C., Prezbindowski, D. R., Dunham, J. B., and Logan, B. W., 1984, Salina-margin tepees, pisolites, and aragonite cements, Lake MacLeod, Western Australia: Their significance in interpreting ancient analogs: Geology, v. 12, pp. 523-527.

Hanley, P. L., 1986, Regional diagenetic trends and uranium mineralization in the Morrison Formation across the Grants uranium region; *in* Turner-Peterson, C. E., Santos, E. S., Fishman, N. S. (eds.), A basin analysis case study: The Morrison Formation, Grants uranium region, New Mexico: American Association of Petroleum Geologists, Studies in Geology no. 22, pp. 277-301.

Haq, B. U., Hardenbol J., and Vail, P. R., 1988, Mesozoic and Cenozoic chronostratigraphy and cycles of sea level change; *in* Wilgus, C. K. et al. (eds.), Sea-level changes: An integrated approach: Society of Economic Paleontologists and Mineralogists, Special Publication 42, pp. 71-108.

Hardie, L. D. (ed.) 1977, Sedimentation of the modern tidal flats of northwest Andros Island, Bahamas: Studies in Geology no. 22, Johns Hopkins University Press, Baltimore, 202 pp.

Hardie, L. A., 1991, On the significance of evaporites: Annual Review of Earth and Planetary Science, v. 19, pp. 131-168.

Hardie, L. A., Smoot, J. P., and Eugster, H. P., 1978, Saline lakes and their deposits: A sedimentological approach; *in* Matter, A., and Tucker, M. E. (eds.), Modern and ancient lake sediments: International Association of Sedimentologists, Special Publication 2, pp. 7-41.

Harland, W. B., Armstrong, R. L., Cox, A. V., Craig, L. E., Smith, A. G., Smith, D. G., 1990, A geologic time scale 1989: Cambridge University Press, 263 pp.

Harshbarger, J. W., Repenning, C. A., and Irwin, J. H., 1957, Stratigraphy of the uppermost Triassic and the Jurassic rocks of the Navajo country: U.S. Geological Survey, Professional Paper 291,74 pp.

Hilpert, L. S., 1969, Uranium resources of northwestern New Mexico: U.S. Geological Survey, Professional Paper 603,166 pp.

Hilpert, L. S., and Moench, R. M., 1960, Uranium deposits of the southern part of the San Juan Basin, New Mexico: Economic Geology, v. 55, no. 3, pp. 429-464.

Jones, C. A., 1978, Uranium occurrence in sedimentary rocks exclusive of sandstone; *in* Mickle, D. G., and Mathews, G. W. (eds.), Geologic characteristic of environment favorable for uranium deposits: U.S. Department of Energy, Report GJBX67-78, 86 pp.

Kendall, A. C., 1984, Evaporites; *in* Walker, R. G. (ed.), Facies models: Geoscience Canada, Reprints Series 1, pp. 259-296.

Kendall, C. G. St. C., and Warren, J., 1987, A review of the origin and setting of tepees and their associated fabrics: Sedimentology, v. 34, pp. 1007-1027.

Kietzke, K., 1992, Reassignment of the Jurassic Todilto Limestone ostracode *Metacypris todiltoensis* Swain, 1946, to *Cytheridella,* with notes on the phylogeny and environmental implications of this ostracode: New Mexico Geological Society, Guidebook 43, pp. 173-183.

Kirkland, D. W., and Evans, R., 1981, Source-rock potential of evaporitic environments: American Association of Petroleum Geologists, Bulletin, v. 65, no. 2, pp. 182-190.

Kocurek, G., and Dott, R. H., Jr., 1983, Jurassic paleogeography and paleoclimate of the central and southern Rocky Mountains region; *in* Reynolds, W. W., and Dolly, E. D. (eds.), Mesozoic paleogeography of west-central United States: Society of Economic Paleontologists and Mineralogists, Rocky Mountain Section, pp. 101-116.

Land, L. S., Behrens, E. W., and Frishman, S. A., 1979, The ooids of Baffin Bay: Journal of Sedimentary Petrology, v. 49, no. 4, pp. 1269-1278.

Lienert, B. R., and Helsley, C. E., 1980, Magnetostratigraphy of the Moenkopi Formation at Bears Ears, Utah: Journal of Geophysical Research, v. 85, pp. 1475-1480.

Logan, B. W., 1987, The MacLeod evaporite basin, western Australia, Holocene environments, sediments and geologic evolution: American Association of Petroleum Geologists, Memoir 44,140 pp.

Logan, B. W., Rezak, R., and Ginsburg, R. N., 1964, Classification and environmental significance of algal stromatolites: Journal of Geology, v. 72, pp. 68-83.

Love, L. G., Al-Kaisy, Adil T. H., and Brockley, H., 1984, Mineral and organic material in matrices and coatings of framboidal pyrite from Pennsylvanian sediments, England: Journal of Sedimentary Petrology, v. 54, no. 3, pp. 867-876.

Lucas, S. G., Kietzke, K. K., and Hunt, A. P., 1985, The Jurassic system in east-central New Mexico: New Mexico Geological Society, Guidebook 36, pp. 213-242.

Ludwig, K. R., Simmons, K. R., and Webster, J. D., 1984, U-Pb isotope systematics and apparent ages of uranium ores, Ambrosia Lake and Smith Lake districts, Grants Mineral Belt, New Mexico: Economic Geology, v. 79, pp. 322-337.

Maclntyre, I. G., 1985, Submarine cements-the peloid question; *in* Schneidermann, N., and Harris, P. (eds.) Carbonate cements: Society of Economic Paleontologists and Mineralogists, Special Publication 36, pp. 109-116.

Mankin, C. J., 1972, Jurassic strata in northeastern New Mexico: New Mexico Geological Society, Guidebook 23, pp. 91-97.

Maxwell, C. H., 1990, Geologic map of the Broom Mountain quadrangle, New Mexico: U.S. Geological Survey, Map GQ1666,1:24,000.

McCrary, M. M., 1985, Depositional history and petrography of the Todilto Formation (Jurassic), New Mexico and Colorado: Unpublished MA thesis, University of Texas at Austin, 183 pp.

McKee, E., and Gutschick, R. C., 1969, History of the Redwall Limestone of northern Arizona: Geological Society of America, Memoir 114,726 pp.

McLaughlin, E. D., 1963, Uranium deposits in the Todilto Limestone of the Grants district; *in* Kelley, V. C. (compiler), Geology and technology of the Grants uranium region: New Mexico Bureau of Mines & Mineral Resources, Memoir 15, pp. 136-149.

McLemore, V. T., and Chenoweth, W. L., 1989, Uranium resources of New Mexico: New Mexico Bureau of Mines & Mineral Resources, Resource Map 18,39 pp.

Milliman, J. D., Freile, D., Steinen, R. R., and Wilber, R. J., 1993, Great Bahama Bank aragonitic muds: Mostly inorganically precipitated, mostly exported: Journal of Sedimentary Petrology, v. 63, no. 4, pp. 589-595.

Moench, R. H., and Schlee, J. S.,1967, Geology and uranium deposits of the Laguna district, New Mexico: U.S. Geological Survey, Professional Paper 519,117 pp.

Monty, C. L. V., 1976, The origin and development of cryptoalgae fabrics; *in* Walter, M. R. (ed.), Stromatolites: Elsevier, Developments in Sedimentology, v. 20, pp. 193-249.

Mulholland, J. W., and Kuryvial, R. J., 1992, Sequence boundaries: A proposed nomenclature for the Mesozoic and Cenozoic: The Mountain Geologist, v. 29, no. 3, pp. 71-74.

Perry, B. L., 1963, Limestone reefs as an ore control in the Jurassic Todilto Limestone of the Grants district; *in* Kelley, V. C. (compiler), Geology and technology of the Grants uranium region: New Mexico Bureau of Mines & Mineral Resources, Memoir 15, pp. 150-156.

Platt, N. H., and Wright, V. P., 1991, Lacustrine carbonates: Facies models, facies distribution and hydrocarbon aspects; *in* Anadón, P., Cabrera, L., and Kelts, K. (eds.), Lacustrine facies analysis: International Association of Sedimentologists, Special Publication no. 13, pp. 57-74.

Poole, F. G., 1962, Wind direction in late Paleozoic to middle Mesozoic time on the Colorado Plateau: U.S. Geological Survey, Professional Paper 450-D, pp. 147-151.

Pray, L. C., and Esteban, M., 1977, Upper Guadalupian facies, Permian reef complex, Guadalupe Mountains, New Mexico and Texas: Society of Economic Paleontologists and Mineralogists, Permian Basin Section, Field Conference Guidebook, v. 2,194 pp.

Prezbindowski, D. R., 1985, Burial cementation-is it important? A case study, Stuart City Trend, south-central Texas; *in* Schneidermann, N., and Harris, P. M. (eds.), Carbonate cements: Society of Economic Paleontologists and Mineralogists, Special Publication no. 36, pp. 241-275.

Rapaport, I., Hadfield, J. P., and Olsen, R. H., 1952, Jurassic rocks of the Zuni uplift, New Mexico: U.S. Atomic Energy Commission, RMO-642, 47 pp.

Rawson, R. R., 1980, Uranium in Todilto Limestone (Jurassic) of New Mexico-example of a sabkha-like deposit; *in* Rautman, C. A. (compiler), Geology and mineral technology the Grants uranium region, 1979: New Mexico Bureau of Mines & Mineral Resources, Memoir 38, pp. 304-312.

Reese, R. S., 1981, Stratigraphy and petroleum trapping mechanisms of Upper Jurassic Entrada Sandstone, northwestern New Mexico (abs.): American Association of Petroleum Geologists, Bulletin, v. 65, no. 3, p. 567.

Reijers, T. J. A., and Hsü, K. J., 1986, Manual of carbonate sedimentology: A lexicographical approach: Academic Press, London, 302 pp.

Ridgley, J. L., 1984, Paleogeography and facies distribution of the Todilto Limestone and Pony Express Limestone, north-central New Mexico (abs.): Geological Society of America, Abstracts with Programs, v. 16, no. 4, pp. 414.

Ridgley, J. L., 1986, Diagenesis of the Todilto Limestone Member of the Wanakah Formation, Chama Basin, New Mexico; *in* Mumpton, F. A. (ed.), Studies in diagenesis: U.S. Geological Survey, Bulletin 1578, pp. 197-206.

Ridgley, J. L., 1989, Trace fossils and mollusks from the upper Member of the Wanakah Formation, Chama Basin, New Mexico: Evidence for a lacustrine origin: U.S. Geological Survey, Bulletin 1880-C, pp. 1-16.

Ridgley, J. L., and Goldhaber, M., 1983, Isotopic evidence for a marine origin of the Todilto Limestone, north-central New Mexico (abs.): Geological Society of America, Abstracts with Programs, v. 16, no. 4, p. 414.

Sandberg, P. A., 1975, New interpretation of Great Lake ooids and of ancient non-skeletal carbonate mineralogy: Sedimentology, v. 25, pp. 673-702.

Santos, E. S., and Turner-Peterson, C. E., 1986, Tectonic setting of the San Juan Basin in the Jurassic; *in* Turner-Peterson, C. E., Santos, E. S., Fishman, N. S. (eds.), A basin analysis case study: The Morrison Formation, Grants uranium region, New Mexico: American Association of Petroleum Geologists, Studies in Geology no. 22, pp. 27-33.

Shearman, D. J., 1981, Sabkha facies evaporites; *in* Busson, G. (ed.), Evaporite deposits, illustration and interpretation of some environmental sequences: Gulf Publishing, Paris, pp. 19,96-109.

Shearman, D. J., and Fuller, J. G., 1969, Anhydrite diagenesis,

calcitization, and organic laminites, Winnipegosis, Middle Devonian, Saskatchewan: Canadian Petroleum Geology, Bulletin, v. 17, no. 4, pp. 496-525.

Shinn, E. A., 1969, Submarine lithification of Holocene carbonate sediments in the Persian Gulf: Sedimentology, v. 12, pp. 109-144.

Shinn, E. A., 1983, Tidal flats; *in* Scholle, P. A., Bebout, D. G., and Moore, C. H. (eds.), Carbonate depositional environments: American Association of Petroleum Geologists, Memoir 33, pp. 345-440.

Shinn, E. A., Lloyd, R. N., and Ginsburg, R. N., 1969, Anatomy of a modern carbonate tidal-flat, Andros Island, Bahamas: Journal of Sedimentary Petrology, v. 39, pp. 1202-1228.

Shinn, E. A., Steiner, R. P., Lidz, B. H., and Swart, P. K., 1989, Whitings, a sedimentological dilemma: Journal of Sedimentary Petrology, v. 59, no. 1, pp. 147-161.

Silver, C., 1948, Jurassic overlap in western New Mexico: American Association of Petroleum Geologists, v. 32, pp. 68-81.

Singh, U., 1987, Ooids and cements from the Late Precambrian of the Flinders Range, South Australia: Journal of Sedimentary Petrology, v. 57, pp. 117-127.

Smith, C. T., 1951, Problems of Jurassic stratigraphy of the Colorado Plateau and adjoining regions: New Mexico Geological Society, Guidebook 2, pp. 99-102.

Smith, D. B., 1974, Origin of tepees in the Upper Permian shelf carbonate rocks of Guadalupe Mountains, New Mexico: American Association of Petroleum Geologists, v. 58, pp. 63-70.

Southgate, P. N., Lambert, I. B., Donnelly, T. H., Henry, R., Etminan, H., and Weste, G., 1989, Depositional environments and diagenesis in Lake Parakeelye: A Cambrian alkaline playa from the Officer Basin, South Australia: Sedimentology, v. 36, pp. 1091-1112.

Steiner, M. B., 1978, Magnetic polarity during the Middle Jurassic as recorded in the Summerville and Curtis Formations: Earth Planetary Science Letters, v. 38, pp. 331-345.

Steiner, M. B., and Helsley, C. E., 1975, Reversal patterns and apparent polar wander for the Late Jurassic: Geologic Society of America, Bulletin, v. 86, pp. 1537-1543.

Swain, F. M., 1946, Middle Mesozoic nonmarine ostracodes from Brazil and New Mexico: Journal of Paleontology, v. 20, pp. 543-555.

Tanner, W. F., 1974, History of Mesozoic lakes in northern New Mexico: New Mexico Geological Society, Guidebook 25, pp. 219-223.

Thaden, R. E., and Ostling, E. J., 1967, Geologic map of the Bluewater quadrangle, Valencia and McKinley Counties, New Mexico: U.S. Geological Survey, Map GQ-679,1:24,000.

Thaden, R. E., Santos, E. S., and Ostling, E. J., 1967, Geologic map of the Dos Lomas quadrangle, Valencia and McKinley Counties, New Mexico: U.S. Geological Survey, Map GQ-680, 1:24,000.

Truesdell, A. H., and Weeks, A. D., 1959, Relation of the Todilto Limestone uranium deposits to Colorado Plateau uranium deposits in sandstones: Geological Society of America, Bulletin, v. 70, no. 12, pt. 2, pp. 1689-1690.

Truesdell, A. H., and Weeks, A. D., 1960, Paragenesis of uranium ores in Todilto Limestone near Grants, New Mexico: U.S. Geological Survey, Professional Paper 400-B, pp. 52-54.

Tucker, M. E., 1984, Calcite, aragonite and mixed calcitic--aragonitic ooids from the mid-Proterozoic Belt Supergroup, Montana: Sedimentology, v. 31, pp. 627-644.

Vakhrameev, V. A., 1991, Jurassic and Cretaceous floras and climate of the Earth: Cambridge University Press, 318 pp.

Vincelette, R. R., and Chittum, W. E., 1981, Exploration for oil accumulations in Entrada Sandstone, San Juan Basin, New Mexico: American Association of Petroleum Geologists, Bulletin, v. 65, no. 12, pp. 2546-2570.

Warren, J. K., 1982, The hydrological significance of Holocene tepees, stromatolites, and boxwork limestone in coastal Salinas in South Australia: Journal of Sedimentary Petrology, v. 52, pp. 1171-1201.

Warren, J. K., 1983, Tepees, modern (southern Australia) and ancient (Permian-Texas and New Mexico)-a comparison: Sedimentary Geology, v. 34, pp. 1-19.

Warren, J. K., 1990, Sedimentology and mineralogy of dolomitic Coorong Lakes, South Australia: Journal of Sedimentary Petrology. v. 60, pp. 843-858.

Warren, J. K., 1991, Sulfate dominated sea-marginal and platform evaporative settings: Sabkhas and salinas, mudflats and salterns; *in* Melvin, J. L. (ed.), Evaporites, petroleum and mineral resources: Elsevier, Developments in Sedimentology, v. 59, pp. 69-187.

Warren, J. K., and Kendall, C. G., St. C., 1985, Comparison of sequences formed in marine sabkha (subaerial) and saliva (subaqueous) settings-modern and ancient: American Association of Petroleum Geologists, Bulletin, v. 69, no. 6, pp. 1013-1023.

Wilkinson, B. H., Buczynski, C., and Owen, R. M., 1984, Chemical control of carbonate phases: Implications from Upper Pennsylvanian calcite-aragonite ooids of southeastern Kansas: Journal of Sedimentary Petrology, v. 54, pp. 932-947.

Wray, J. L., 1977, Calcareous algae: Elsevier, Developments in Paleontology and Stratigraphy, no. 4,185 pp.

Selected conversion factors*

TO CONVERT	MULTIPLY BY	TO OBTAIN	TO CONVERT	MULTIPLY BY	TO OBTAIN
Length			**Pressure stress**		
inches, in	2.540	centimeters, cm	lb in^{-2} (= lb/in^2), psi	7.03×10^{-2}	kg cm^{-2} (= kg/cm^2)
feet, ft	3.048×10^{-1}	meters, m	lb in^{-2}	6.804×10^{-2}	atmospheres, atm
yards, yds	9.144×10^{-1}	m	lb in^{-2}	6.895×10^{3}	newtons (N)/m^2, N m^{-2}
statute miles, mi	1.609	kilometers, km	atm	1.0333	kg cm^{-2}
fathoms	1.829	m	atm	7.6×10^{2}	mm of Hg (at 0° C)
angstroms, Å	1.0×10^{-8}	cm	inches of Hg (at 0° C)	3.453×10^{-2}	kg cm^{-2}
Å	1.0×10^{-4}	micrometers, µm	bars, b	1.020	kg cm^{-2}
Area			b	1.0×10^{6}	dynes cm^{-2}
in^2	6.452	cm^2	b	9.869×10^{-1}	atm
ft^2	9.29×10^{-2}	m^2	b	1.0×10^{-1}	megapascals, MPa
yds^2	8.361×10^{-1}	m^2	**Density**		
mi^2	2.590	km^2	lb in^{-3} (= lb/in^3)	2.768×10^{1}	gr cm^{-3} (= gr/cm^3)
acres	4.047×10^{3}	m^2	**Viscosity**		
acres	4.047×10^{-1}	hectares, ha	poises	1.0	gr cm^{-1} sec^{-1} *or* dynes cm^{-2}
Volume (wet and dry)			**Discharge**		
in^3	1.639×10^{1}	cm^3	U.S. gal min^{-1}, gpm	6.308×10^{-2}	l sec^{-1}
ft^3	2.832×10^{-2}	m^3	gpm	6.308×10^{-5}	m^3 sec^{-1}
yds^3	7.646×10^{-1}	m^3	ft^3 sec^{-1}	2.832×10^{-2}	m^3 sec^{-1}
fluid ounces	2.957×10^{-2}	liters, l *or* L	**Hydraulic conductivity**		
quarts	9.463×10^{-1}	l	U.S. gal day^{-1} ft^{-2}	4.720×10^{-7}	m sec^{-1}
U.S. gallons, gal	3.785	l	**Permeability**		
U.S. gal	3.785×10^{-3}	m^3	darcies	9.870×10^{-13}	m^2
acre-ft	1.234×10^{3}	m^3	**Transmissivity**		
barrels (oil), bbl	1.589×10^{-1}	m^3	U.S. gal day^{-1} ft^{-1}	1.438×10^{-7}	m^2 sec^{-1}
Weight, mass			U.S. gal min^{-1} ft^{-1}	2.072×10^{-1}	l sec^{-1} m^{-1}
ounces avoirdupois, avdp	2.8349×10^{1}	grams, gr	**Magnetic field intensity**		
troy ounces, oz	3.1103×10^{1}	gr	gausses	1.0×10^{5}	gammas
pounds, lb	4.536×10^{-1}	kilograms, kg	**Energy, heat**		
long tons	1.016	metric tons, mt	British thermal units, BTU	2.52×10^{-1}	calories, cal
short tons	9.078×10^{-1}	mt	BTU	1.0758×10^{2}	kilogram-meters, kgm
oz mt^{-1}	3.43×10^{1}	parts per million, ppm	BTU lb^{-1}	5.56×10^{-1}	cal kg^{-1}
Velocity			**Temperature**		
ft sec^{-1} (= ft/sec)	3.048×10^{-1}	m sec^{-1} (= m/sec)	°C + 273	1.0	°K (Kelvin)
mi hr^{-1}	1.6093	km hr^{-1}	°C + 17.78	1.8	°F (Fahrenheit)
mi hr^{-1}	4.470×10^{-1}	m sec^{-1}	°F – 32	5/9	°C (Celsius)

**Divide by* the factor number to reverse conversions.
Exponents: for example 4.047×10^{3} (see acres) = 4,047; 9.29×10^{-2} (see ft^2) = 0.0929.

Editors: Jiri Zidek, Jane Love

Typeface: Palatino

Presswork: Miehle Single Color Offset
Harris Single Color Offset

Binding: Saddlestitched with
Softbound cover

Paper: Cover on 12-pt. Kivar Text
on 70-lb White Matte

Ink: Cover—PMS 320
Text—Black

Quantity: 1,000